Aus dem Pathologischen Institut

der Ludwig-Maximilians-Universität München

Vorstand: Prof. Dr. med. Thomas Kirchner

Characterization of a p53/miR-34a/CSF1R/STAT3 feedback-loop in colorectal cancer

Dissertation

zum Erwerb des Doktorgrades der Naturwissenschaften

an der Medizinischen Fakultät der

der Ludwig-Maximilians-Universität zu München

vorgelegt von

Xiaolong Shi

aus

Shaanxi, Volksrepublik China

2020

Mit Genehmigung der Medizinischen Fakultät

der Universität München

Betreuer: Prof. Dr. rer. nat. Heiko Hermeking

Zweitgutachter: Prof. Dr. rer. nat. Roland Kappler

Dekan: Prof. Dr. med. dent. Reinhard Hickel

Tag der mündlichen Prüfung: 30.09.2020

Eidesstattliche Versicherung

Xiaolong Shi

Ich erkläre hiermit an Eides statt, dass ich die vorliegende Dissertation mit dem Thema

"Characterization of a p53/miR-34a/CSF1R/STAT3 feedback-loop in colorectal cancer"

selbständig verfasst, mich außer der angegebenen keiner weiteren Hilfsmittel bedient und alle Erkenntnisse, die aus dem Schrifttum ganz oder annähernd übernommen sind, als solche kenntlich gemacht und nach ihrer Herkunft unter Bezeichnung der Fundstelle einzeln nachgewiesen habe.

Ich erkläre des Weiteren, dass die hier vorgelegte Dissertation nicht in gleicher oder in ähnlicher Form bei einer anderen Stelle zur Erlangung eines akademischen Grades eingereicht wurde.

Ort, Datum: Munich, 25.03.2020 Unterschrift: Xiaolong Shi

Publication

Parts of this thesis have been submitted for publication:

Characterization of a p53/miR-34a/CSF1R/STAT3 feedback-loop in colorectal cancer.
Xiaolong Shi, Markus Kaller, Matjaz Rokavec, Thomas Kirchner, David Horst and Heiko Hermeking, *Cellular and Molecular Gastroenterology and Hepatology* (revised version submitted)

Table of Contents

Eidesstattliche Versicherung ..... **Error! Bookmark not defined.**
Publication I
Table of Contents II
Abbreviations 1
1. Introduction 3
1.1 Colorectal Cancer: 3
1.2 Molecular Subtypes of CRC 6
1.2.1 Consensus Molecular Subtypes (CMS) 6
1.2.2 CRC Intrinsic Subtypes (CRIS) 7
1.3 CRC Metastasis and EMT 8
1.3.1 CRC Metastasis 8
1.3.2 Epithelial-mesenchymal transition (EMT) 9
1.3.2 EMT regulation in CRC 9
1.4 p53/miR-34a 10
1.4.1 The tumor suppressor p53 10
1.4.2 miRNAs and miR-34a family 11
1.5 CSF1R signaling pathway 15
2. Aims of the study 18
3. Materials 19
3.1 Chemicals and Reagents 19
3.2 Cell Lines 22
3.3 Buffers and Solutions 22
3.4 Kits 25
3.5 Enzymes 26
3.6 Oligonucleotides 26
3.6.1 Oligonucleotides used for qPCR 26
3.6.2 Oligonucleotides used for MSP and BSP 27
3.6.3 Oligonucleotides used for qChIP 28
3.6.4 Oligonucleotides used for cloning and mutagenesis of the *CSF1R* 3'-UTR 28
3.6.5 Oligonucleotides (*pre-miR-34a*, antagomir miR-34a) 29
3.7 Antibodies 29
3.7.1 Primary Antibodies 29
3.7.2 Secondary Antibodies 30
3.8 Vectors 30

3.9 siRNAs ... 31
3.10 Softwares ... 31
3.11 Laboratory equipment ... 32
4. Methods ... 34
4. 1 Cell culture and treatments ... 34
4. 2 Modified Boyden-chamber assay ... 34
4. 3 Western blot analysis ... 35
4. 4 Chromatin immunoprecipitation (ChIP) ... 35
4. 5 Generation of cell pools stably expressing conditional alleles ... 36
4. 6 Dual 3'-UTR luciferase reporter assays ... 37
4. 7 Bioinformatic analysis of online databases ... 37
4. 8 Clinical samples and immunohistochemistry ... 38
4. 9 Colony formation assay ... 39
4. 10 Wound healing assay ... 39
4. 11 Detection of apoptosis ... 39
4. 12 MTT assay ... 40
4. 13 Establishment of a 5-FU-resistant cell pool ... 40
4. 14 RNA isolation and qPCR analysis ... 41
4. 15 Methylation-specific PCR ... 41
4. 16 Bisulfite sequencing ... 42
4. 17 Metastasis formation in NOD/SCID mice ... 43
4. 18 Statistics ... 43
4. 19 Study approval ... 44
5. Results ... 45
5.1 Association of *CSF1R, CSF1* and *IL34* expression with clinical parameters in CRCs ... 45
5.2 *CSF1R* represents a direct target of miR-34a ... 56
5.3 p53 represses *CSF1R* via inducing miR-34a ... 59
5.4 Coherent feed-forward regulation of *CSF1R* by SNAIL and miR-34a ... 61
5.5 Repression of *miR-34a* after CSF1R activation is mediated by STAT3 ... 66
5.6 CSF1R activation induces EMT, migration, and invasion ... 69
5.7 CSF1R mediates resistance to 5-FU in CRC cells ... 78
5.8 CSF1R mediates EMT, migration, and invasion of 5-FU in CRC cells ... 82
5.9 Epigenetic silencing of *miR-34a* contributes to CSF1R up-regulation, 5-FU resistance and CRC progression ... 86
6. Discussion ... 91

8. Zusammenfassung 96
9. Acknowledgements 97
10. References 98
11. Curriculum Vitae 113

Abbreviations	
CDH1	E-cadherin
CMS	consensus molecular subtype
COAD	colon adenocarcinoma
CRC	colorectal cancer
CRIS	colorectal cancer intrinsic subtypes
EMT	epithelial-mesenchymal transition
MET	mesenchymal-epithelial transition
EMT-TF	EMT-inducing transcription factor
GSEA	gene set enrichment analyses
MSP	methylation-specific PCR
STAT3	signal transducers and activators of transcription 3
FCS	fetal calf serum
DMSO	dimethyl-sulfoxide
APS	ammonium peroxodisulfate
TEMED	tetramethylethylendiamin,1,2-bis (dimethylamino) –ethan
SDS	sodium dodecyl sulfate
WB	Western blot analysis
IHC	immunohistochemical analysis
cDNA	complementary DNA
E.coli	*Escherichia coli*
DNA	deoxyribonucleic acid
DOX	doxycycline
HBSS	Hank's balanced salt solution
PCR	polymerase chain reaction
siRNA	small interfering rna
PDX	patient-derived xenografts
PTP- ζ	protein-tyrosine phosphatase ζ
qChIP	quantitative chromatin immunoprecipitation
READ	rectal adenocarcinoma
TCGA	the cancer genome atlas
TSA	trichostatin A
TSS	transcriptional start site

VIM	vimentin
3′-UTR	three primed untranslated region
5-aza	5-aza-2'deoxycytidine
5-FU	5-fluoro-uracil
ZEB	zinc finger E-box-binding homeobox protein
miRNAs	micro RNAs

1. Introduction

1.1 Colorectal Cancer:

Colorectal cancer (CRC) is the third most common cancer but second in terms of mortality globally (Dekker, Tanis, Vleugels, Kasi, & Wallace, 2019) (Figure 1.1). Despite the big efforts in prevention, diagnosis, and treatment in the past decades, more than 1.81 million new CRC patients were diagnosed and 881,000 deaths are estimated to occur in 2018 (Bray et al., 2018).

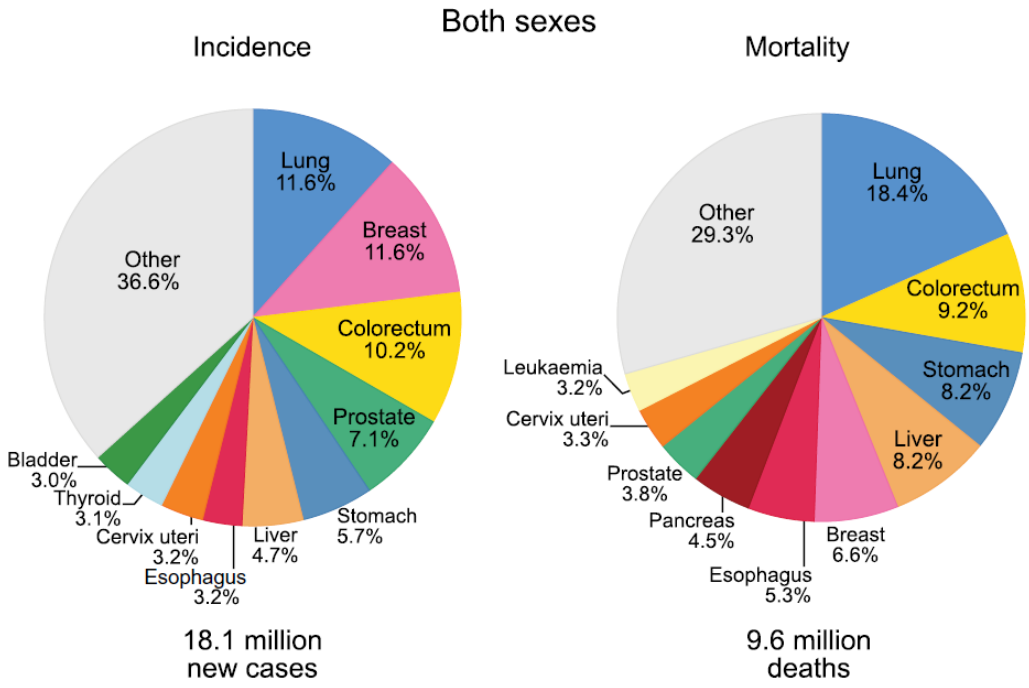

Figure 1.1: The distribution of the new diagnosed cases and death in 2018.
(Figure taken from Freddie Bray, et al. CA: A Cancer Journal for Clinicians, 2018 (Bray et al., 2018))

Although genetic inheritance is an important risk factor for CRC, the majority of CRC cases occurred in people without a family history of CRC or inherited gene

mutation that could increase the risk of CRC, suggesting the acquired somatic genetic and epigenetic alterations largely contributed to the CRC risk (Smith et al., 2018). The CRC incidence rates between countries show a great variation and are correlated with the human development index (HDI) that used to reflect the county's economic development (Khazaei et al., 2016) (Figure 1.2). Accordingly, developed countries have higher CRC incidence rates than undeveloped countries, which is probably due to the sedentary lifestyle, westernized dietary and increasing obesity, since all of them are major risk factors for CRC. Moreover, age-standardized incidence rates also vary, highlighting that CRC is a consequence of combined risk factors, including genetics and lifestyle. Of note, the rising incidence of CRC at younger ages is an emerging trend.

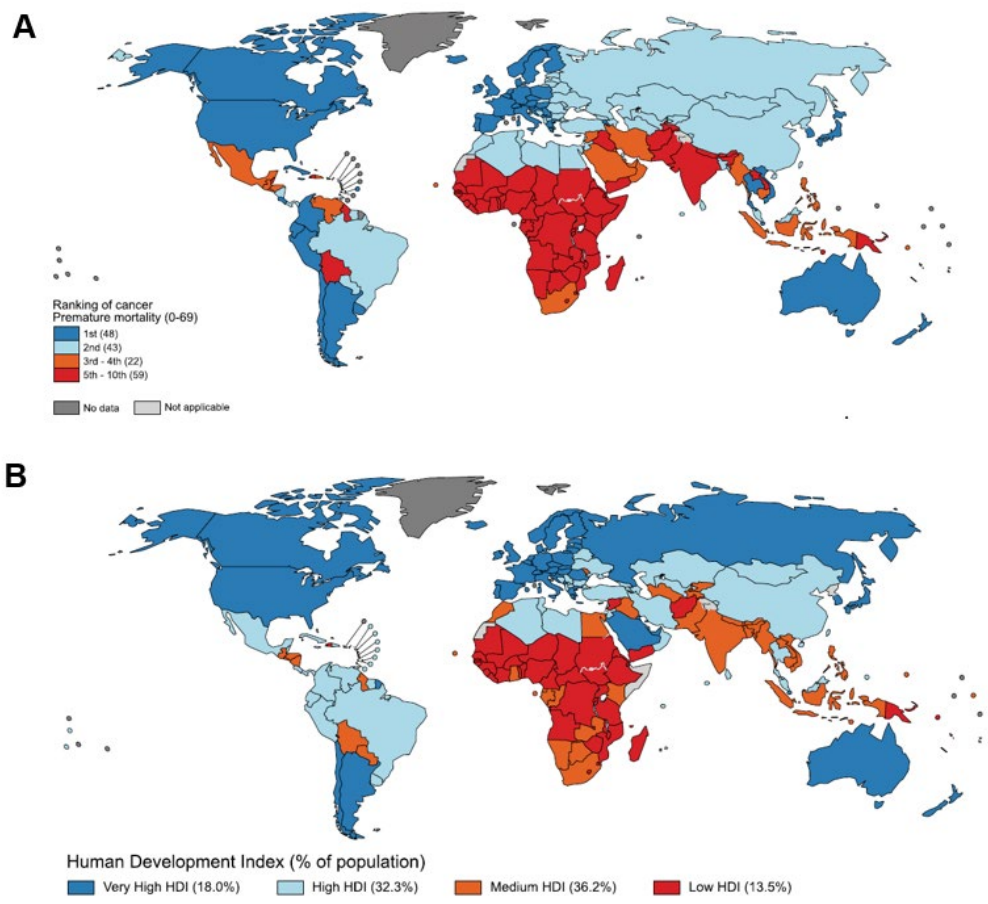

Figure 1.2

A, The ranking of cancer mortality of countries.

B, Global Maps Present the 4-Tier Human Development Index.

Figures taken from (Bray et al., 2018)

CRC carcinogenesis is considered to represent a stepwise process and each step is associated with distinct molecular changes. In the past, Fearon and Vogelstein described a model in which the accumulation of sequential alterations of several tumor-suppressive and tumor-driven genes results in the “adenoma to carcinoma cascade” (Fearon & Vogelstein, 1990) (Figure 1.3). In this cascade, the inactivation of APC initiates the transformation from mucosa to adenoma, followed by the alteration of KRAS and p53, which further drives the aggressiveness of subclones. This model was well-accepted as it was the foundation on which the strategy of CRC prevention is based. However, some of the CRC lack alterations of APC and KRAS showing that CRC is a heterogeneous disorder and indicating that the linear theory is not applicable to all the cases of CRC (Jass, 2007).

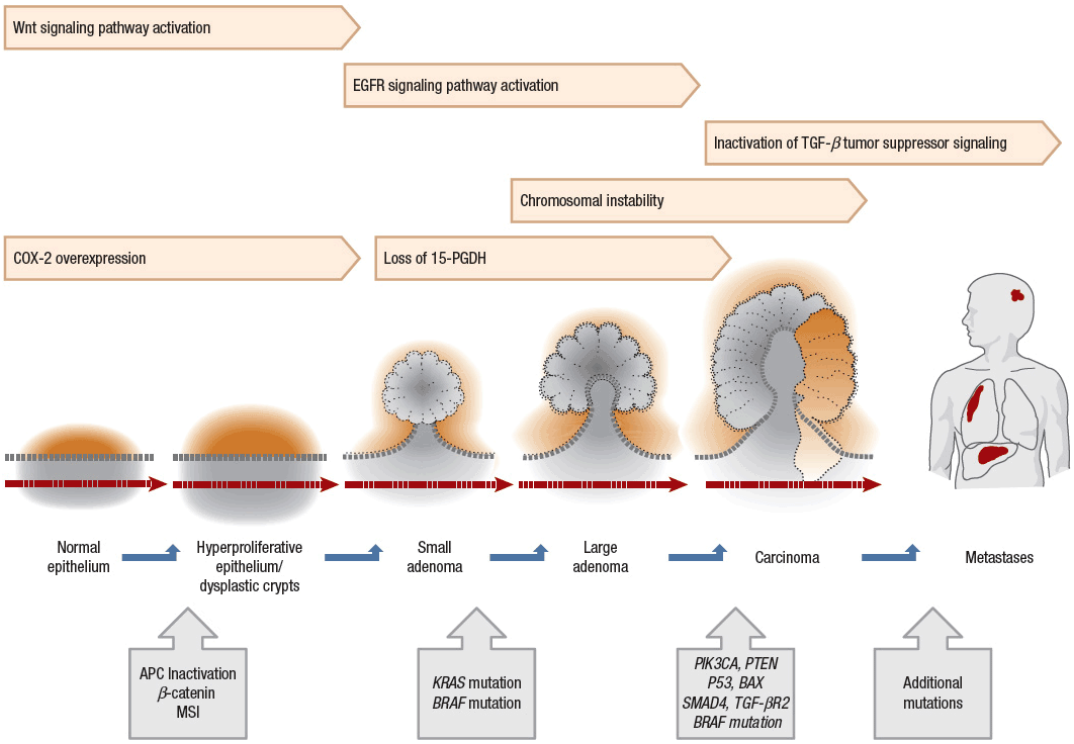

Figure 1.3: Genetic changes associated with the "adenoma to carcinoma cascade". Figure taken from https://basicmedicalkey.com/colorectal-cancer-2/

1.2 Molecular Subtypes of CRC

CRC is a heterogeneous disease and composed of biologically and clinically diverse subtypes. An appropriate subtype classification that correlates molecular changes in tumors with clinical relevance can better describe the tumor behavior and may improve prognosis and treatment strategies.

1.2.1 Consensus Molecular Subtypes (CMS)

With the increasing molecular and genomic study of CRC, a number of genes expression-based CRC classification systems were proposed which grouped colorectal cancer into subgroups with distinct molecular and clinical features (Jass, 2007). Among those classifications, the consensus molecular subtypes (CMS)

classification is one of the most robust colorectal cancer classifications and widely accepted. It grouped CRCs into 4 subtypes (CMS1-CMS4) with distinguishing features: CMS1, hyper-mutated, microsatellite unstable, strong immune activation; CMS2, epithelial, chromosomally unstable, marked WNT and MYC signaling activation; CMS3, epithelial, evident metabolic dysregulation; and CMS4, prominent transforming growth factor β activation, stromal invasion, and angiogenesis (Guinney et al., 2015). The CMS classification has prognostic value independent of the cancer stage. For example, patients with CMS4 subtype have poor survival, even when treated with standard adjuvant chemotherapies (Sveen et al., 2018). In addition, it also shows the advantage of predicting the response to treatments. Okita et al. studied the association between CMS subtypes and treatment outcomes, showing that this classification could be a predictive factor for the efficacy of chemotherapy against CRC (Okita et al., 2018).

1.2.2 CRC Intrinsic Subtypes (CRIS)

The CMS classification was created by using 18 datasets and collectively more than 4000 CRC samples (Guinney et al., 2015). However, the tumor samples might be contaminated by infiltrated stromal cells. Thus the molecular features in each CMS subtype represent a mixture of those from tumor cells and stromal cells (Isella et al., 2015). For example, a large portion of the genes involved in the CMS4 signature may be derived from tumor stroma. Such stromal cells may, for instance, be tumor-associated macrophages (TAMs) and cancer-associated fibroblasts (CAFs), which are strong indicators of tumor aggressiveness, but do not represent tumor cell inherent functions (Calon et al., 2015; Isella et al., 2015). To solve this problem, patient-derived xenografts (PDX) have been used to generate mRNA expression signatures by

microarray analyses. By the use of human-specific probe sets the contribution of (murine) stromal mRNAs to whole tumor mRNA expression patterns was selectively eliminated (Isella et al., 2017). Thereby, five different colorectal cancer intrinsic subtypes (CRIS-A to CRIS-E) were defined. Among those five CRIS subtypes, CRIS-B shows the poorest prognosis and is enriched with signatures associated with EMT. Apart from classifying PDX-derived tumors, this classification system was used to re-classify previously established publicly available CRC patient cohorts into CRIS subtypes, such as the TCGA-COAD cohort (Isella et al., 2017)

1.3 CRC Metastasis and EMT

1.3.1 CRC Metastasis

Metastasis, which is defined as the spread of tumor cells from the original tumor site to a secondary site within the patients, is the main cause of cancer-related death in the vast majority of cancer types, including CRC (Boire, Brastianos, Garzia, & Valiente, 2020; Favoriti et al., 2016). The most common site of metastasis for CRC is the liver (Dekker et al., 2019). In addition, metastatic tumors were also found in the lungs, brain, bones, or spinal cord. While surgery still remains the most effective and mainstay treatment option for CRC, most CRC patients with distant metastasis are not suitable for conventional therapy, leading to poor 5-year survival of <10% (Brenner, Kloor, & Pox, 2014; Manfredi et al., 2006). In most of CRC patients, metastasis occurred before the surgical resection or was found at the time of surgery, resulting in a high risk of recurrence. However, the mechanism underlying metastasis has not been fully discovered, which limits the strategy of prevention, early diagnosis, therapeutic

treatment, and prognosis. Therefore, a better understanding of the molecular mechanism is urgently needed.

1.3.2 Epithelial-mesenchymal transition (EMT)

Epithelial-mesenchymal transition (EMT) of primary tumor cells is one of the first steps of the metastatic cascade in epithelium-derived carcinomas (Nieto, Huang, Jackson, & Thiery, 2016). EMT is accompanied by the downregulation of epithelial gene expression and the upregulation of mesenchymal gene expression. The key events in EMT are the dissolution of the epithelial cell-cell junctions to detach from the primary tumor and get into the surrounding tissues. Tumor cells that underwent an EMT acquire an increased capability of motility and invasion by expressing matrix metalloproteinase that can degrade extracellular matrix proteins (De Craene & Berx, 2013; Thiery, Acloque, Huang, & Nieto, 2009). Therefore, tumor cells are able to invade into the bloodstream or lymphatic system, and subsequently establish metastasis.

1.3.3 EMT regulation in CRC

Several transcription factors that repress the epithelial phenotype and induce the mesenchymal phenotype are critical for EMT, such as SNAIL, TWIST and zinc-finger E-box-binding (ZEB) transcription factors (Hahn & Hermeking, 2014; Hahn, Jackstadt, Siemens, Hunten, & Hermeking, 2013). One of the hallmarks of EMT is the down-regulation of E-cadherin. SNAIL represses E-cadherin and other epithelial genes by binding to their promoter, thereby decreasing cell-cell adhesion (Peinado, Ballestar, Esteller, & Cano, 2004). In addition, SNAIL also down-regulates mesenchymal-to-

epithelial transition (MET)-inducing genes, such as miR-200c and miR-34a/b/c, by directly binding to the promoter (Gill et al., 2011; Hahn et al., 2013; Siemens et al., 2011). As a member of the SNAIL family, SLUG is also responsible for EMT and tumor metastasis via repression of E-Cadherin (Bolos et al., 2003). The expression of ZEB1 and ZEB2 often follows the activation of SNAIL expression. ZEB1 and ZEB2 act as both transcriptional repressors and activators, thereby repress some epithelial junction and polarity genes and activate mesenchymal genes that define the EMT phenotype (Krebs et al., 2017). Besides, TWIST also plays an essential role in EMT and cancer metastasis (Kang & Massague, 2004). TWIST directly induces SLUG by binding its promoter. Additionally, TWIST represses E-cadherin independently SNAIL. Moreover, TWIST cooperates with SNAIL in the induction of ZEB1 expression.

1.4 p53/miR-34a

1.4.1 The tumor suppressor p53

p53 is one of the most important suppressors of tumor formation and is also the most frequently mutated gene in human cancer. For instance, up to 50%-70% of colorectal tumors harbor *p53* mutations (Chung, 2000). In unstressed cells, the p53 protein is degraded through the ubiquitin-proteasome pathway and is thereby maintained at a low level. A number of intracellular and extracellular stresses, such as DNA damage, induce the activation of p53. Upon the stimulation, the half-life of p53 protein is increased, leading to an accumulation of p53 protein in cells. The activated p53 binds to specific DNA sequences in the promoter of target genes, thereby regulating cancer cell metabolism, invasion, metastasis, apoptosis, cell cycle arrest and DNA repair (Rokavec, Li, Jiang, & Hermeking, 2014a) (Figure 1.4). Thereby, p53

eliminates damaged or mutant cells that could potentially become cancer cells. On the contrary, defective p53 allows abnormal cells to proliferate. Besides protein-encoding genes, microRNA can also be targeted directly by p53.

1.4.2 miRNAs and miR-34a family

microRNAs (miRNAs) are a class of short, endogenous RNAs of 19-25 nucleotides in size (Hermeking, 2012). So far, hundreds of miRNAs have been found and identified in animals, plants, and viruses. miRNAs are critical for a variety of biological processes by targeting mRNAs for degradation or translation repression. In general, the host genes of miRNA are transcribed to a primary miRNA (pri-miRNA), which is further processed to a precursor miRNA (pre-miRNA) by a class 2 RNase enzyme Drosha in nuclear (Rokavec et al., 2014a; Rokavec, Li, Jiang, & Hermeking, 2014b). Next, the pre-miRNAs are transported to the cytoplasm by exportin-5. In the cytoplasm, the pre-miRNAs are cleaved by another RNase III nuclease Dicer, resulting in a 22 bp double-stranded RNA (miRNA: miRNA* duplex). Mostly one strand is loaded into the RNA-induced silencing complex (RISC) in which the miRNA interacts with its target mRNA, whereas the other strand is degraded. After loading, the miRNA guides the RISC to its target mRNA to repress translation or induce mRNA degradation.

Certain miRNAs are induced by p53 and displayed a tumor-suppressive function (Hermeking, 2012). Among these p53-induced miRNAs, miRNAs of the miR-34 family often show the most pronounced induction by p53 (Rokavec, Li, Jiang, & Hermeking, 2014). The miR-34 family consists of miR-34a, miR-34b, and miR-34c. Of the 3 members of the miR-34 family, the expression of miR-34a was found in most of the human tissue, while the miR-34b/c were mainly expressed in specific organs, such as

lungs and brain. In humans, the host gene of miR-34a is located on chromosome 1, whereas the host gene of miR-34b and miR-34c is located on chromosome 11. Chromatin immunoprecipitation and luciferase reporter assays showed that both host genes of the miR-34 family contain p53-responsive elements where p53 binds directly to activate the transcription (Hermeking, 2007; Tarasov et al., 2007). Upon p53 induction, the elevated expression of miR-34a/b/c inhibits the progression of cancer by down-regulation of multiple proteins, such as SNAIL, ZNF281, IL6R, INH3 and PAI-1, suggesting miR-34 family represent important mediators of tumor suppressor p53 (Hahn et al., 2013; Li, Rokavec, Jiang, Horst, & Hermeking, 2017; Oner et al., 2018; Rokavec, Oner, et al., 2014; Siemens et al., 2011) (Figure 1.4). Besides p53-induced expression of miR-34 family, the level of miR-34a/b/c can be regulated by other factors, such as FoxO3a, ELK1, STAT3 and HIF1alpha (Christoffersen et al., 2010; Li, Rokavec, et al., 2017; Natarajan et al., 2017; Rokavec, Oner, et al., 2014).

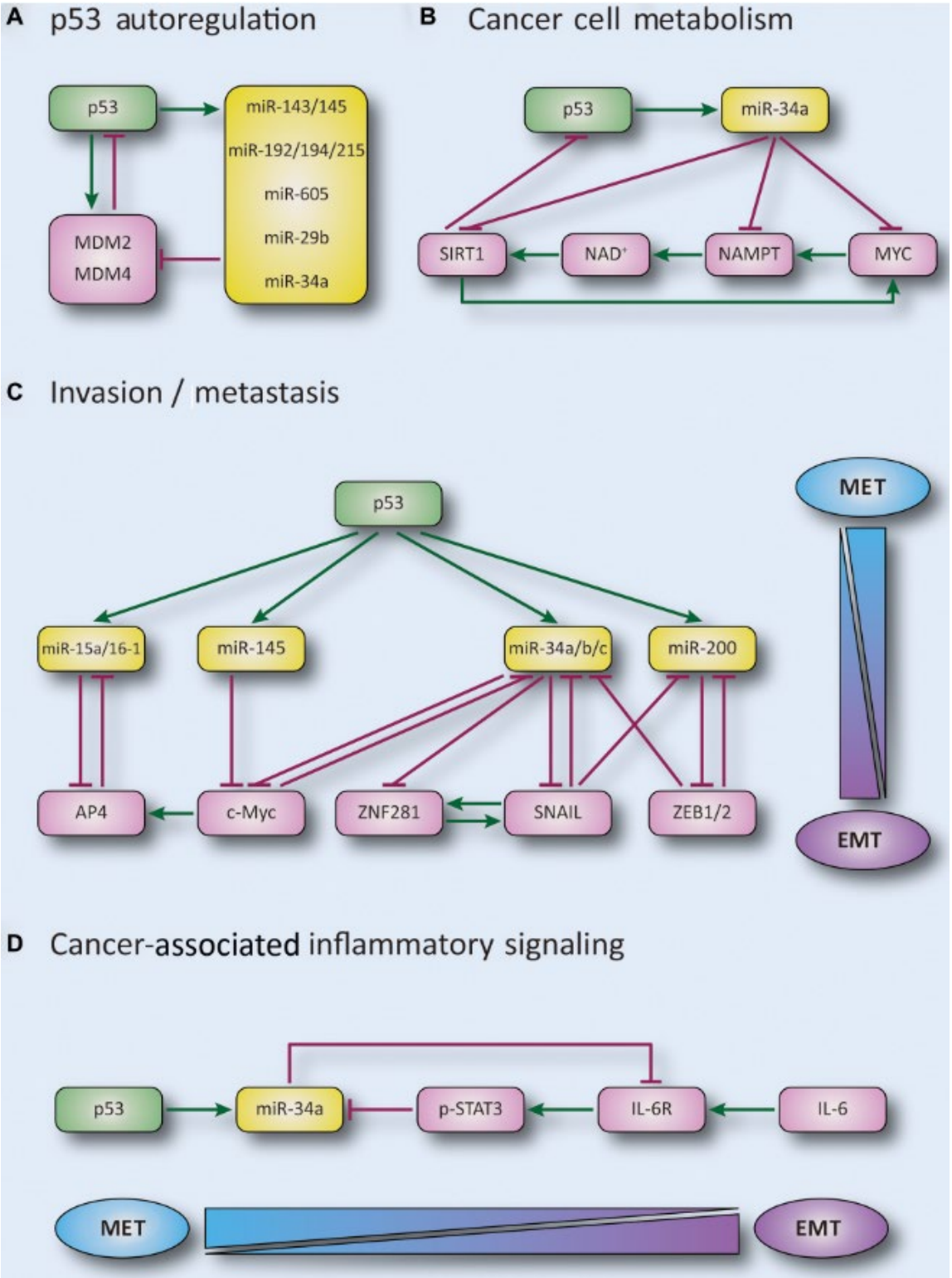

Figure 1.4

The role of p53/miRNA axis in (A) p53 autoregulation, (B) cancer cell metabolism, (C) invasion, and metastasis, as a result of the regulation of EMT/MET (D) cancer-associated inflammatory signaling. Figure taken from (Rokavec, Li, et al., 2014)

1.4.3 miR-34 in CRC

The potential tumor-suppressive effect of the miR-34 family attracted researchers to investigate their role in cancer. The members of the miR-34 family exhibit tumor suppressor effects, by inhibiting the process that promotes tumor development, such as EMT, cell cycle, and stemness, and promoting processes that inhibit tumor growth, such as apoptosis and senescence. These processes are regulated via the repression of miR-34target mRNA.

In CRC, it has been shown miR-34 inhibits cell migration, invasion and metastasis by downregulation of IL6R, ZNF281, c-Kit and Pai-1. In a model of *Apc*$^{min/+}$ mice with deletions of the *miR-34a* and/or *miR-34b/c* genes, the tumor burden was increased while the life-span survival was decreased (Jiang & Hermeking, 2017). In another AOM/DSS treated mice model for the study of colon carcinogenesis, loss of miR-34a facilitated tumor invasion, accompanied by characteristics of EMT and enhanced IL-6R/STAT3 signaling. These findings demonstrated the tumor-suppressive function of miR-34 in CRC. Moreover, miR-34a directly suppresses the EMT transcriptional factor SNAIL, therefore inhibiting EMT. Interestingly, miR-34a is also repressed by SNAIL, thus the balance between miR-34a and SNAIL determines, at least in part, the epithelial or mesenchymal state of tumor cells.

Notably, the expression of the miR-34 family is frequently inactivated in a number of tumor types. In CRC, the expression of miR-34a and miR-34b/c is downregulated in tumors when compared with adjacent non-tumor tissues. Besides the mutation of *p53*, the CpG methylation in the promoter of *miR-34a/b/c* genes significantly contributes to the lower expression of miR-34 in CRCs and has been associated with distant metastasis (Lodygin et al., 2008; Oner et al., 2018; Siemens, Neumann, et al., 2013; Vogt et al., 2011). The methylation of *miR-34a* and *miR-34b/c* was frequently found in

CRC samples, with a rate of 74% and 99% of samples respectively. Compared with miR-34b/c, the level of miR-34a is higher in CRC. Therefore, many studied in CRC focused on the regulation and function of miR-34a.

1.5 CSF1R signaling pathway

Together with the PDGFR and c-kit receptors, the colony-stimulation factor 1 receptor (CSF1R), which is encoded by the c-*fms* proto-oncogene, belongs to the group of type III RTKs (Heisterkamp N Fau - Groffen, Groffen J Fau - Stephenson, & Stephenson, 1983; Roussel, Sherr, Barker, & Ruddle, 1983; Yarden & Ullrich, 1988). Transforming potential has been assigned to the viral homolog (v-*fms*) and c-*fms* (Coussens et al., 1986; Roussel et al., 1987). Binding of its ligand CSF1 or the more recently identified ligand, IL-34, induces homodimerization and activation of CSF1R (Ullrich & Schlessinger, 1990; Y. Wang et al., 2012). Subsequently, the Ras/Raf/MAPK, PI3K/AKT, and JAK/STAT pathways are activated (Lemmon & Schlessinger, 2010; Novak et al., 1995; Ullrich & Schlessinger, 1990) (Figure 1.5). CSF1R was initially identified and shown to be mainly expressed in macrophages and their progenitors (Byrne, Guilbert, & Stanley, 1981; Guilbert & Stanley, 1980), where the CSF1R-mediated signaling is crucial for the survival and differentiation. Tumor-associated macrophages (TAM), which are recruited to tumors through the secretion of various chemotactic molecules, such as CSF1, have been associated with poor survival in various tumor types (Cannarile et al., 2017; Chockalingam & Ghosh, 2014). In early stage as well as metastatic cancer, the dominant TAM phenotype was reported to be tumor-promoting M2 macrophages as opposed to tumor suppressive M1 macrophages. CSF1/CSF1R signaling is critical for the polarization and maintenance of M2

macrophages, that promote tumor growth, angiogenesis, invasion, and metastasis as well as resistance to therapy (Zhao et al., 2015). In addition, paracrine interactions between tumor cells and TAMs facilitate the spread of a tumor by promoting migration, invasion, and metastasis (Wyckoff et al.). Accordingly, the intra-tumoral presence of TAM is associated with poor survival. Thus, targeting the CSF1/CSF1R axis in tumor-promoting TAM has been represented as a potential and attractive strategy to eliminate or repolarize these cells. For example, CSF1R inhibition reduced the M2 macrophage polarization and blocked tumor progression in glioma (Pyonteck et al., 2013). Moreover, various approaches targeting CSF1R signaling are currently in clinical development (Cannarile et al., 2017).

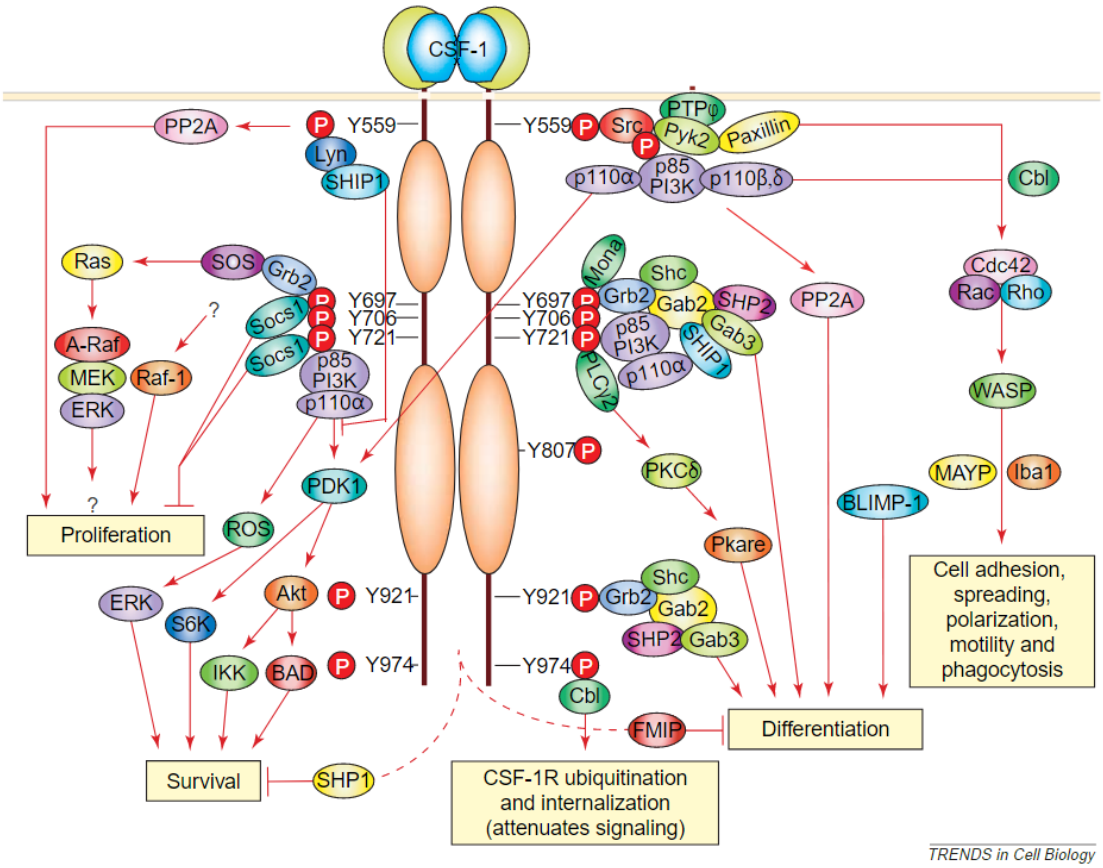

Figure 1.5 Signaling pathways regulated by CSF1R in myeloid cells (Figure taken from (Pixley & Stanley, 2004).)

In addition to macrophages, the expression of CSF1R and its ligands can be detected in several types of tumors, including CRC (Cioce et al., 2014; Julia Menke et al., 2012; Patsialou et al.). As a receptor tyrosine kinase, the biological activity of CSF1R is largely based upon ligand stimulation. It has been shown that not only CSF1R but also CSF1 and IL34, are overexpressed in CRC (Franze et al., 2018b; H. Wang et al., 2016). In the human colon expression of CSF1 is significantly higher than that of IL34, suggesting CSF1 is the main ligand for activation of CSF1R in CRC (Zwicker et al., 2015). However, the significance of CSF1R-expressing tumor cells of epithelial origin is less well characterized. Interestingly, elevated expression of CSF1 and CSF1R in breast cancer has been associated with metastases and progression (Richardsen, Uglehus, Johnsen, & Busund, 2015). Notably, colorectal cancer patients with a more advanced tumor stage display elevated serum levels of CSF1, implying that CSF1R signaling may be involved in CRC progression (Mroczko, Szmitkowski, & Okulczyk, 2003).

2. Aims of the study

The present study had the following aims:

- Analysis of the putative associations and prognostic value of *CSF1R, CSF1* and *IL34* expression in CRC patient cohorts
- Characterization of the putative regulation of CSF1R by miR-34a in colorectal cancer cells.
- Determination of the relevance of CSF1R regulation by miR-34a for EMT, migration, invasion, metastasis, and chemo-resistance in CRC
- Analysis of the potential association of miR-34a silencing with CSF1R up-regulation in CRC cells and patient samples

3. Materials

3.1 Chemicals and Reagents

Chemical compound	Supplier
FCS	Life Technologies
Penicillin-Streptomycin (10,000 U/mL)	Life Technologies
DMEM medium	Life Technologies
Mc Coy's medium	Life Technologies
HBSS, no calcium, no magnesium, no phenol red	Life Technologies
etoposide	Sigma-Aldrich
5-FU	Sigma-Aldrich
DMSO	Carl Roth
Boric acid	Sigma-Aldrich
Fast SYBR® Green Master Mix	Applied Biosystems
Fast SYBR Green Master Mix Universal RT	Exiqon A/S
Protein A-Sepharose® from Staphylococcus aureus	Sigma-Aldrich
Rotiphorese gel 30 (37,5:1)	Carl Roth
APS	Carl Roth
TEMED	Carl Roth
Nonidet®P40 substitute	Sigma-Aldrich
sodium deoxycholate	Carl Roth
SDS	Carl Roth
β-mercaptoethanol	Sigma-Aldrich
glycerol	Carl Roth
Tris base	Sigma-Aldrich
bromophenol blue	Carl Roth
complete mini protease inhibitor cocktail	Roche

Chemical compound	Supplier
PhosSTOP Phosphatase Inhibitor Cocktail	Roche
Bradford reagent	Bio-Rad
PageRuler™ Prestained Protein Ladder	Fermentas
Immobilon-P PVDF,0.45µm Membrane	Merck Millipore
skim milk powder	Sigma-Aldrich
Methanol	Carl Roth
ECL/HRP substrate	Merck Millipore
DAPI	Carl Roth
EDTA	Sigma-Aldrich
BD Matrigel™ Basement Membrane Matrix	BD Bioscience
Triton X 100	Carl Roth
Protein G Sepharose®, Fast Flow	Sigma-Aldrich
BSA fatty acid free	Sigma-Aldrich
Salmon Sperm DNA	Promega
37% formaldehyde	Merck Millipore
ampicillin	Sigma-Aldrich
water (molecular biological grade)	Life Technologies
LB-Agar (Lennox)	Carl Roth
LB-Medium (Luria/Miller)	Carl Roth
Hi-Di™ Formamide	Applied Biosystems
sea plaque® agarose	Lonza
O'Gene Ruler 1kb DNA ladder	Fermentas
ethidium bromide	Carl Roth
HiPerFect Transfection Reagent	Qiagen
Opti-MEM® Reduced Serum Medium	Life Technologies
ampicillin	Sigma-Aldrich

Chemical compound	Supplier
water (molecular biological grade)	Life Technologies
LB-Agar (Lennox)	Carl Roth
LB-Medium (Luria/Miller)	Carl Roth
Hi-Di™ Formamide	Applied Biosystems
sea plaque® agarose	Lonza
O'Gene Ruler 1kb DNA ladder	Fermentas
ethidium bromide	Carl Roth
Lipofectamine® 2000 Transfection Reagent	Invitrogen
Chloroquine	Sigma-Aldrich
Opti-MEM® Reduced Serum Medium	Life Technologies
puromycin dihydrochloride	Sigma-Aldrich
Doxycycline	Sigma-Aldrich
Crystal violet	Carl Roth
Acetic acid	Carl Roth
Methanol	Carl Roth
Mitomycin C	Sigma-Aldrich

3.2 Cell Lines

Cell lines	Medium
DLD-1	McCoy's 5A medium with 10% FBS and 1% Pen/strep
HT29	
HCT15	
RKO *TP53*$^{-/-}$	
RKO *TP53*$^{+/+}$	
SW480	DMEM medium with 10% FBS and 1% Pen/strep
SW620	

3.3 Buffers and Solutions

3.3.1 Buffers for Western Blot:

Laemmli buffer (2x):

125 mM TrisHCl (pH 6.8)

4% SDS

20% glycerol

0.05% bromophenol blue (in H_2O)

10% β-mercaptoethanol (added right before use)

RIPA buffer:

1% NP40

0.5% sodium deoxycholate;

0.1% SDS

250 mM NaCl

50 mM TrisHCl (pH 8.0)

Tris-glycine-SDS running buffer (10x):

720 g Glycin

150 g Tris base

50 g SDS

pH 8.3-8.7

add ddH_2O up to 5 l

Towbin buffer:

200 mM glycine

20% methanol

25 mM Tris base (pH 8.6)

TBST (10x):

500 ml 1M Tris (pH 8.0)

438.3 g NaCl

50 ml Tween20

add ddH_2O up to 5 l

3.3.2 Buffers for MTT:

SDS-0.01M HCl:

10g SDS

0.1ml HCl (10M)

add ddH_2O up to 100 ml

3.3.3 Buffer for PCR:

‘Vogelstein‘ PCR buffer (10x):

166 mM NH_4SO_4

670 mM Tris (pH 8.8)

67 mM $MgCl_2$

100 mM β-mercaptoethanol

3.3.4 Cell Culture Medium:

90% Mc Coy’s 5A medium or DMEM medium

10% FBS

100 U/ml penicillin

100 µg/ml streptomycin

3.3.5 Cell Freezing Medium:

40% Mc Coy's 5A medium or DMEM medium

50% FBS

10% DMSO

3.3.6 Buffers for Methylation-specific PCR

TBE buffer (10X, 1L):

54 g of Tris base (CAS# 77-86-1)

27.5 g of boric acid (CAS# 10043-35-3，H3BO3)

20 ml of 0.5 M EDTA (CAS# 60-00-4) (pH 8.0)

Adjust pH to 8.3 by HCl.

3.4 Kits

Kit	Supplier
High Pure RNA Isolation Kit	Roche
BCA Protein Assay Kit	Thermo Fisher Scientific
QIAamp DNA Micro Kit	QIAGEN
High Pure RNA Isolation Kit	Roche
Verso cDNA Kit	Thermo Fisher Scientific
QIAquick Gel Extraction Kit	QIAGEN
QIAquick PCR Purification Kit	QIAGEN
Pure Yield™ Plasmid Midiprep System	Promega
QIAprep Spin Miniprep Kit	QIAGEN

Kit	Supplier
BigDye® Terminator v3.1 Cycle Sequencing Kit	Life Technologies
DyeEx® 2.0 Spin Kit	QIAGEN
EZ DNA Methylation Kits	Zymo Research
QuikChange II XL Site-Directed Mutagenesis Kit	Agilent Technologies
DNeasy Blood & Tissue Kit	Qiagen
Dual-Luciferase® Reporter Assay System	Promega

3.5 Enzymes

Enzyme	Use	Supplier
Trypsin-EDTA	cell culture	Invitrogen
DNase I	qPCR	Sigma-Aldrich
restriction endonucleases	vectors generation	New England Biolabs
Platinum® *Taq* DNA polymerase	vectors generation	Invitrogen
Pfu polymerase	vectors generation	Thermo Fisher Scientific
T4 DNA ligase	vectors generation	Thermo Fisher Scientific

3.6 Oligonucleotides

3.6.1 Oligonucleotides used for qPCR

Gene	Sequence (5'-3')
*β-actin*_For	TGACATTAAGGAGAAGCTGTGCTAC
*β-actin*_Rev	GAGTTGAAGGTAGTTTCGTGGATG
*CSF1R*_For	CCTCGCTTCCAAGAATTGCA
*CSF1R*_Rev	CCCAATCTTGGCCACATGA

Gene	Sequence (5'-3')
*CSF1*_For	GCAAGAACTGCAACAACAGC
*CSF1*_Rev	ATCAGGCTTGGTCACCACAT
*pri-miR-34a*_For	CGTCACCTCTTAGGCTTGGA
*pri-miR-34a*_Rev	CATTGGTGTCGTTGTGCT
*CDH1*_For	CCCGGGACAACGTTTATTAC
*CDH1*_Rev	GCTGGCTCAAGTCAAAGTCC
*VIM*_For	TACAGGAAGCTGCTGGAAGG
*VIM*_Rev	ACCAGAGGGAGTGAATCCAG
*SNAIL*_For	GCACATCCGAAGCCACAC
*SNAIL*_Rev	GGAGAAGGTCCGAGCACAC
*ZEB1*_For	TCAAAAGGAAGTCAATGGACAA
*ZEB1*_Rev	GTGCAGGAGGGACCTCTTTA

3.6.2 Oligonucleotides used for MSP and BSP

	Sequence (5'-3')
MSP_M_For	GGTTTTGGGTAGGCGCGTTTC
MSP_M_Rev	TCCTCATCCCCTTCACCGCCG
MSP_U_For	(Inosine)(Inosine)GGTTTTGGGTAGGTGTGTTTT
MSP_U_Rev	AATCCTCATCCCCTTCACCACCA
BSP_For	TAGAGATAATAGGTTTTGATTCGGGATAGA
BSP_Rev	CAAAACTCCCACAAAATCTCCAAATACCCCC

3.6.3 Oligonucleotides used for qChIP

Gene	Sequence (5'-3')
*CSF1R*_For	ACAACTTTCCCACCAGTCCT
*CSF1R*_Rev	GGGGTGAGTAGTTTGGTGGG
*MiR-200c*_For	CAGGAGGACACACCTGTGC
*MiR-200c*_Rev	TCCCCTGGTGGCCTTTAC
*AchR*_For	CCTTCATTGGGATCACCACG
*AchR*_Rev	AGGAGATGAGTACCAGCAGGTTG

3.6.4 Oligonucleotides used for cloning and mutagenesis of the *CSF1R* 3'-UTR

gene	Sequence (5'-3')
*Human CSF1R 3'UTR*_For	CGGAATTCGGAGTTGACGACAGGGAG
*Human CSF1R 3'UTR*_Rev	CGCTGCAGATGTGGACAGAGACATCC
*Human CSF1R 3'UTR mutant*_For	CCTGAGCATGGGCCATCAGTCGGAGT
*Human CSF1R 3'UTR mutant*_Rev	CCCCCAGCCCCTGACTCCGACTGATG
Human CSF1R (L301S) _For	GAGAGTGCCTACTCGAACTTGAGCTCT
Human CSF1R (L301S) _Rev	AGAGCTCAAGTTCGAGTAGGCACTCTC

3.6.5 Oligonucleotides (*pre-miR-34a*, antagomir miR-34a)

product	Sequence (5'-3')	Company
pre-miR-34a	GGCCAGCUGUGAGUGUUUCUUU GGCAGUGUCUUAGCUGGUUGUU GUGAGCAAUAGUAAGGAAGCAA UCAGCAAGUAUACUGCCCUAGA AGUGCUGCACGUUGUGGGGCCC	Thermo Fisher Scientific
antagomir miR-34a	UUGCCAGGCAGUGUAGUUAGCU GAUUGACGAGGCAACAGUCACU AACAACACGGCCAGGUGA	Thermo Fisher Scientific

3.7 Antibodies

3.7.1 Primary Antibodies

epitope	catalog no.	company	use	dilution	source
α-tubulin	# T-9026	Sigma-Aldrich	WB	1:1000	mouse
β-actin	# A2066	Sigma-Aldrich	WB	1:1000	rabbit
p53	# sc-126	Santa Cruz	WB	1:1000	mouse
E-cadherin	# 334000	Invitrogen	WB	1:1000	mouse
CSF1R	# HPA012323	Sigma-Aldrich	WB	1:1000	rabbit
Vimentin	# 2707-1	Epitomics	WB	1:1000	rabbit
SNAIL	# 3879S	Cell Signaling	WB	1:500	rabbit
ZEB1	# sc-25388	Santa Cruz	WB	1:1000	rabbit
STAT3^{pS727}	# 9134	Cell Signaling	WB	1:1000	rabbit
STAT3	# sc-482	Santa Cruz	WB	1:1000	rabbit
VSV	# V4888	Sigma-Aldrich	WB; ChiP	1:1000	rabbit
CSF1R	# sc-692	Santa Cruz	WB	1:500	rabbit

3.7.2 Secondary Antibodies

name	ordering no.	company	use	dilution	source
anti-mouse HRP	# W4021	Promega	WB	1:10.000	goat
anti-rabbit HRP	# A0545	Sigma	WB	1:10.000	goat

3.8 Vectors

Name	Insert	Reference
pRTR	--	(Jackstadt et al., 2013)
pRTR-*p53*-VSV	human *p53*	(Hunten et al., 2015)
pRTR-*miR-34a*	human *miR-34a*	(Kaller et al., 2011)
pRTR-*SNAIL*	human *SNAIL*	(Siemens et al., 2011)
pRTR-*SLUG*	human *SLUG*	(Rokavec, Kaller, Horst, &
pRTR-*CSF1R*	human *CSF1R*	
pRTR-*CSF1R* (L301S)	human *CSF1R* (L301S)	
pGL3-control-MCS	--	(Welch, Chen, & Stallings,
pGL3-*CSF1R* wt	human *CSF1R* 3'UTR	
pGL3-*CSF1R* mut	human *CSF1R* 3'UTR	
pRL	Renilla	(Pillai et al., 2005)

3.9 siRNAs

siRNA	Supplier
negative control	#4611, Ambion
siRNA STAT3	#6880, Ambion
siRNA *CSF1R*	SMART pool, Dharmacon

3.10 Softwares

Application	Software	Supplier
Data analysis	SPSS Statistics 23.0	IBM
Data analysis and figure generation	Graphpad Prism8.0	Graph Pad Software Inc.
Figure composition	Adobe Illustrator	Adobe
WB	Varioskan Flash Spectral Scanning Multimode Reader	Thermo Scientific
	Image Studio™ Lite	LI-COR Biosciences
qPCR	NanoDrop 1000 Spectrophotometer	Thermo Scientific
Sequencing analysis	DNASTAR Lasergene Software	DNASTAR
	BioEdit	BioEdit
qPCR	LightCycler 480	Roche
Wound healing assay	Axiovision	Zeiss
Morphology	Axiovision	Zeiss
IHC	Axiovision	Zeiss
Luciferase reporter assays	SIMPLICITY software package	DLR

Application	Software	Supplier
Modified Boyden-chamber	Axiovision	Zeiss
Xenograft	IVIS Illumina System	Caliper Life Sciences
Ectopic expression	BD Accuri™ C6 Cytometer	BD Biosciences

3.11 Laboratory equipment

Device	Supplier
Cell culture flasks, Multiwall plates and Conical Tubes	Corning Incorporated, USA
Neubauer counting chamber	Carl Roth
Axiovert 25 Inverted Microscope	Carl Zeiss Meditec AG, Germany
AxioPlan 2 Microscope System	Carl Zeiss Meditec AG, Germany
Microcentrifuge	Thermo Fisher Scientific Inc.,USA
Mastercycler™ pro PCR System	Eppendorf GmbH, Germany
NanoDrop® ND-1000 Spectrophotometer	Thermo Fisher Scientific Inc.,USA
Boyden chamber transwell membranes	Corning
Culture-Insert 2 Well	ibidi
Waterbath WNB 45	Memmert GmbH + Co. KG,Germany
ABI 3130 genetic analyzer capillary sequencer	Applied Biosystems
biophotometer plus	eppendorf
BD AccuriTM C6 Flow Cytometer Instrument	BD Accuri
Forma scientific CO_2 water jacketed incubator	Thermo Fisher Scientific
EPS 600 power supply	Pharmacia Biotech

Device	Supplier
Orion II luminometer	Berthold Technologies
IVIS Illumina System	Caliper Life Sciences
Mini-PROTEAN®-electrophoresis system	Bio-Rad
PerfectBlue™ SEDEC ‘Semi-Dry’ blotting system	Peqlab Biotechnologie
HTU SONI130	G. Heinemann Ultraschall- und Labortechnik

4. Methods

4.1 Cell culture and treatments

The CRC cell lines HCT-15, RKO, HT29, and DLD-1 were maintained in McCoy's 5A Medium (Invitrogen) containing 10% fetal bovine serum (FBS, Invitrogen), SW480 and SW620 cell lines were maintained in Dulbecco`s Modified Eagles Medium (DMEM, Invitrogen) containing 10% FBS. *p53*-/- and *p53*+/+ RKO cell lines were kindly provided by Bert Vogelstein (Johns Hopkins University, Baltimore). All cells were cultivated in the presence of 100 units/ml penicillin and 0.1 mg/ml streptomycin at 20% O_2, 5% CO_2 and 37°C. Doxycycline (Dox) (Sigma-Aldrich) was dissolved in water (100 µg/ml stock solution) and always used at a final concentration of 100 ng/ml. Recombinant Human CSF1 (BioLegend) was dissolved in water and used at a final concentration of 50 ng/ml with daily refreshment. pre-miRNAs mimics (PM11030, Ambion), miRNA antagomirs, and respective negative controls (Ambion-Applied Biosystems) were transfected using HiPerfect (Qiagen). siRNAs (Ambion silencer siRNA: negative control [ID#4611], siRNA STAT3 [ID#6880], and Dharmacon: siRNA *CSF1R* [SMART pool]) were transfected at a final concentration of 20 nM using Lipofectamine 2000 (Invitrogen).

4.2 Modified Boyden-chamber assay

Migration and invasion analyses were performed as described previously (Rokavec, Oner, et al., 2014). In brief, cells were serum-starved for 24 hours. For the migration assay, $5x10^4$ cells were seeded in the upper chamber (8.0 µm pore size membrane; Corning) in a serum-free medium. For invasion assays, chamber membranes were first coated with Matrigel (BD Bioscience) at a dilution of 3.3 ng/ml in medium without serum.

Then $5x10^5$ cells were seeded on the Matrigel in the upper chamber in serum-free medium. As chemo-attractant, 10% FCS was placed in the lower chamber. After cells were cultured for 36 hours, non-motile cells at the top of the filter were removed and the cells in the bottom chamber were fixed with methanol, stained with crystal violet. Relative invasion/migration was normalized to the corresponding control.

4.3 Western blot analysis

SDS-PAGE and Western blot analyses were performed as described previously (Li, Rokavec, et al., 2017). Cells were lysed in RIPA lysis buffer (50 mM Tris/HCl, pH 8.0, 250 mM NaCl, 1% NP40, 0.5% (w/v) sodium deoxycholate, 0.1% sodium dodecyl sulfate, complete mini protease inhibitors (Roche) and PhosSTOP Phosphatase Inhibitor Cocktail Tablets (Roche)). Lysates were sonicated and centrifuged at 16.060 g for 20 min at 4°C. 30-80 µg protein were separated on 7.5%, 10% or 12% SDS-acrylamide gels. Gel electrophoresis and transfer to Immobilon PVDF membranes (Millipore) were carried out using standard protocols (Bio-Rad laboratories). Primary antibodies were used in combination with HRP-coupled secondary antibodies. ECL (Millipore) signals were recorded with a 440CF imaging system (Kodak). Antibodies used here are listed in chapter 3.7.

4.4 Chromatin immunoprecipitation (ChIP)

DLD1/pRTR-SNAIL-VSV cells were cultured as described above. Before cross-linking, cells were treated with Dox [100 ng/ml] for 24 hours to induce ectopic expression of VSV-tagged proteins. Cross-linking was conducted with formaldehyde (Merck) at 1%

final concentration and terminated after 5 minutes by addition of glycine at a final concentration of 0.125 M. Cells were harvested in SDS buffer (50 mM Tris pH 8.1, 0.5% SDS, 100 mM NaCl, 5 mM EDTA), pelleted and resuspended in IP buffer (2 parts of SDS buffer and 1 part Triton dilution buffer (100 mM Tris-HCl pH 8.6, 100 mM NaCl, 5 mM EDTA, pH 8.0, 0.2% NaN_3, 5.0% Triton X-100)). Chromatin was sheered by sonication (HTU SONI 130, G. Heinemann) to generate DNA fragments with an average size of 500 bp. Preclearing and incubation with polyclonal VSV antibody (V4888, Sigma) for 16 hours was performed as previously described (Hahn et al., 2013; Menssen et al., 2007). Washing and reversal of cross-linking was performed as described (Amati, Frank, Donjerkovic, & Taubert, 2001). Immunoprecipitated DNA was analyzed by qRT-PCR and the enrichment was expressed as a percentage of the input for each condition. The sequences of oligonucleotides used as qChIP primers are listed in chapter 3.6.3.

4.5 Generation of cell pools stably expressing conditional alleles

Stably transfected cells were generated by transfection of the episomal expression vector pRTR using Fugene6 (Roche) and selected with incrementally increasing concentrations of Puromycin (0.5-6.0 µg/ml) for 10 days (Siemens et al., 2011). The frequency of GFP-positive cells was determined 48 hours after the addition of Dox at a final concentration of 100 ng/ml by flow cytometry.

4.6 Dual 3'-UTR luciferase reporter assays

The full-length 3'-UTRs of the human *CSF1R* mRNA were PCR-amplified from cDNA of human diploid fibroblasts. The PCR product was cloned into the shuttle vector pGEM-T-Easy (Promega), and then transferred into the pGL3-control-MCS vector (Welch et al., 2007) and verified by sequencing. For mutagenesis of the miR-34a seed-matching sequences, the QuikChange II XL Site-Directed Mutagenesis Kit (Stratagene) was used according to the manufacturer's instructions and verified by sequencing. H1299 cells were seeded in 12-well plate at 3×10^4 cells/well for 24 hours and transfected for 72 hours with 100 ng of the indicated firefly luciferase reporter plasmid, 20 ng of Renilla reporter plasmid as a normalization control and 25 nM of *miR-34a* pre-miRNA oligonucleotide (Ambion, PM11030), or a negative control oligonucleotide (Ambion, neg. control #1) with HiPerFect Transfection Reagent (Qiagen) for 48 hours. The analysis was performed with the Dual-Luciferase Reporter assay (Promega) according to the manufacturer's instructions. Fluorescence intensities were measured with an Orion II luminometer (Berthold) in 96-well format and analyzed with the SIMPLICITY software package (DLR). The sequences of oligonucleotides used for cloning and mutagenesis of human 3'-UTR are listed in chapter 3.6.4.

4.7 Bioinformatic analysis of online databases

The Cancer Genome Atlas (TCGA) gene expression data and follow-up information of colon adenocarcinomas (COAD) were downloaded from the NCI's Genomic Data Commons (GDC) (https://gdc.cancer.gov/) (Network, 2012). Normalized RSEM counts were used to determine the expression of relevant mRNAs. Pearson for analysis of expression correlation was performed with the Prism5 program (Graph Pad Software

Inc.). Association of patient samples with the different CMS categories was obtained from the Cancer Subtyping Consortium (CRCSC) at www.synapse.org. The CMS subtypes were described in (Guinney et al., 2015). CMS-specific signature gene sets were obtained from (Sveen et al., 2018). PDX RNA expression data of human CRC specimens (GSE76402), the classification of CRC intrinsic subtypes (CRIS) and the respective signature genes for each CRIS subtype were obtained from (Isella et al., 2017). Single-cell RNA expression data of normal colonic and CRC cells (GSE81861) were obtained from (Li, Courtois, et al., 2017) and analysed with the RCA *R* package as described. Expression and clinical data of GSE37892, GSE39582, and GSE14333 datasets were downloaded from NCBI GEO (www.ncbi.nlm.nih.gov/geo). Gene Set Enrichment Analysis (GSEA) was performed on pre-ranked gene lists based on expression correlation coefficients (Pearson) with *CSF1R* using the GSEA software obtained from http://software.broadinstitute.org/gsea/index.jsp (Subramanian et al., 2005). Hallmark gene sets were obtained from the Molecular Signatures Database (MSigDB) (Liberzon et al., 2015). Heatmaps were generated with GENE-E (Broad Institute).

4.8 Clinical samples and immunohistochemistry

CSF1R expression was evaluated using formalin-fixed, paraffin-embedded (FFPE) colon cancer samples of 90 patients who underwent surgical tumor resection at the Ludwig-Maximilians University Munich. Tissue microarrays (TMAs) were generated with 6 representative 1 mm cores of each case, for which the methylation status of *miR-34a* had been determined previously (Siemens, Neumann, et al., 2013). The TMA sections were deparaffinized and stained with the human CSF1R antibody (ab183316,

Abcam) on a Benchmark XT Autostainer with UltraView Universal DAB and alkaline phosphatase detection kits (Ventana Medical Systems). The stainings were evaluated according to the score shown in Figure 5.40A.

4.9 Colony formation assay

For low-density, colony formation assays, 500 cells were seeded into a 6-well plate and cultivated for 24 hours in the presence or absence of Dox or CSF1 for 24 hours, and subsequently treated with or without 5-FU for 72 hours. Cells were washed once with HBSS, a new medium was added and cells were allowed to recover for two days before fixation and crystal violet staining.

4.10 Wound healing assay

Mitomycin C [10 ng/ml] was added two hours before generating a scratch using a Culture-Insert (IBIDI, 80241). Cells were allowed to close the wound for the indicated periods and images were captured on an Axiovert Observer Z.1 microscope connected to an AxioCam MRm camera using the Axiovision software (Zeiss) at the respective time-points.

4.11 Detection of apoptosis

Apoptosis rates were determined by flow cytometry after staining with Annexin V-FITC (apoptotic cell marker) and PI (necrotic cell marker) according to the Annexin V-FITC/PI staining kit (BD Pharmingen, 556570). In brief, treated and control cells were

harvested by the addition of trypsin (without EDTA) and washed twice with HBSS. Then cells were resuspended in 1 x binding-buffer (0.01 M HEPES/NaOH (pH 7.4), 0.14 M NaCl, 2.5 mM $CaCl_2$) at a concentration of 1 x 10^6 cells/ml. 100 µl of the solution (1 x 10^5 cells) was incubated with 5 µl of FITC Annexin V and 5 µl propidium iodide. Cells were gently agitated and incubated for 15 minutes at room temperature in the dark. Then 400 µl of the 1x binding-buffer was added to each tube and the samples were analyzed within 1 hour by flow cytometry (CFlow6, Accuri).

4.12 MTT assay

Cell viability was measured with a modified MTT assay (Septisetyani, Ningrum, Romadhani, Wisnuwardhani, & Santoso, 2014). In brief, CRC cells were seeded in 96-well plates and treated with different doses of 5-FU for 48 hours, MTT was added at a concentration of 0.5 µg/µL four hours before addition of formazan solvents (10% SDS in 0.01 M HCL). Following overnight incubation in the dark, plates were agitated and the absorbance was measured at 570 nm.

4.13 Establishment of a 5-FU-resistant cell pool

5-FU-resistant cell pools were established by exposure to stepwise increasing concentrations of 5-FU. Initially, DLD1 and HT29 cells were cultured in medium containing 0.1 µmol/l 5-FU. The drug concentration was then increased in steps of 1.25x increases from 0.1 µmol/l up to 30 µmol/l. Cells were cultured for at least one week at each step, with medium exchange every three days. The 5-FU-resistant cell

pool was designated DLD1_5FU and HT29_5FU, respectively. The tolerance towards 5-FU was determined with an MTT assay.

4.14 RNA isolation and qPCR analysis

Total RNA was isolated with the High Pure RNA Isolation Kit (Roche) or RNAeasy Kit (Qiagen) according to the manufacturer´s protocol. cDNA was generated from 1 µg of total RNA per sample using the Verso cDNA synthesis kit (Thermo scientific). Quantitative real-time PCR (qPCR) was performed with the Fast SYBR Green Master Mix (Applied Biosystems) by using the LightCycler 480 (Roche). Expression was normalized using the detection of GAPDH or β-actin using the ΔΔCt method (Livak & Schmittgen, 2001). Results are represented as fold induction of the treated/transfected condition compared with the control condition. Experiments were performed in triplicates. The sequences of oligonucleotides used as qPCR primers are listed in chapter 3.6.1.

4.15 Methylation-specific PCR

Genomic DNA was isolated from cell lines using the DNeasy Blood & Tissue Kits (Qiagen). 400 ng of gDNA was treated with bisulfite using the EZ DNA methylation kit (Zymo Research, D5001 & D5002). The modified DNA was eluted with a final volume of 10 µl elution buffer. 3 µl were amplified by PCR. The MSP primers used for detection of CpG-methylation of the *miR-34a* promoter are depicted in chapter 3.6.2 and were previously established (Lodygin et al., 2008). The PCR protocol entailed 5 min at 95°C; two cycles of 95°C for 20 seconds, 68°C for 30 seconds, and 72°C for 30 seconds,

followed by two cycles with 66°C annealing temperature, then 34 cycles with 65°C annealing temperature, and a final elongation step at 72°C for 10 minutes. For the methylated allele a 122-bp fragment and for the unmethylated allele a 126-bp fragment were obtained. The PCR products were separated by electrophoresis on 8% polyacrylamide gels and then visualized by ethidium bromide staining.

4.16 Bisulfite sequencing

5 µl of bisulfite-treated genomic DNA was used as a template to amplify fragments of a 776 bp region upstream of the *miR-34a* promoter encompassing the transcription start site and p53 binding site with a high CpG content (Lodygin et al., 2008; Vogt et al., 2011). The bisulfite sequencing PCR (BSP) primers used here are depicted in Table 2, with PCR settings of 95°C for 5 minutes, followed by 38 cycles of 95°C for 20 seconds, 65°C for 30 seconds, and 72°C for 60 seconds, with a final elongation step at 72°C for 10 minutes. Amplification products were purified using a QIAquick Gel Extraction Kit, and then subcloned into the shuttle vector pGEM-T-Easy (Promega). For each cell line at least 9 individual clones were sequenced on both strands using SP6 and T7 sequencing primers. The sequencing reactions were analysed on a capillary sequencer (ABI 3130, Applied Biosystems). Clones with a cytosine conversion rate of < 90% were excluded. Methylation data from bisulfite sequencing were trimmed, aligned and displayed as lollipop graphs using QUMA.

4.17 Metastasis formation in NOD/SCID mice

Immune-compromised NOD/SCID mice were obtained from Jackson Laboratories. DLD-1 cells stably expressing Luc2 were produced as described previously (Shi et al., 2014). DLD1-Luc/pRTR-CSF1R were generated by stable transfection of pRTR plasmids and maintained in medium with puromycin. 1 x 10^6 cells were resuspended in 0.2 ml HBSS and injected into the lateral tail vein of a 6- to 8-week-old age-matched male NOD/SCID mouse using a 25-gauge needle. For monitoring of the injected cells, anesthetized mice were injected i.p. with D-luciferin (150 mg/kg) and imaged with the IVIS Illumina System (Caliper Life Sciences) 10 minutes after injection. The acquisition time was set to 2 min and imaging was performed once a week. After 8 weeks, mice were sacrificed and the whole lungs were resected and subjected to H&E staining. All studies involving mice were performed with approval by the local Animal Experimentation Committee (Regierung of Oberbayern). All experiments were conducted following relevant guidelines and regulations.

4.18 Statistics

Calculations of significant differences between two groups of samples were analyzed by a Student's t-test (unpaired, two tailed). For the comparison of multiple groups, a one-way analysis of variance followed by a Tukey multiple comparisons post-hoc test was performed. Log-rank test was used for the statistical analysis of the Kaplan-Meier curves. Cox proportional hazards models were applied for multiple regression analyses of survival data. The Association of CSF1R expression with clinical parameters was analyzed using chi-square tests. For mRNA expression correlation analyses, Pearson

´ s correlation was applied. P-values ≤ 0.05 were considered as significant. Asterisks generally indicate: *$P < 0.05$, **$P < 0.01$, ***$P < 0.001$ and ****$P < 0.0001$. Statistics were calculated with Prism5 (Graph Pad Software Inc.) and SPSS (IBM).

4.19 Study approval

All experimentations involving mice were approved by the Government of Upper Bavaria, Germany (AZ-ROB-55.2-2532.Vet_02-18-57). Since the human tumor biopsies analyzed in Figure 5.40 and Figure 5.41 underwent dual anonymization a specific approval was not requested by the ethics committee of the Medical Faculty, Ludwig-Maximilians-University Munich.

5. Results

5.1 Association of *CSF1R, CSF1* and *IL34* expression with clinical parameters in CRCs

In order to determine the potential clinical relevance of CSF1R and its ligands in CRC, we analyzed their expression in 440 primary colorectal cancer (CRC) samples represented within the Cancer Genome Atlas (TCGA) database (Cancer Genome Atlas, 2012). Thereby, we found that increased expression of *CSF1R*, as well as *CSF1* and *IL-34* mRNAs, in primary CRCs was significantly associated with decreased survival of patients (Figure 5.1).

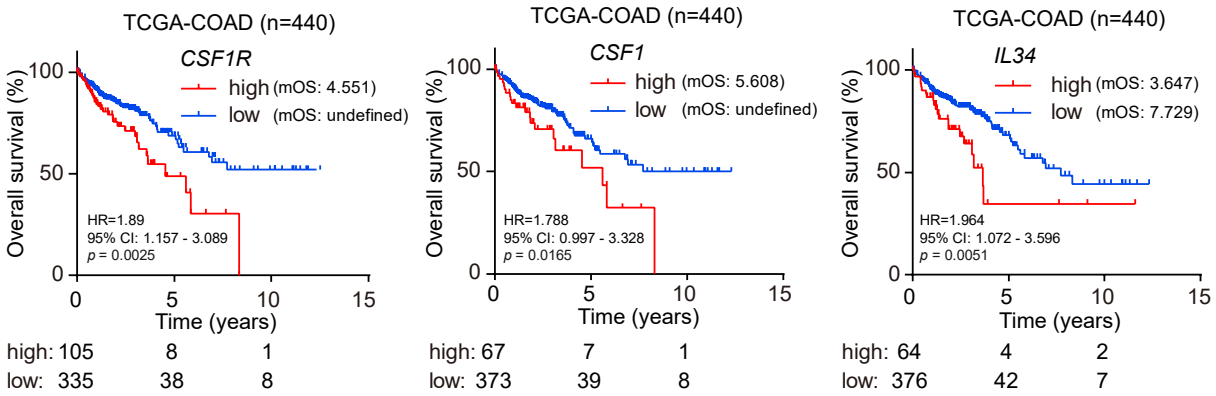

Figure 5.1

Kaplan-Meier analyses of survival with data from the TCGA database using log-rank tests. Below the graphs the numbers of patients with high or low expression of the indicated mRNA at the respective time point is provided. COAD: colorectal adenomas. mOS: median overall survival. HR: hazard ratio, CI: confidence interval.

In another cohort of 566 CRC patient samples (Marisa et al., 2013), elevated *CSF1R* and *CSF1*, but not *IL34*, mRNA expression was associated with poor overall survival (Figure 5.2 A). Moreover, elevated *CSF1R, CSF1, and IL-34* mRNA expression was also associated with decreased relapse-free survival in an

independent cohort comprising 130 patients (Laibe et al., 2012) (Figure 5.2 B). Therefore, we could confirm the findings obtained within the TCGA-COAD cohort in two independent CRC cohorts.

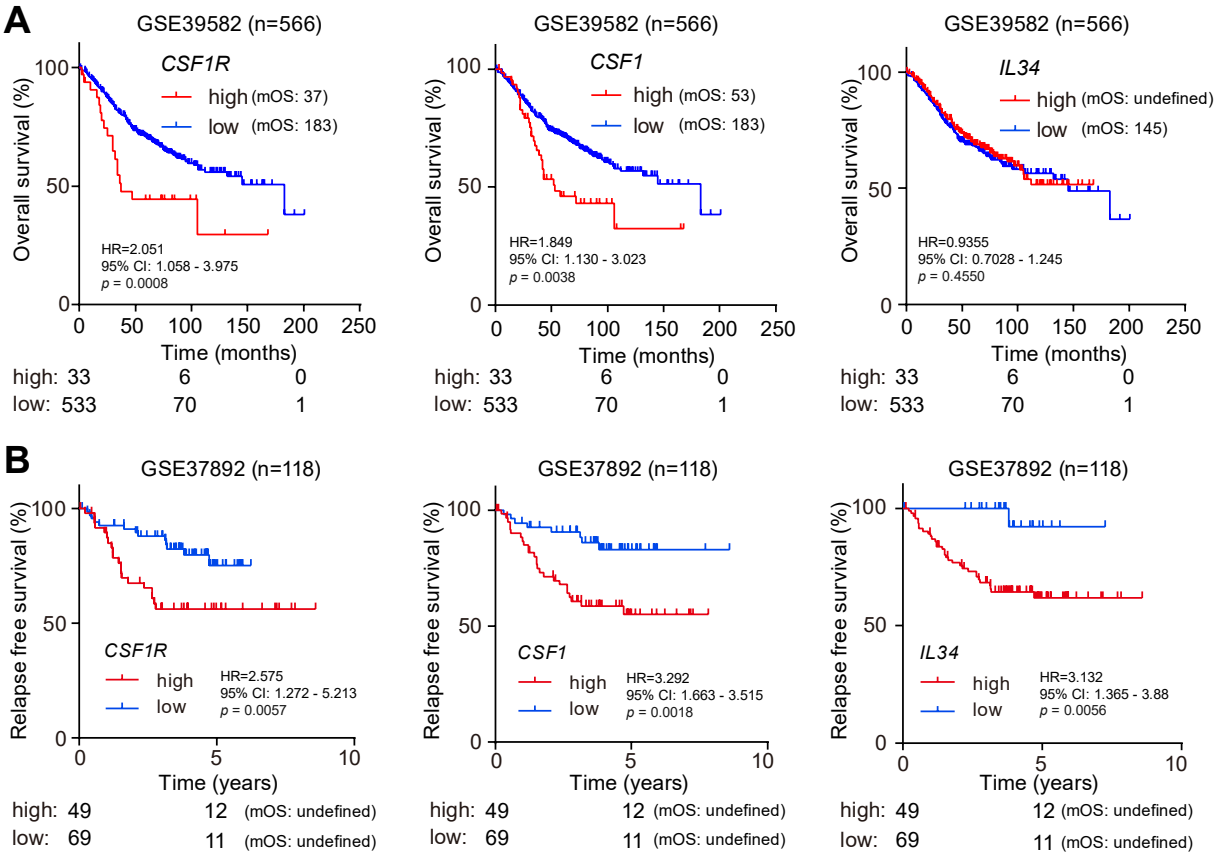

Figure 5.2

A, B, Kaplan-Meier analyses of survival with data from the (A) GSE39582 and the (B) GSE37892 cohorts using log-rank tests. Below the graphs the numbers of patients with high or low expression of the indicated mRNA at the respective time point is provided. COAD: colorectal adenomas. mOS: median overall survival. HR: hazard ratio, CI: confidence interval.

The consensus molecular subtypes (CMS) classification is one of the most robust classification system for CRCs and is based on comprehensive gene expression profiles (Guinney et al., 2015). CRCs belonging to the consensus

molecular subtype 4 (CMS4), which displays a mesenchymal signature and the worst prognosis among the 4 different CMSs (Guinney et al., 2015), showed the highest expression of *CSF1R*, *CSF1*, and *IL-34* (Figure 5.3 A). Next, we stratified CMS4 tumors into *two* subgroups with either elevated or low expression of *CSF1R*, *CSF1* and *IL-34* mRNAs (Figure 5.3 B): Patients with CMS4 CRCs that displayed either high *CSF1R*, *CSF1* or IL34 expression had a significantly shorter overall survival than patients with CRCs classified as CMS1-3 or CMS4 with low *CSF1R* or *CSF1* or *IL34* expression.

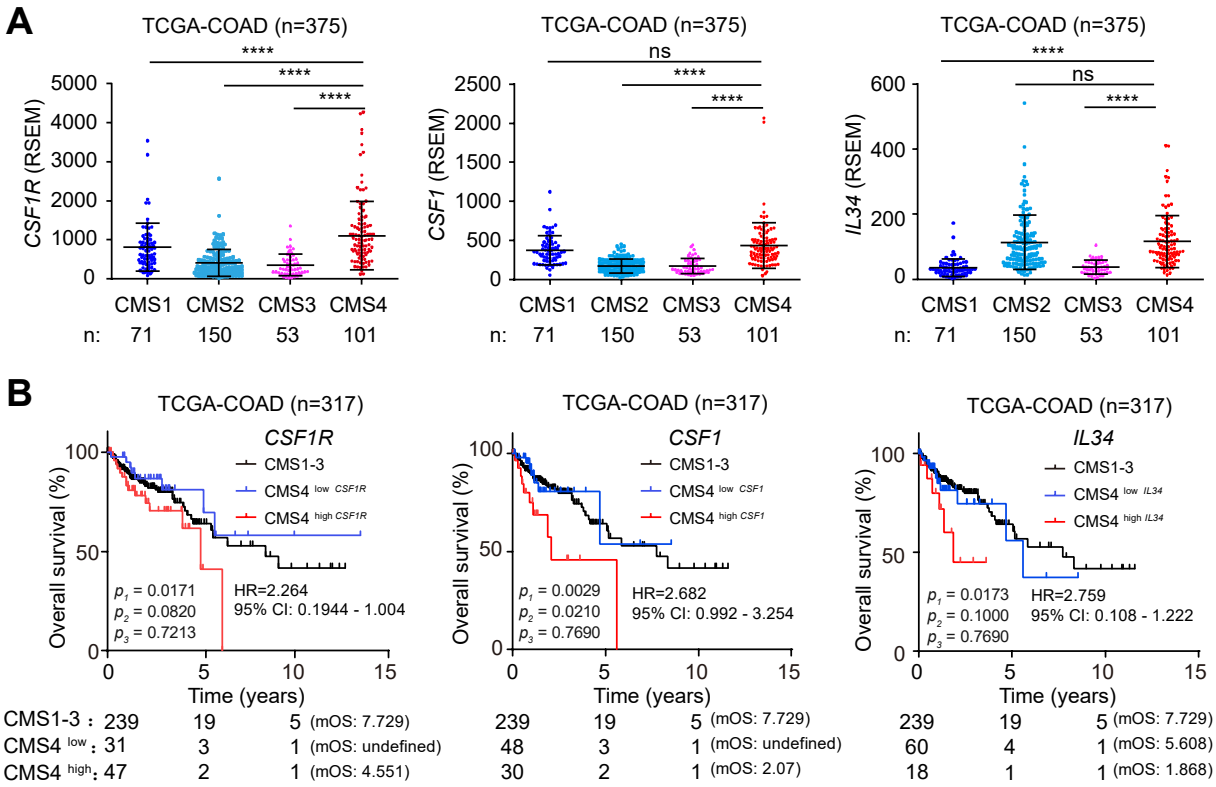

Figure 5.3

A, *CSF1R, CSF1* and *IL34* mRNA expression in CRCs belonging to the indicated consensus molecular subtypes (CMS). RSEM: RNA-Seq by Expectation Maximization. **B**, Kaplan-Meier analysis of overall survival of patients with primary CRCs classified as CMS1-3 or CMS4 with either high *CSF1R/CSF1/IL34* or low *CSF1R/CSF1/IL34* expression levels. *P1*: CMS^{high} vs CMS^{low}; *P2*: CMS^{high} vs CMS1-3; *P3*: CMS^{low} vs

CMS1-3. The number of patients in each group was listed below the graph. mOS: median overall survival.
(*) $P < 0.05$, (**) $P < 0.01$, (***) $P < 0.001$ and (****) $P < 0.0001$.

Furthermore, also in the two other cohorts, expression levels of *CSF1R* and *CSF1* were elevated in CMS4 tumors (Figure 5.4 A and B).

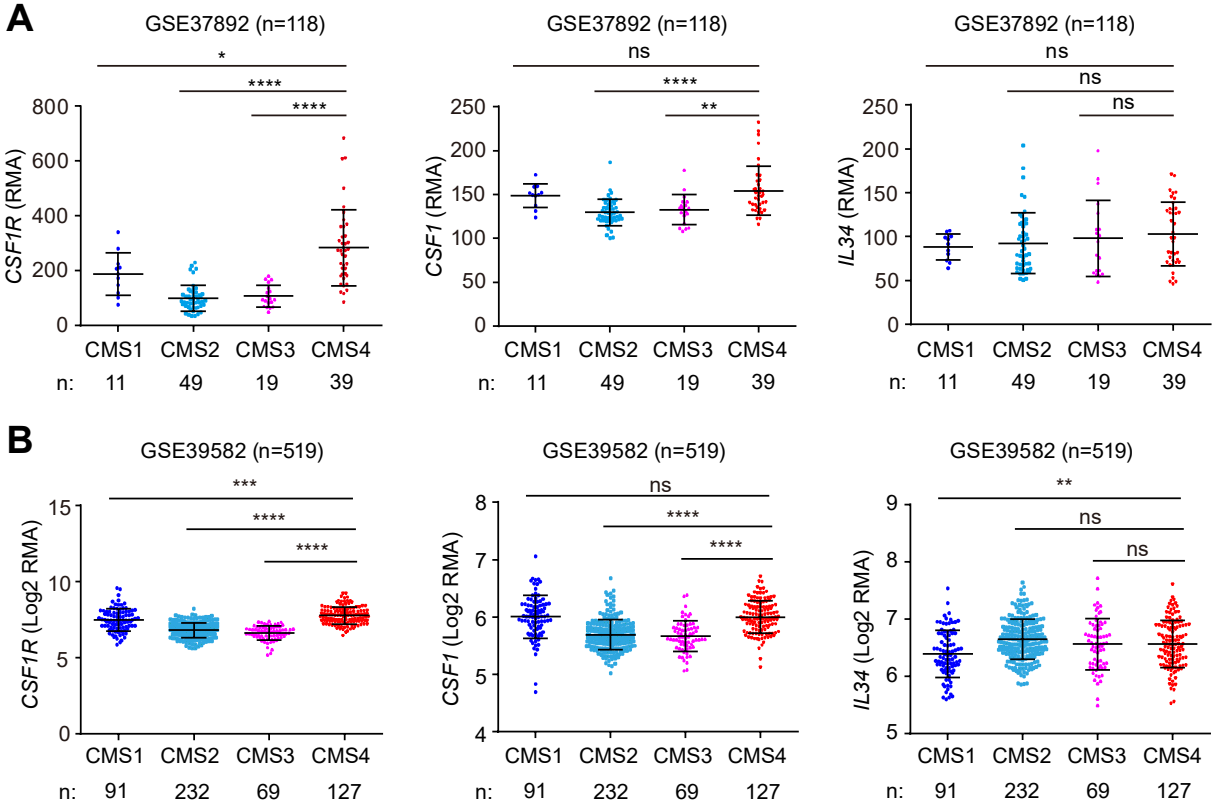

Figure 5.4

A, B, *CSF1R, CSF1* and *IL34* mRNA expression in CRC patient samples from the GSE37892 (A) and GSE39582 (B) datasets classified according to the indicated consensus molecular subtypes (CMS). (*) $P < 0.05$, (**) $P < 0.01$, (***) $P < 0.001$ and (****) $P < 0.0001$.

However, mRNAs displaying elevated expression in CMS4 type tumors may originate from stromal cells and therefore confound the gene expression profiles of

CRCs (Calon et al., 2015; Isella et al., 2017; Isella et al., 2015). To overcome this caveat, patient-derived xenografts (PDX) have been used to generate mRNA expression signatures by microarray analyses, where the contribution of (murine) stromal mRNAs to whole tumor mRNA expression patterns was selectively eliminated by the use of human-specific probe sets (Isella et al., 2017). Thereby, five different colorectal cancer intrinsic subtypes (CRIS) were defined. Apart from classifying PDX-derived tumors, these were used to re-classify previously established publicly available CRC patient cohorts into CRIS subtypes, such as the TCGA-COAD cohort (Isella et al., 2017). Notably, *CSF1R* mRNA expression within the TCGA-COAD cohort was elevated in the CRIS-B subtype (Figure 5.5 A), which is characterized by TGF-β pathway activity, epithelial-mesenchymal transition and poor prognosis (Isella et al., 2017). Moreover, expression of the *CSF1* ligand, but not of *IL34*, was elevated in the CRIS-B subtype of tumors within the TCGA-COAD cohort. We validated these findings in the additional cohort comprising 566 cases. Again, expression of both *CSF1R* and its ligand *CSF1*, but not *IL34*, was elevated in CRIS-B tumors (Figure 5.5 B).

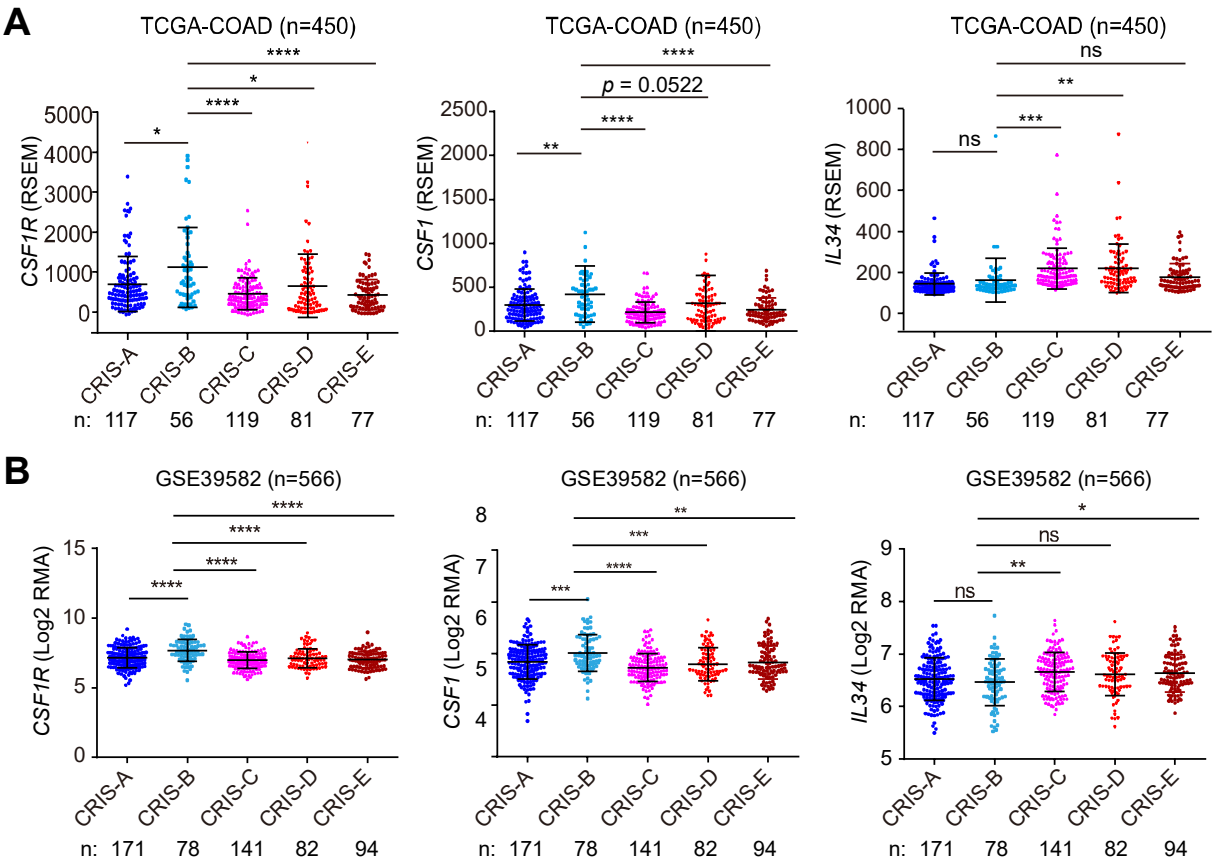

Figure 5.5

A, B, The indicated mRNA expression in CRC patient samples from the TCGA-COAD (A) and GSE39582 (B) cohorts classified according to the indicated CRC intrinsic subtypes (CRIS).

(*) $P < 0.05$, (**) $P < 0.01$, (***) $P < 0.001$ and (****) $P < 0.0001$.

To further validate our findings, we also analyzed *CSF1R* expression in CRIS subtypes of PDX samples. *CSF1R* expression was elevated in the CRIS-B subtype when compared to the other subtypes, albeit without statistical significance in case of the CRIS-A and CRIS-D subtypes (Figure 5.6 A). Gene Set Enrichment Analyses (GSEA) showed a strong positive correlation of *CSF1R* mRNA expression with CRIS-B and CMS4 gene signatures, whereas either negative or non-significant correlations of *CSF1R* mRNA with signatures from all other CRIS or CMS subclasses in PDX

samples were observed (Figure 5.6 B and C), indicating that tumor intrinsic *CSF1R* expression is associated with a mesenchymal tumor phenotype. In addition, elevated *CSF1R* expression was associated with CRIS-B/CMS4 associated signatures, such as EMT and IL6/JAK/STAT3 signalling. Moreover, mRNA expression data from whole tumors showed strong positive correlations of *CSF1R* with both CRIS-A and -B and CMS1 and -4, as well as EMT and IL6/JAK/STAT3 signalling associated signatures in the majority of analyzed patient cohorts.

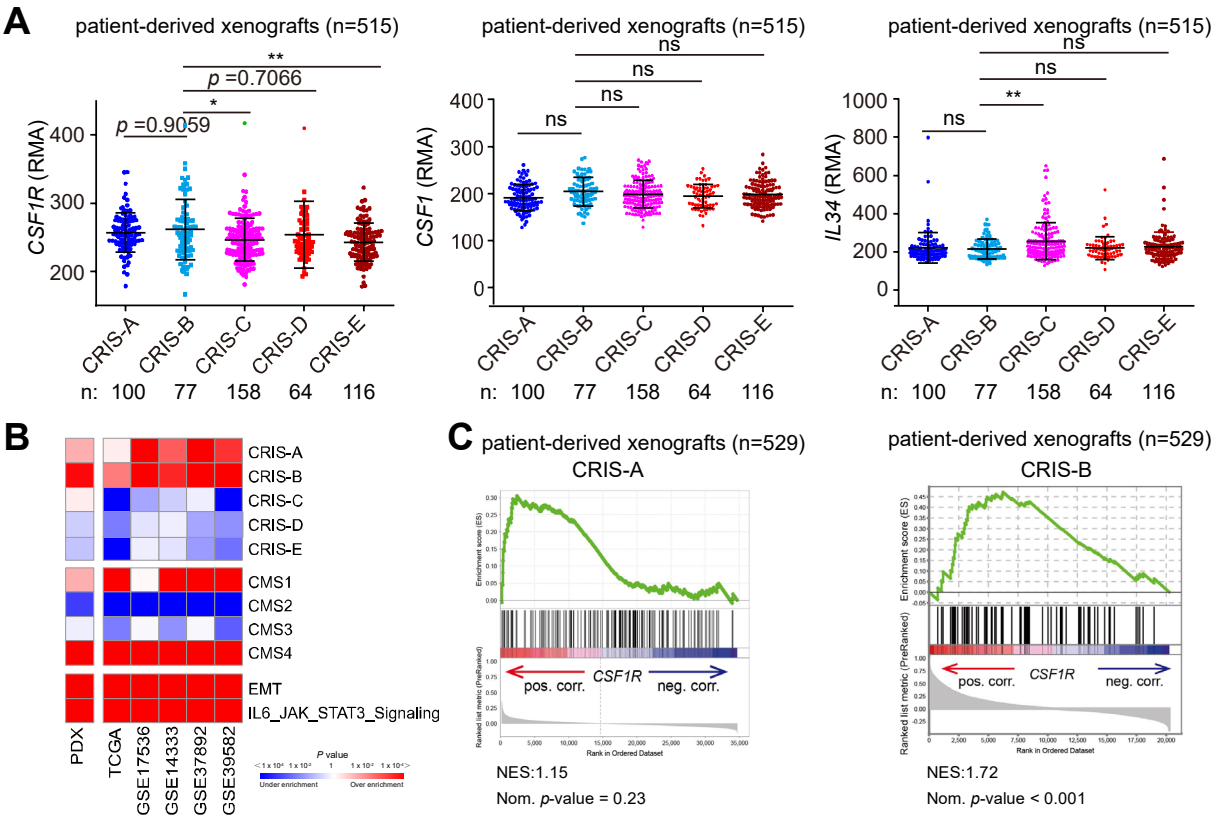

Figure 5.6

A, The indicated mRNA expression in CRC patient samples from the PDX cohorts classified according to the indicated CRC intrinsic subtypes (CRIS).

B, GSEA results for CSF1R expression from PDX, TCGA, and indicated GEO data sets. Genes were preranked by expression correlation coefficient (Pearson r) with *CSF1R* for each data set.

C, *CSF1* and *IL34* mRNA expression in CRC patient samples from the GSE76402 cohort classified according to the indicated CRC intrinsic subtypes (CRIS).

C: Figures and analysis were made by Dr. Markus Kaller.

(*) $P < 0.05$, (**) $P < 0.01$, (***) $P < 0.001$ and (****) $P < 0.0001$.

Furthermore, analysis of published single cell RNA sequencing results (Li, Courtois, et al., 2017) obtained from primary colorectal tumors and matched normal mucosa revealed that *CSF1R* is specifically expressed in colonic epithelial and tumor cells with stem/TA-like features (Figure 5.7 A and B).

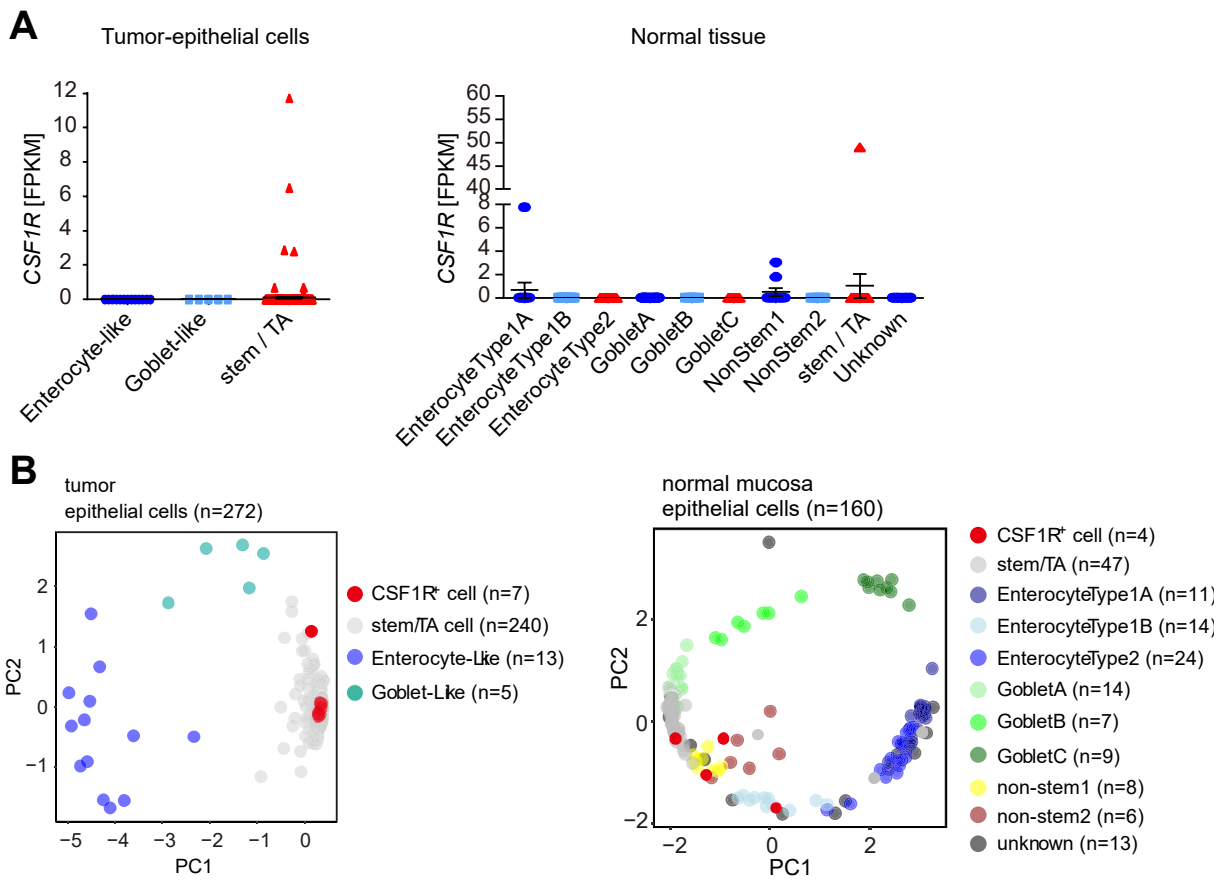

Figure 5.7

A, *CSF1R* mRNA expression derived from single-cell sequencing data of normal colonic (n=160) and CRC tissue (n=271) (GSE81861).

B, PCA plot based on the reference component analysis (RCA) scRNA–seq clustering algorithm showing the clustering of different cell types in tumor epithelial cells and cells from normal mucosa. *CSF1R*-expressing cells are highlighted as indicated.

A, B: Figures and analysis were made by Dr. Markus Kaller.

(*) $P < 0.05$, (**) $P < 0.01$, (***) $P < 0.001$ and (****) $P < 0.0001$.

Next we also evaluated association of CSF1R expression with other clinical/pathological variables in both the TCGA-COAD and the GSE39582 cohort in order to exclude potentially confounding factors that might affect patient survival. CSF1R expression did not display a significant association with age, gender and tumor stage (UICC). However, elevated CSF1R expression in CRCs was associated with mismatch-repair-deficient/MSI (microsatellite-instability), as well as with the CMS4 or CRIS-B molecular subtypes of CRCs (Table 1). A Cox multiple regression analysis demonstrated prognostic power of high CSF1R expression independent from age, gender, MSI status and tumor stage (Table 2). The GSE37892 cohort was not included here, since the necessary data was incomplete.

Table 1.

Clinical data and *CSF1R* mRNA expression in colon cancer cases from two independent patient cohorts

	TCGA-COAD				GSE39582			
Characteristics	**Total**	***CSF1R***		***P***	**Total**	***CSF1R***		***P***
		Low	**High**			**Low**	**High**	
All patients	440 (100.0)	335 (76.1)	105 (23.9)		566 (100.0)	532 (76.1)	34 (23.9)	
Age (years)								
< median	206 (46.9)	164 (79.6)	42 (20.4)	0.109	283 (51.2)	272 (96.1)	11 (3.9)	**0.033**
≥ median	234 (53.1)	171 (73.1)	63 (26.9)		282 (48.8)	259 (91.8)	23 (8.2)	
Gender								
Male	235 (53.4)	182 (77.4)	53 (22.6)	0.490	310 (54.8)	290 (93.5)	20 (6.5)	0.624
Female	205 (46.6)	153 (74.6)	52 (25.4)		256 (45.2)	242 (94.5)	14 (5.5)	
UICC stage								
I	73 (17.0)	58 (79.5)	15 (20.5)	0.378	33 (5.9)	33 (100)	0 (0)	0.497
II	169 (39.4)	122 (72.2)	47 (27.8)		264 (47.0)	248 (93.9)	16 (6.1)	
III	126 (29.4)	97 (77.0)	29 (23.0)		205 (36.5)	191 (93.2)	14 (6.8)	
IV	61 (14.2)	50 (82.0)	11 (18.0)		60 (10.7)	56 (93.3)	4 (6.7)	
MSI status								
MSS/MSI-low	323 (81.2)	253 (78.3)	70 (21.7)	**0.005**	444 (85.5)	424 (95.5)	20 (4.5)	**0.029**
MSI-high	75 (18.8)	47 (62.7)	28 (37.3)		75 (14.5)	67 (89.3)	8 (10.7)	
CMS subtype								
CMS1-3	253 (73.3)	219 (86.6)	34 (13.4)	**< 0.0001**	360 (73.9)	351 (97.5)	9 (2.5)	**< 0.0001**
CMS4	92 (26.7)	41 (44.6)	51 (55.4)		127 (26.1)	107 (84.3)	20 (15.7)	
CRIS subtype								
CRIS-A/C-E	283 (87.9)	219 (77.4)	64 (22.6)	**0.002**	488 (86.2)	468 (95.9)	20 (4.1)	**< 0.0001**
CRIS-B	39 (12.1)	21 (53.8)	18 (46.2)		78 (13.8)	64 (82.1)	14 (17.9)	

Percentage values are given in parentheses. Association of CSF1R expression with clinical parameters was analyzed using chi-square tests. CSF1R low / high status was defined according to Figure 5.1 and Figure 5.2 A, respectively. Statistics were calculated with SPSS (IBM). Table and analysis were made by Dr. Markus Kaller.

Table 2.

Multiple regression analysis of overall survival in colon cancer cases from two independent cohorts

	TCGA-COAD			GSE395823		
Variables	**overall survival**			**overall survival**		
	HR	**(95% CI)**	***P***	**HR**	**(95% CI)**	***P***
Age ≥ median	2.02	(1.26-3.24)	0.003	2.11	(1.55-2.88)	0.001
Male vs. Female	1.08	(0.69-1.68)	0.745	0.71	(0.52-0.96)	0.025
UICC stage	2.27	(1.74-2.96)	< 0.0001	2.14	(1.67-2.58)	< 0.0001
MSI status	1.01	(0.55-1.82)	0.985	0.82	(0.49-1.32)	0.392
CSF1R high	1.80	(1.10-2.93)	**0.018**	1.96	(1.18-3.26)	**0.009**

Cox proportional hazards models were used for multiple regression analyses. Statistics were calculated with SPSS (IBM). HR: Hazard Ratio; CI: Confidence interval. Table and analysis were made by Dr. Markus Kaller.

5.2 *CSF1R* represents a direct target of miR-34a

In order to determine whether the up-regulation of CSF1R expression in CRCs may be due to the down-regulation of microRNAs that negatively control the *CSF1R* mRNA, we examined the 3'-UTR of *CSF1R* for the presence of potential seed-matching sites. Only three different microRNAs were identified by all five algorithms used here (Figure 5.8 A): miR-34a and miR-449a share the same, whereas miR-765 has a different seed-sequence. Since analysis of TCGA revealed that miR-449a and miR-765 expression is almost not detectable in CRCs, whereas miR-34a is expressed at a higher level and represents a p53 target, we decided to focus miR-34a (Figure 5.8 B).

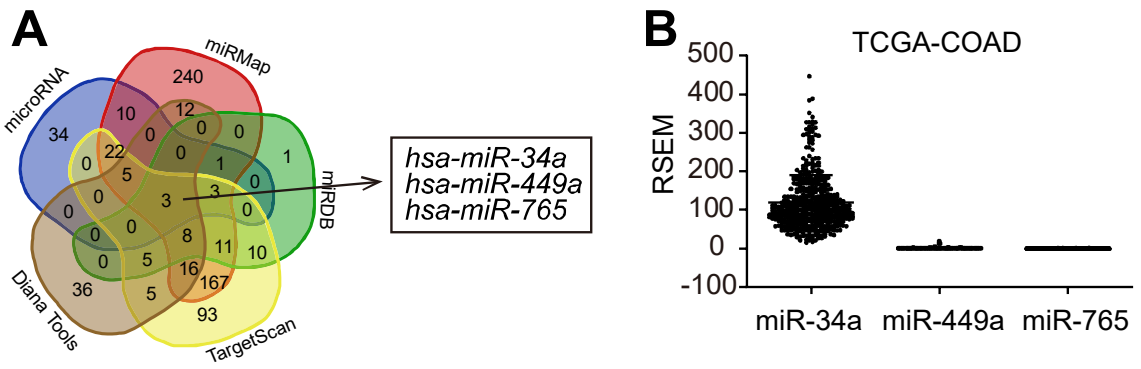

Figure 5.8

A, Bioinformatics prediction of matching seed sequences in the *CSF1R* 3'-UTR using five different algorithms.

B, Expression of miR-34a, miR-449a, and miR-765 in CRC patient samples from TCGA.

Notably, the miR-34a seed-matching sequence within the *CSF1R* 3'-UTR is highly conserved in other species (Figure 5.9 A). In line with these observations, expression of miR-34a showed an inverse correlation with *CSF1R* and *CSF1* in primary CRCs (Figure 5.9 B and C).

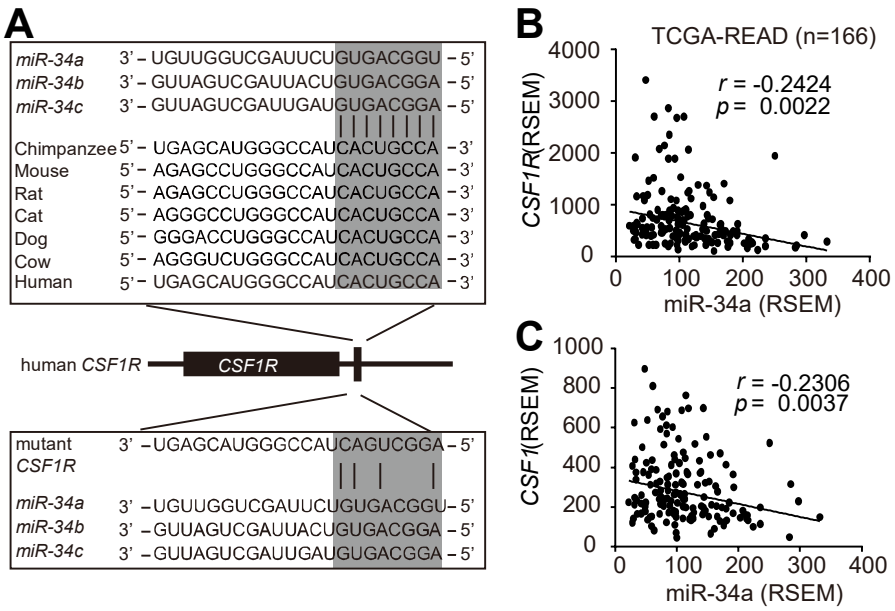

Figure 5.9

A, Scheme of the miR-34a seed, the seed-matching sequences and its targeted mutation in the 3'-UTR of the *CSF1R* mRNA. The seed and seed-matching sequences are high-lighted in grey. Black vertical bars indicate complementarity between the miR-34a seed and the CSF1R seed-matching sequence.

B, **C,** Correlative analysis between miR-34a and the indicated mRNAs in the samples of the TCGA collection of rectal adenocarcinomas (READ; n = 166) using the Pearson coefficient.

A: Figure and analysis were made by Dr. Markus Kaller.

However, we did not detect a miR-34a seed-matching site in the *CSF1* mRNA (data not shown). Ectopic expression of an Doxycycline(Dox)-inducible *pri-miR-34a* allele resulted in a significant down-regulation of *CSF1R* mRNA levels in four different human CRC lines (Figure 5.10 A). Furthermore, ectopic expression of *pri-miR-34a* in mesenchymal-like SW480 cells, which display low expression of endogenous miR-34a, also resulted in down-regulation of CSF1R protein expression (Figure 5.10 B).

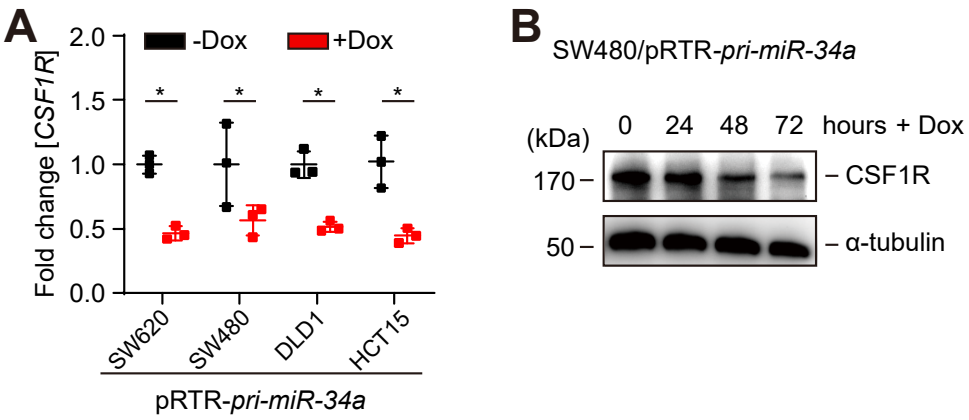

Figure 5.10

A, qPCR analysis of *CSF1R* expression in three different colorectal cancer cell lines 72 hours after induction of *pri-miR-34a* expression by addition of doxycyclin (Dox).

B, Western Blot analysis of CSF1R expression after induction of *pri-miR-34a* in SW480 cells by addition of Dox for the indicated periods.

A, B: Figures and analysis were made by Dr. Markus Kaller.

In panels A, mean values ± SD are provided. (*) $P < 0.05$

In a dual-reporter assay, ectopic miR-34a significantly repressed the activity of a wild-type *CSF1R* 3'-UTR reporter and also repressed a *TPD52* (a known miR-34a target) reporter. However, a *CSF1R* 3'-UTR reporter with mutations in the miR-34a seed-matching sequence was refractory to miR-34a (Figure 5.11). Therefore, miR-34a directly represses *CSF1R* expression via a conserved miR-34a seed-matching sequence.

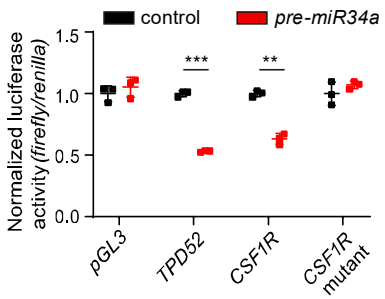

Figure 5.11 Dual-reporter assay after transfection with the indicated *pre-miR-34a* oligonucleotides and human *CSF1R* 3'-UTR reporter constructs. Mean values ± SD are provided. (*) $P < 0.05$. Figure and analysis were made by Dr. Markus Kaller.

5.3 p53 represses *CSF1R* via inducing miR-34a

Since *miR-34a* is directly induced by p53, we determined whether p53 activation would also repress CSF1R. Indeed, ectopic expression of p53 repressed CSF1R mRNA and protein expression in SW480 cells (Figure 5.12 A and B). In addition, p53 activation suppressed *CSF1* expression (Figure 5.12 A).

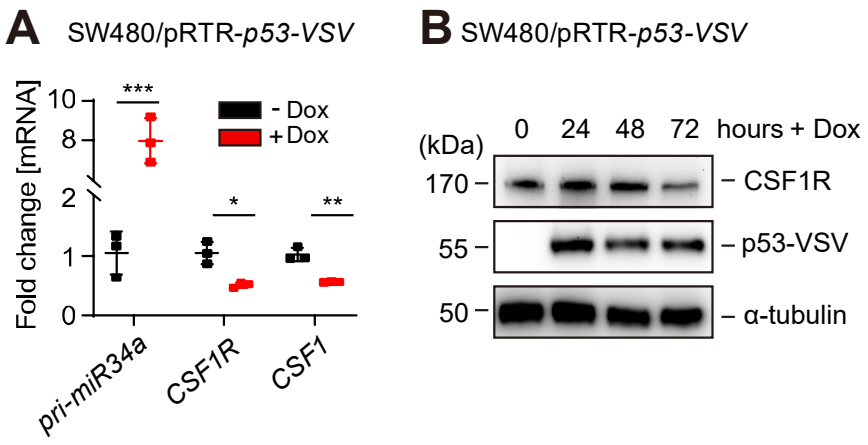

Figure 5.12

A, B qPCR analysis (A) of the indicated mRNAs and Western blot analysis (B) of CSF1R expression 72 hours after induction of ectopic *p53* by addition of Dox to SW480/pRTR-*p53-VSV* cells. B: Figure and analysis were made by Dr. Markus Kaller. In panels A, mean values ± SD are provided. (*) $P < 0.05$, (**) $P < 0.01$ and (***) $P < 0.001$.

Furthermore, the repression of CSF1R by p53 was alleviated by inactivation of miR-34a via treatment with miR-34a-specific antagomirs, demonstrating that miR-34a mediates the repression of CSF1R by ectopic p53 (Figure 5.13 A). In addition, treatment with the DNA damaging agents etoposide or 5-FU caused the down-regulation of CSF1R protein expression in *p53*$^{+/+}$, but not in isogenic *p53*$^{-/-}$ RKO cells

(Figure 5.13 B). Moreover, the repression of CSF1R by activation of endogenous p53 by treatment with etoposide was prevented by miR-34a-specific antagomirs (Figure 5.13 C).

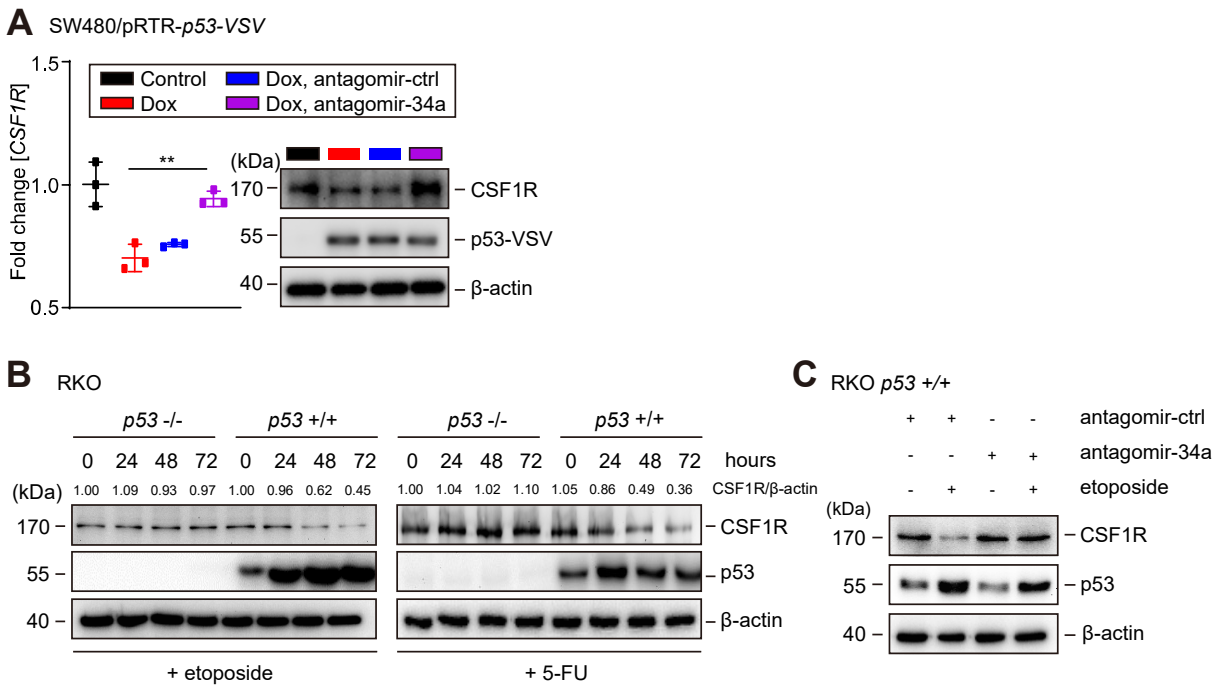

Figure 5.13

A, qPCR (left) and Western blot (right) analysis of SW480/pRTR-*p53-VSV* cells transfected with antago-*miR-34a* or control oligonucleotides for 24 hours and/or subsequently treated with Dox for 48 hours.

B, Western blot analysis of CSF1R expression in RKO $p53^{+/+}$ and RKO $p53^{-/-}$ cells after addition of etoposide (20 µM) or 5-FU (25 µg/mL) for the indicated periods.

C, Western blot analysis of CSF1R proteins in RKO p53+/+ cells transfected with antagomir-miR-34a or antagomir control oligonucleotides for 24 hours and subsequent exposure to etoposide (20 µM) for 48 hours or DMSO.

In panels A mean values ± SD are provided. (*) $P < 0.05$, and (**) $P < 0.01$.

Taken together, these results show that p53 activation leads to a miR-34a-mediated repression of CSF1R expression.

5.4 Coherent feed-forward regulation of *CSF1R* by SNAIL and miR-34a

Since *CSF1R* expression was elevated in CRCs classified as CRIS-B subtype, which is characterized by a mesenchymal expression profile, we determined whether *CSF1R* expression is associated with EMT-specific gene expression profiles. Gene Set Enrichment Analyses (GSEA) showed that *CSF1R* mRNA expression is strongly associated with the expression of EMT-specific signature mRNAs represented by the EMT hallmark gene set (Liberzon et al., 2015) in PDX samples (Figure 5.14 A). A similar correlation was found in the TCGA-COAD cohort and the additional cohort containing 566 CRC samples (Figure 5.14 B and C). More specifically, *CSF1R* mRNA expression was positively associated with the expression of “canonical” EMT-TFs, such as *SNAIL* and *SLUG,* and mesenchymal markers such as *Vimentin* (*VIM*), whereas it displayed an inverse correlation with *E-Cadherin* (*CDH1)* (Figure 5.14 D, E and F).

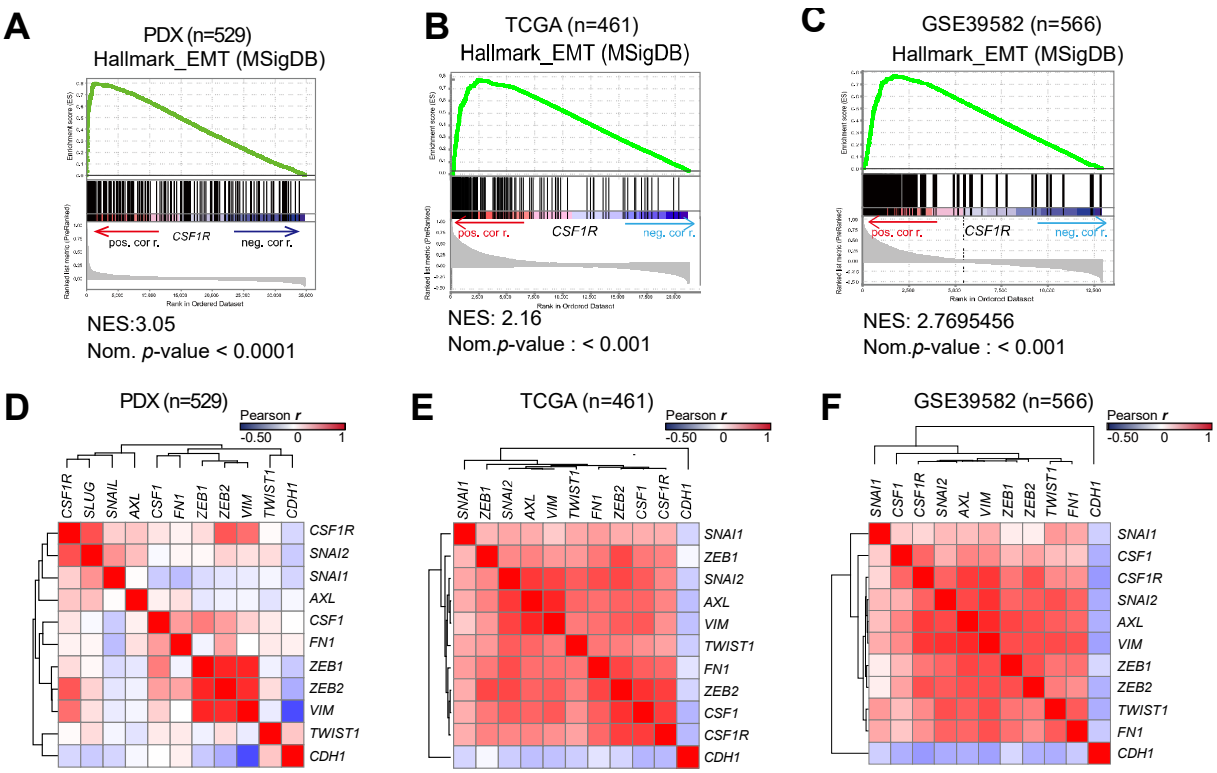

Figure 5.14

A, B, C, Genes were preranked by expression correlation coefficient (Pearson r) with *CSF1R* in descending order from left (positive correlation) to right (negative correlation) based on RNA expression data obtained from GSE76402 (A), TCGA-COAD (B) and GSE39582 (C) and association of EMT_hallmark genes with *CSF1R* expression was subsequently analyzed by GSEA. Pos. corr.: positive correlation, neg. corr.: negative correlation. NES: normalized enrichment score.

D, E, F, Heat-map depicting a hierarchically clustered correlation matrix of pairwise expression correlation coefficients (Pearson r) between previously described direct miR-34a target genes, EMT markers and *CSF1R* mRNA.

D, E, and F: Figures and analysis were made by Dr. Markus Kaller.

We have previously shown that the EMT-TFs SNAIL and SLUG negatively regulate *miR-34a* expression by directly binding to its promoter (Siemens et al., 2011). Since *CSF1R* is repressed by miR-34a, a down-regulation of *miR-34a* by *SNAIL* should

presumably lead to induction of CSF1R. Therefore, we determined CSF1R expression levels after ectopic expression of SNAIL or SLUG in epithelial-like DLD1 cell pools harbouring Dox-inducible expression vectors encoding either SNAIL or SLUG. Indeed, *CSF1R* mRNA showed robust induction concomitantly with repression of *pri-miR-34a* transcription after ectopic expression of SNAIL or SLUG in DLD1 cells (Figure 5.15 A). Consistent with previous reports (Siemens et al., 2011), *pri-miR-200c* was also repressed by SNAIL or SLUG. The up-regulation of *CSF1R* mRNA after activation of SNAIL or SLUG was accompanied by an increase in CSF1R protein levels (Figure 5.15 B).

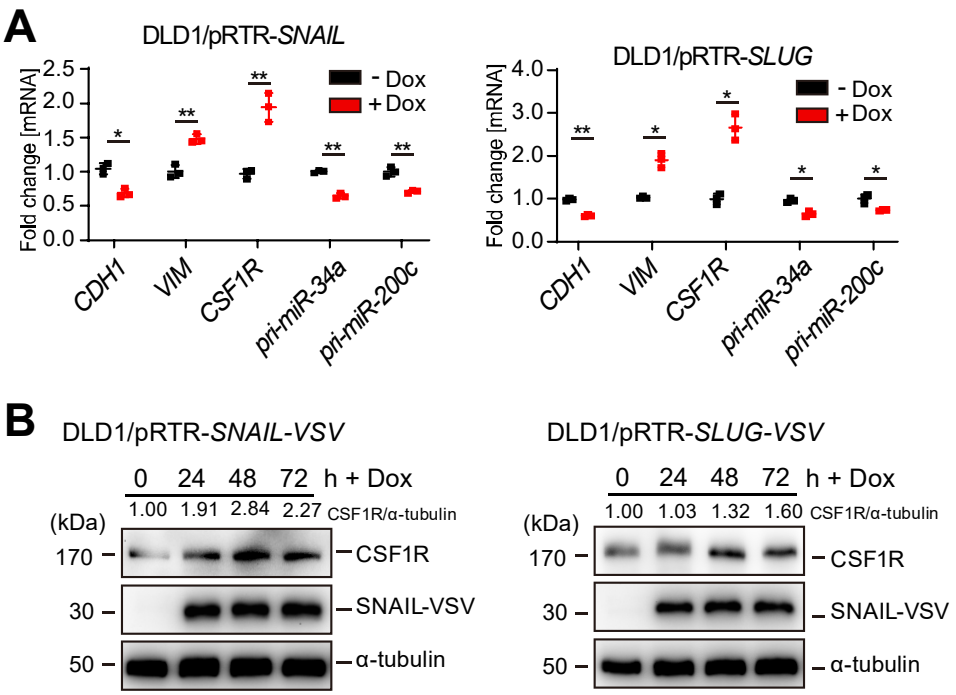

Figure 5.15

A, qPCR analysis of the indicated mRNAs 72 hours after addition of Dox to DLD1/pRTR-*SNAIL-VSV* cells (left) and DLD1/pRTR-*SLUG-VSV* cells (right).

B, Western blot analysis of CSF1R expression after addition of Dox for the indicated periods in DLD1/pRTR-*SNAIL-VSV* cells (left) and DLD1/pRTR-*SLUG-VSV* cells (right).

A, B: Figures and analysis were made by Dr. Markus Kaller.

In panels A mean values ± SD are provided. (*) $P < 0.05$ and (**) $P < 0.01$.

Although repression of *miR-34a* by SNAIL is presumably a critical component in the regulation of CSF1R, we asked whether direct activation by these EMT-TFs may also contribute to the induction of *CSF1R* expression. Indeed, we detected SNAIL occupancy in the first intron of *CSF1R* in a genome-wide ChIP-Seq analysis of DLD-1 cells (Figure 5.16 A), suggesting that *CSF1R* is also directly regulated by SNAIL. Accordingly, we identified a cluster of three closely spaced SNAIL binding sites with the sequence 5'-[CACCTG]-3' within the first intron of the *CSF1R* gene (Figure 5.16 B). By quantitative chromatin immunoprecipitation (qChIP) of this region, SNAIL occupancy at the first intron of the *CSF1R* gene was confirmed (Figure 5.16 C).

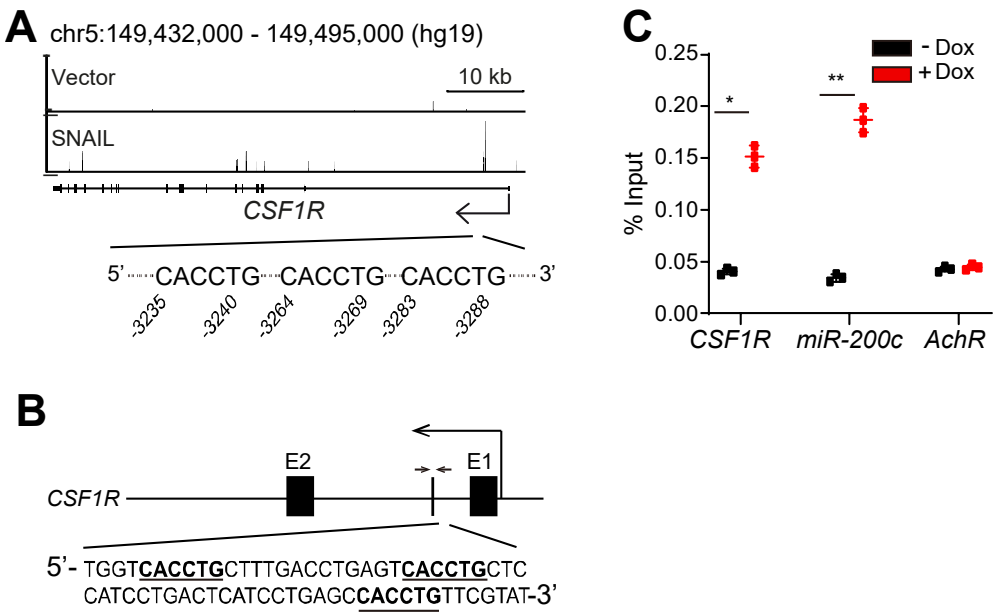

Figure 5.16

A, SNAIL-VSV-derived ChIP-Seq results were obtained after induction of ectopic SNAIL in DLD-1 cells and displayed using the UCSC genome browser.

B, Scheme of the first intron of human *CSF1R*. Putative SNAIL binding sites are indicated as bold letters in the DNA sequence. Small arrows indicate the amplicon used in Figure 5.16 C for qChIP analysis.

C, ChIP analysis of SNAIL occupancy at the first intron of *CSF1R* and promoter of *miR-200c* 24h after addition of Dox or cells left untreated using anti-VSV and anti-rabbit-IgG antibodies. AchR served as negative control.

A: Figure and analysis were made by Dr. Markus Kaller.

In panels A and B mean values ± SD are provided. (*) $P < 0.05$ and (**) $P < 0.01$.

Moreover, siRNA-mediated suppression of CSF1R in SNAIL-expressing DLD1 cells resulted in a decrease in invasion (Figure 5.17). Taken together, these results demonstrate a coherent feed-forward regulation of CSF1R expression by SNAIL and miR-34a. In addition, CSF1R may be a critical downstream mediator of SNAIL-induced invasion in CRC cell lines.

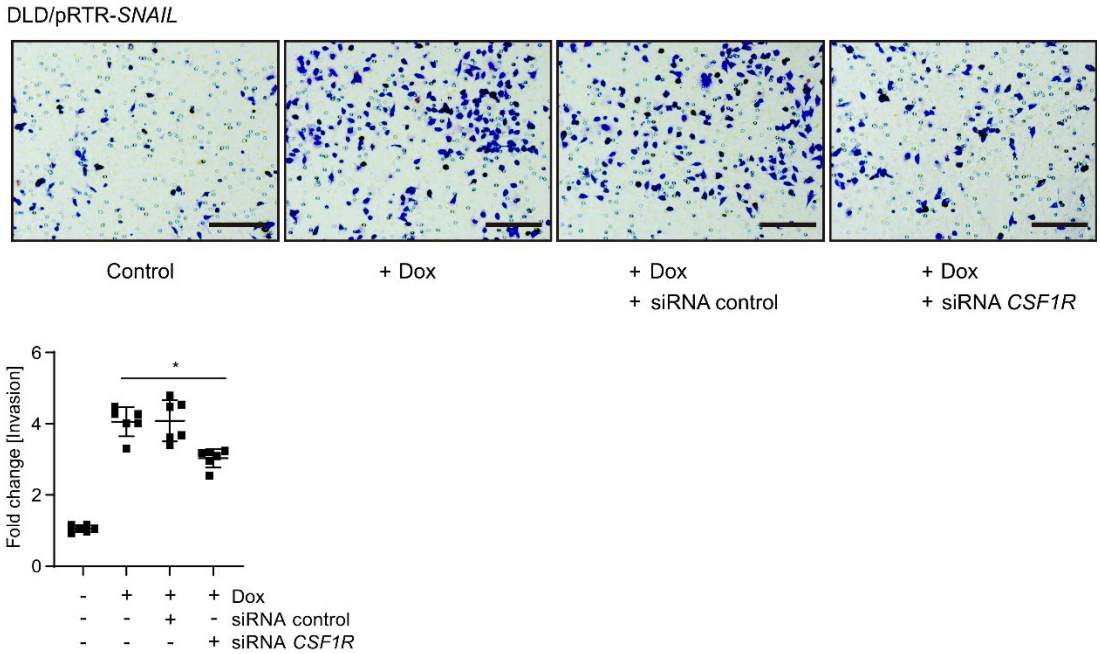

Figure 5.17

Boyden-chamber invasion assay of DLD1/pRTR-*SNAIL-VSV* cells after the indicated treatments. Mean values ± SD are provided. (*) $P < 0.05$.

5.5 Repression of *miR-34a* after CSF1R activation is mediated by STAT3

We have previously found that miR-34a often forms double-negative feed-back loops with its targets (Hahn et al., 2013; Liberzon et al., 2015; Rokavec, Oner, et al., 2014; Siemens et al., 2011). Also here we observed a downregulation of *pri-miR-34a* expression after activation of its target CSF1R either by CSF1 or IL34 (Figure 5.18 A). Also after ectopic expression of a constitutively active form of CSF1R, which was generated previously by changing lysine at position 301 to serine (Roussel, Downing, Rettenmier, & Sherr, 1988), the expression of *pri-miR-34a* was down-regulated in DLD-1 CRC cells (Figure 5.18 B). Furthermore, inhibition of CSF1R by the small molecule inhibitor GW2580 (Bencheikh et al., 2019) resulted in an upregulation of *pri-miR-34a* in SW480 and SW620 cells (Figure 5.18 C and D).

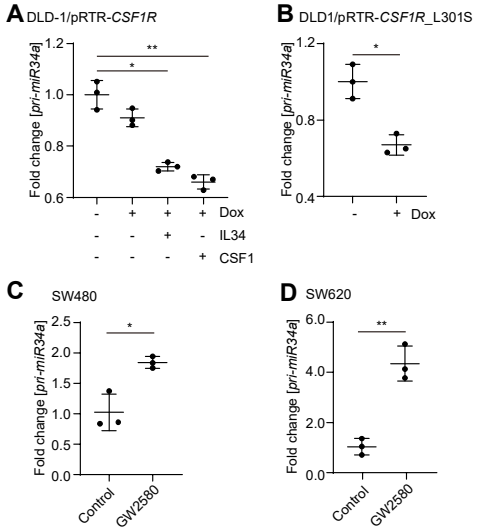

Figure 5.18

A, qPCR analysis of *pri-miR-34a* in DLD1/pRTR-*CSF1R-FLAG* treated with Dox for 96 hours. The last 72 hours also treated with CSF1 or IL34.

B, qPCR analysis of *pri-miR-34a* in DLD1/pRTR-*CSF1R*_L301S-*FLAG* after addition of Dox for 48 hours.

C, D, qPCR analysis of indicated mRNAs in SW480 (C) and SW620 (D) cells after treatment with GW2580 (1 nM) for 72 hours.

In panels A, B, C, and D mean values ± SD are provided. (*) $P < 0.05$ and (**) $P < 0.01$.

Since Gene Set Enrichment Analyses (GSEA) showed a positive correlation between *CSF1R* expression and the IL6_JAK_STAT3 pathway hallmark gene signature (Figure 5.6 B, and Figure 5.19 A), we asked whether STAT3 activation may mediate the repression of *miR-34a* after CSF1R activation. Indeed, treatment of DLD-1 cells ectopically expressing CSF1R with CSF1 resulted in increased phosphorylation of STAT3 at residue S727 which indicates STAT3 activation (Figure 5.19 B). Also, the ectopic expression of the constitutively active *CSF1R_L301S* allele resulted in STAT3 phosphorylation (Figure 5.19 C). Of note, RNAi-mediated down-regulation of STAT3 significantly reversed the suppression of *pri-miR-34a* observed after CSF1R activation, whereas silencing of *SNAIL* only led to a minor de-repression (Figure 5.19 D).

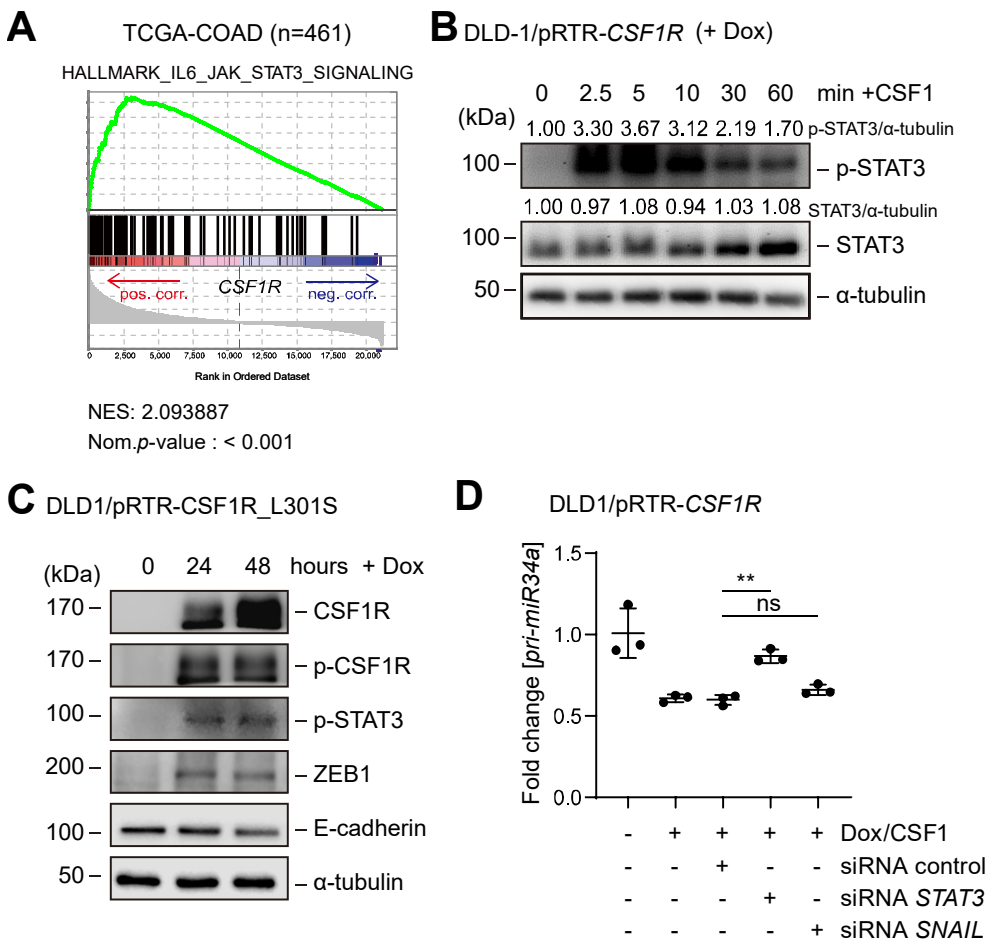

Figure 5.19

A, Genes were preranked by expression correlation coefficient (Pearson r) with *CSF1R* in descending order from left (positive correlation) to right (negative correlation) based on RNA expression data obtained from TCGA-COAD and analyzed by GSEA. Pos. corr.: positive correlation, neg. corr.: negative correlation. NES: normalized enrichment score.

B, Western blot analysis of STAT3 phosphorylation at residue S727 and STAT3 expression after addition of Dox for 24 hours and subsequent exposure to CSF1 for indicated periods in DLD1/pRTR-*CSF1R* cells.

C, Western blot analysis of DLD1/pRTR-*CSF1R*_L301S cells after addition of Dox for indicated periods.

D, qPCR analysis of *pri-miR-34a* expression. DLD1/pRTR-*CSF1R* cells were transfected with indicated siRNAs. After 6 hours they were treated with Dox and CSF1 for 48 hours. The STAT3- and SNAIL-specific siRNAs used here have been validated previously (Rokavec, Oner, et al., 2014).

In panels D mean values ± SD are provided. (**) $P < 0.01$.

Therefore, the down-regulation of *miR-34a* by CSF1R is, at least in part, mediated by STAT3 activation. This effect is presumably mediated via a conserved STAT3-binding site in the *miR-34a* promoter, which we have characterized previously (Rokavec, Oner, et al., 2014). Taken together, *miR-34a, CSF1R* and *STAT3* therefore form a double-negative feed-back loop. In combination with the coherent feed-forward loop described above these regulatory circuitries may allow cells to integrate antagonistic mitogenic (CSF1, WNT) and anti-proliferative (p53) signals (see model in Figure 5.20).

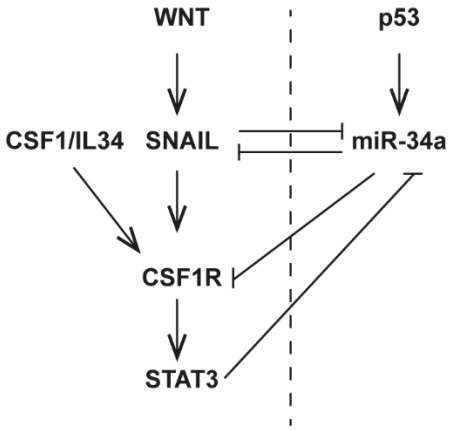

Figure 5.20
Model of the regulations characterized in Figures 5.8-5.19. The dashed line separates p53 on (right) and p53 off states (left).

5.6 CSF1R activation induces EMT, migration, and invasion

Next, we asked whether CSF1R activation is sufficient to induce EMT. Therefore, we treated the epithelial-like CRC cell line HCT15 with CSF1 or IL-34 for 72 hours. Indeed, CSF1 and IL-34 induced the transition from an epithelial morphology with dense islands of cobblestone-shaped cells to a mesenchymal morphology with

spindle-shaped cells forming protrusions and displaying a scattered growth pattern (Figure 5.21 A). In addition, mesenchymal markers, such as Vimentin (VIM), SNAIL, and ZEB1, were induced on mRNA and protein levels, while CDH1 protein expression decreased (Figure 5.21 B and C).

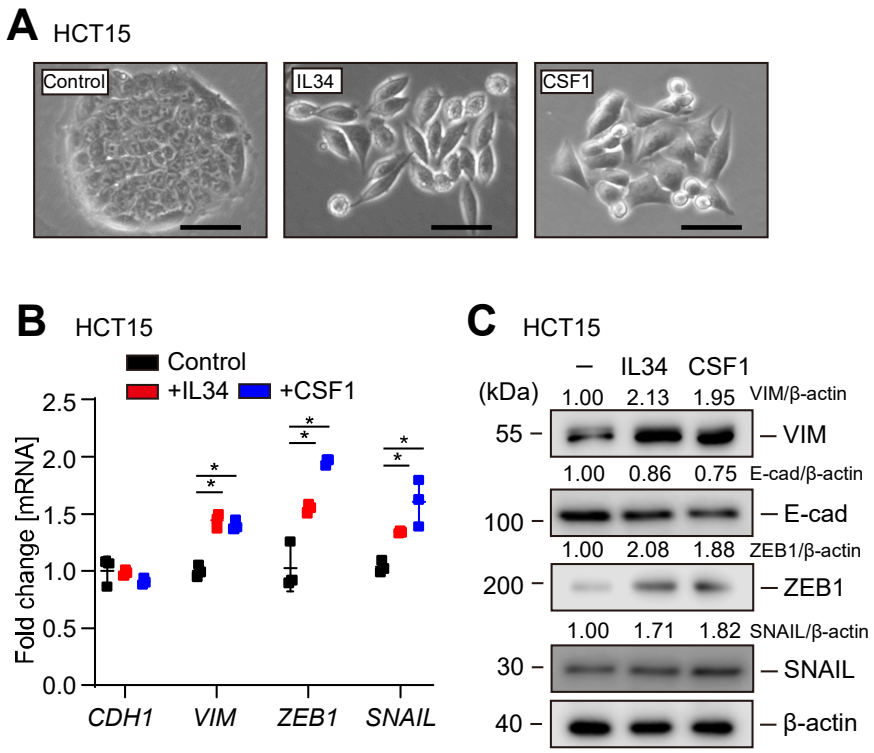

Figure 5.21

A, Representative phase-contrast pictures of HCT15 cells after treatment with IL34 or CSF1 for 72 hours. Scale bar: 25 µm.

B, qPCR analysis of the indicated EMT markers after treatment of HCT15 cells with IL34 or CSF1 for 48 hours.

C, Western blot analysis of indicated EMT markers after treatment of HCT15 cells with IL34 or CSF1 for 72 hours.

In panels B mean values ± SD are provided. (*) $P < 0.05$.

Silencing of *CSF1R* expression by siRNAs prevented the induction of VIM by IL34 (Figure 5.22), excluding the possibility that IL-34-induced EMT in HCT15 cells is

mediated by protein-tyrosine phosphatase ζ (PTP-ζ), which represents an alternative IL34 receptor (Nandi et al., 2013).

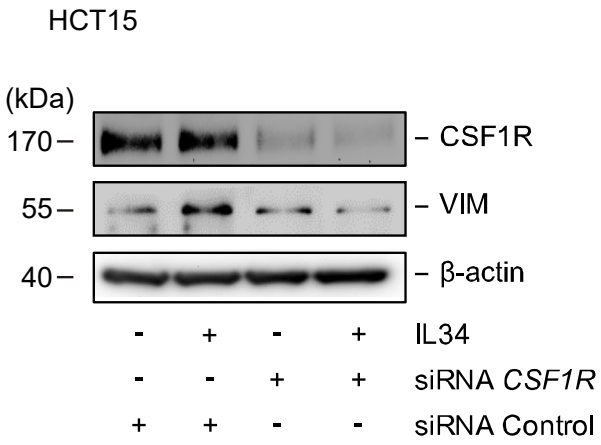

Figure 5.22
Western blot analysis of HCT15 transfected with siRNA *CSF1R* or siRNA Control oligonucleotide for 24 hours and/or subsequently treated with IL34 for 72 hours.

However, treatment of DLD1 CRC cells with CSF1 or IL34 did not significantly affect the expression of epithelial or mesenchymal markers (Figure 5.23 A). This non-responsiveness is presumably due to the relatively low expression of CSF1R protein in DLD1 cells when compared to HCT15 cells (Figure 5.23 B). Indeed, ectopic *CSF1R* expression in DLD1 cells restored their responsiveness to CSF1, as CSF1 induced the hallmarks of EMT in these cells (Figure 5.23 C, D, E, F and G). Taken together, these results demonstrate that CSF1R activation induces EMT in CRC cells.

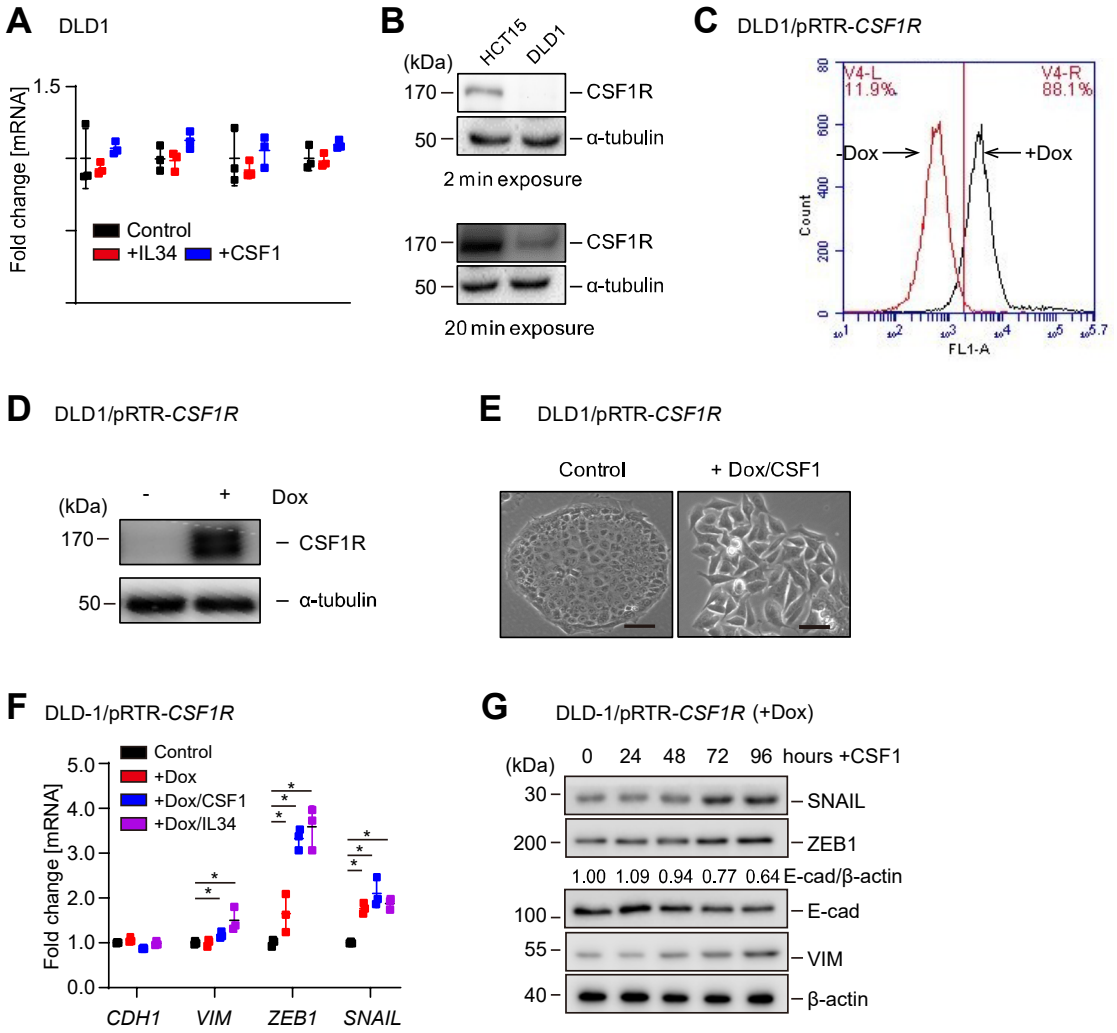

Figure 5.23

A, qPCR analysis of DLD1 cells after treatment with CSF1 or IL34 for 48 hours.

B, Western blot analysis of CSF1R expression in DLD1 and HCT15 cells.

C, Flow cytometric determination of the frequency of cells with inducible expression of eGFP in DLD-1 cell pools harboring a pRTR-*CSF1R* vector after addition of 100 ng/ml Dox for 72 hours.

D, Western blot analysis of CSF1R expression in DLD1/ pRTR-*CSF1R* cells after addition of 100 ng/ml Dox for 72 hours.

E, Representative phase-contrast pictures of DLD1/pRTR-*CSF1R* cells after treatment with Dox for 24 hours, and then exposed to CSF1 for 72 hours. Scale bar: 25 µm.

F, qPCR analysis of DLD1/pRTR-*CSF1R-FLAG* cells that were treated with Dox for 24 hours and then exposed to CSF1 or IL34 for another 48 hours.

G, Western blot analysis of DLD1/pRTR-*CSF1R-FLAG* cells treated with Dox for 24 hours and subsequently exposed to CSF1 for the indicated periods.

In panels A and F mean values ± SD are provided. (*) $P < 0.05$.

Expression of CSF1R was associated with epithelial cell migration by GSEA analysis (Figure 5.24).

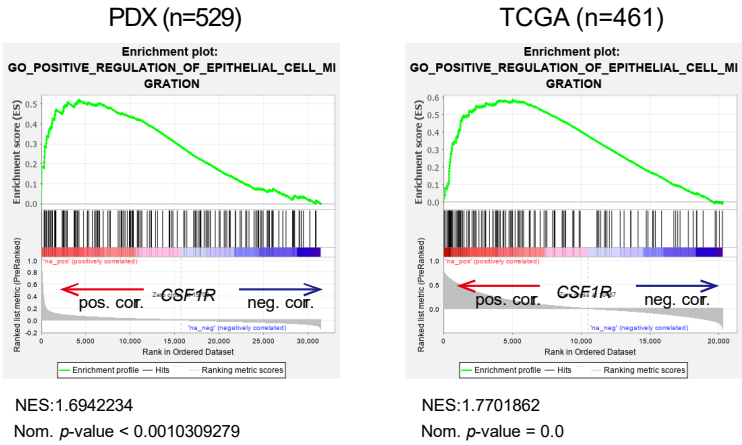

Figure 5.24

Genes were preranked by expression correlation coefficient (Pearson r) with *CSF1R* in descending order from left (positive correlation) to right (negative correlation) based on RNA expression data and association of indicated gene signature with *CSF1R* expression was subsequently analyzed by GSEA. Pos. corr.: positive correlation, neg. corr.: negative correlation. NES: normalized enrichment score.

Therefore, we asked whether activation of CSF1R enhances cell migration, invasion and eventually metastases formation, as these processes are functional consequences of an EMT. Indeed, activation of CSF1R accelerated the closure of a scratch in CSF1R-expressing DLD1 cells (Figure 5.25 A). In addition, migration and invasion were enhanced after CSF1R activation as determined in a Boyden-chamber assay, whereas treatment with the CSF1R inhibitors GW2580 or BLZ925 resulted in a significant decrease of cellular invasion in the mesenchymal-like cell line SW620 (Figure 5.25 B, C and D).

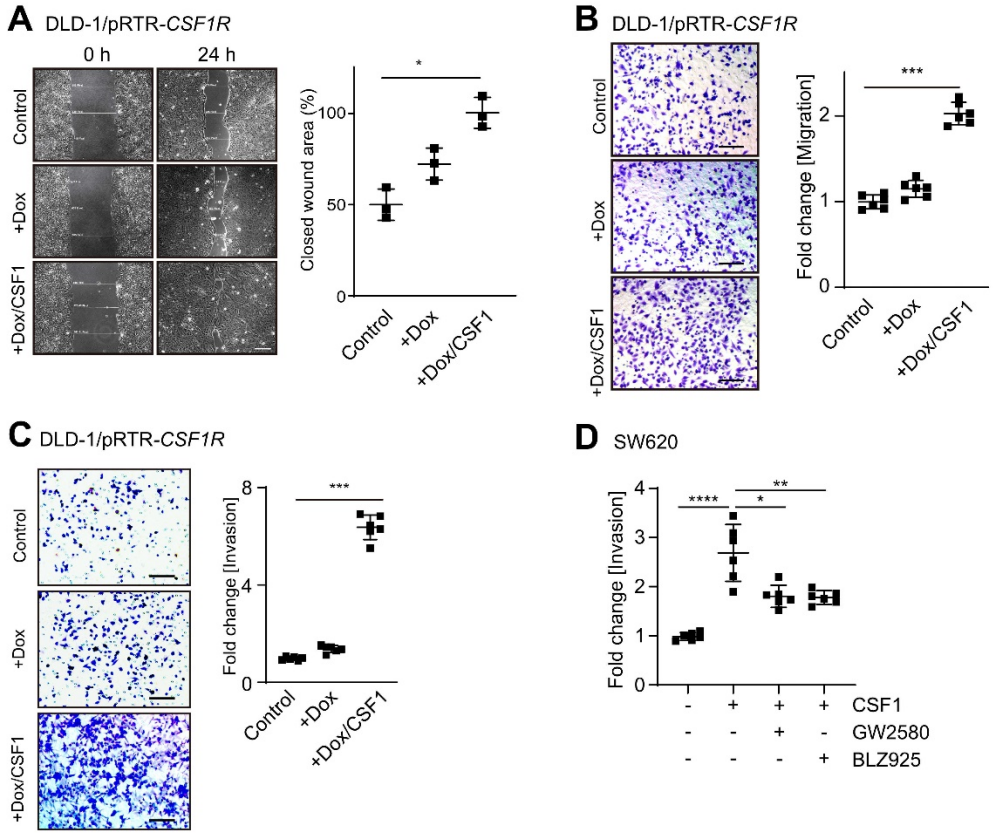

Figure 5.25

A, Scratch assay of DLD1-pRTR-*CSF1R* cells treated with Dox or Dox/CSF1. Scale bar: 200 µm.

B, C, Boyden-chamber assays of cellular migration (B) or invasion (C).

D, SW620 cells were pre-treated with inhibitors as indicated, and subsequently treated with Dox and CSF1. After incubation with CSF1 or 48 hours, cells were subjected to Boyden-chamber assay.

In panels A, B, C and D mean values ± SD are provided. (*) $P < 0.05$, (**) $P < 0.01$, and (***) $P < 0.001$.

Furthermore, ectopic expression of a miR-34a-resistant *CSF1R* cDNA in the mesenchymal-like cell line SW480 prevented the repression of migration and invasion by *pre-miR-34a* (Figure 5.26 A and B). Therefore, the repression of *CSF1R* by miR-34a is presumably required for inhibition of migration and invasion by miR-34a.

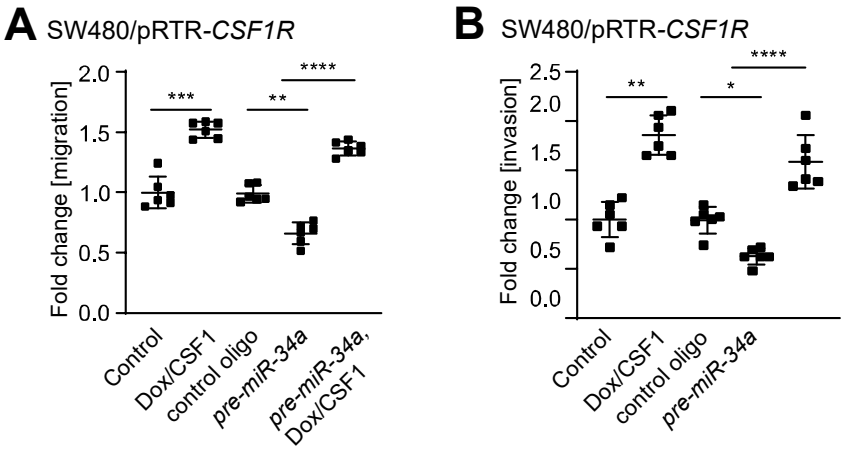

Figure 5.26

A, B, Cells were transfected with or without *pre-miR-34a* oligo one day before the addition of Dox and CSF1, and then subjected to the migration (A) or invasion assay (B). In panels A and B mean values ± SD are provided. (*) $P < 0.05$, (**) $P < 0.01$, and (***) $P < 0.001$.

Next, DLD-1 cells harbouring a luciferase marker gene and an inducible *CSF1R* allele were injected into mice to assess the effect of CSF1R activation on lung metastases formation. Indeed, only cells with activated CSF1R formed lung metastases in mice as evidenced by a significant increase in luciferase signal by week 5 which further increased until week 7 (Figure 5.27 A and B).

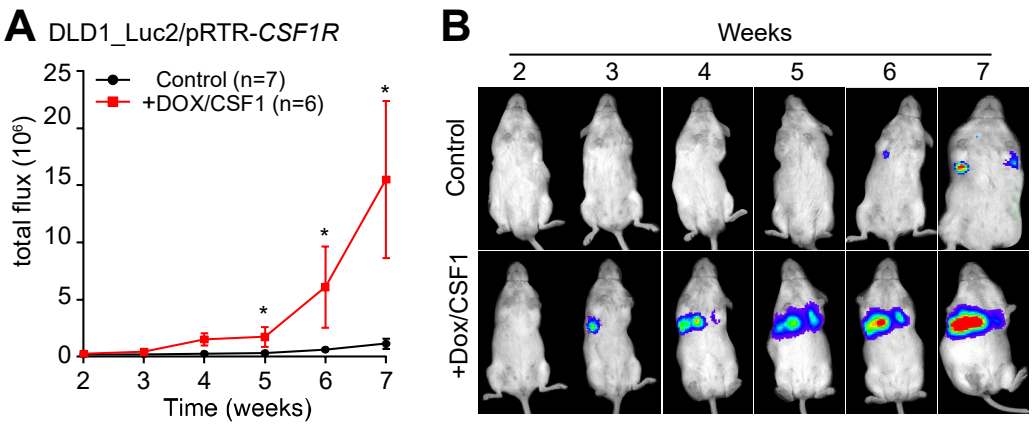

Figure 5.27

A, DLD1-Luc2/pRTR-*CSF1R-FLAG* cells treated with or without Dox and CSF1 were injected into the tail vein of NOD/SCID mice. At the indicated time points, bioluminescence signals were recorded. Bioluminescence signals are presented as "total flux".

B, Representative examples of bioluminescence imaging at the indicated time points after tail vein injection of DLD1-Luc2/pRTR-*CSF1R* cells.

A, B: Figures and analysis were made by Dr. Matjaz Rokavec.

In panels A mean values ± SD are provided. (*) $P < 0.05$.

In SW620 CRC cells down-regulation of CSF1R expression by transfection with *CSF1R*-specific siRNAs or *pre-miR-34a* inhibited invasion as determined in a Boyden-chamber assay (Figure 5.28 A). When SW620 cells treated similarly were injected into the tail veins of mice, a reduced number of metastatic tumor nodules were detected in the lungs 8 weeks later (Figure 5.28 B and C). The stronger inhibitory effect of *pre-miR-34a* oligonucleotides, as compared to *CSF1R*-specific siRNAs, can be explained by the inhibition of other miR-34a targets, which promote the formation of metastases, such as the IL6R (Rokavec, Oner, et al., 2014).

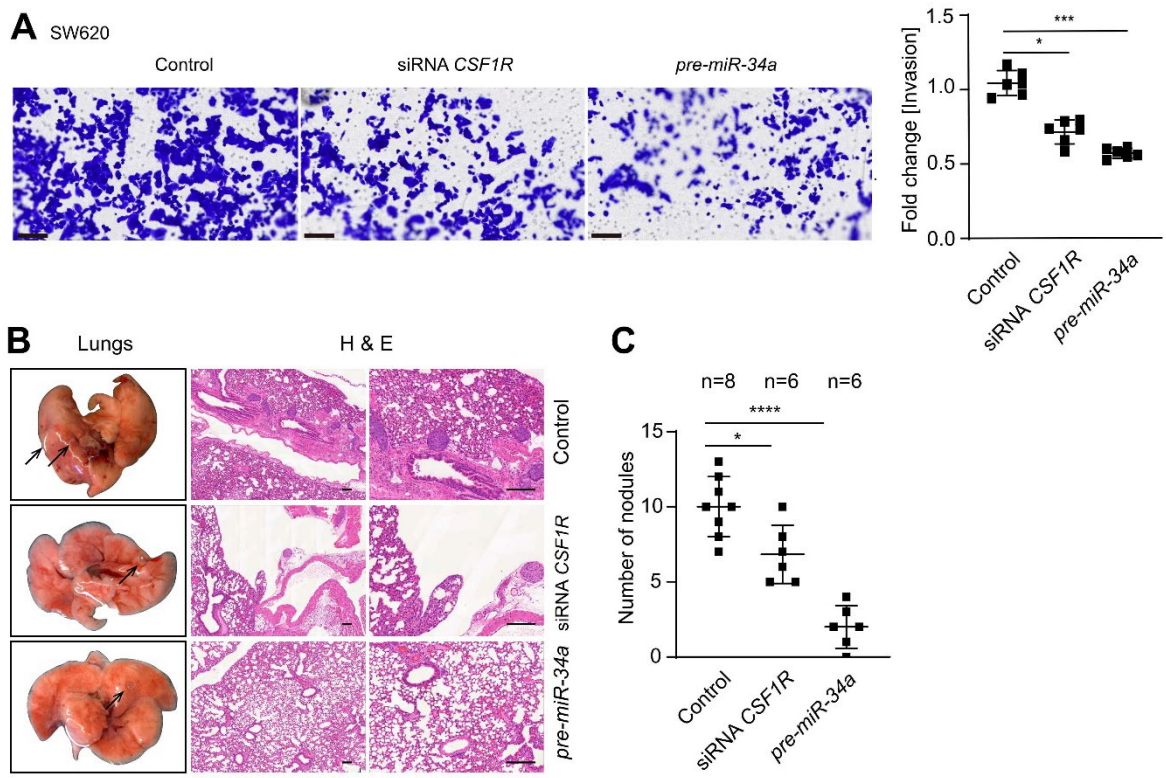

Figure 5.28

A, SW620 cells were transfected with the indicated oligonucleotides for 48 hours and then subjected to an invasion assay in Boyden-chambers for another 36 hours.

B, SW620 cells were transfected as the indicated oligonucleotides for 48 hours and subsequently injected into the tail vein of NOD/SCID mice. Left, lungs were resected 8 weeks after injection. Arrows, metastatic tumor nodules. Right, representative examples of the H&E staining of the resected lungs are shown. Scale bar, 200 µm.

C, Quantification of metastatic tumor nodules in the lung per mouse 8 weeks after tail-vein injection.

B: Xenograft experiments were performed by Dr. Matjaz Rokavec.

In panels A and C mean values ± SD are provided. (*) $P < 0.05$, (***) $P < 0.001$, and (****) $P < 0.0001$.

Taken together, these results show that CSF1R activation is sufficient and necessary for invasion and metastases formation of CRC cells.

5.7 CSF1R mediates resistance to 5-FU in CRC cells

Since CSF1R activation induced EMT, which has been linked to chemo-resistance (Sale et al., 2019), we determined whether CSF1R activity and/or expression influences the sensitivity of CRC cells to the chemo-therapeutic agent 5-FU (5-fluoro-uracil), which is commonly used in CRC therapy. DLD-1 cells ectopically expressing CSF1R were treated with CSF1 for 24 hours and subsequently exposed to 5-FU for 3 days. Cells expressing ectopic CSF1R formed more colonies and were therefore less sensitive to 5-FU, when compared to control cells (Figure 5.29).

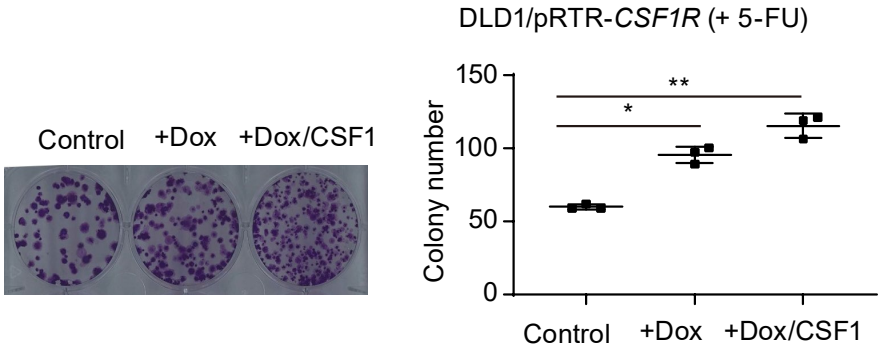

Figure 5.29

For a colony formation assay 500 cells were seeded per well of a 6-well plate and cultivated with or without Dox for 24 hours, then exposed to CSF1 for another 24 hours, and then treated with 5-FU for 72 hours. Subsequently, cells were fixed and stained with crystal violet. Quantification of colony formation (right) and representative examples of crystal violet staining (left). Mean values ± SD are provided. (*) $P < 0.05$, and (**) $P < 0.01$.

The addition of CSF1 further increased the number of colonies formed by cells ectopically expressing CSF1R. Next, we established a 5-FU-resistant cell pool (DLD1_5FU) by exposing DLD-1 cells to increasing concentrations of 5-FU over a period of five months. The tolerance of DLD1_5FU cells to 5-FU was significantly

higher than that of parental DLD1 cells (DLD1_par) (Figure 5.30 A and B). The IC_{50} value of 5-FU for DLD1_5FU cells was 8-fold increased when compared to the parental cells. Accordingly, DLD1_5FU cells exposed to 5-FU underwent less apoptosis than DLD1_par cells (Figure 5.30 C).

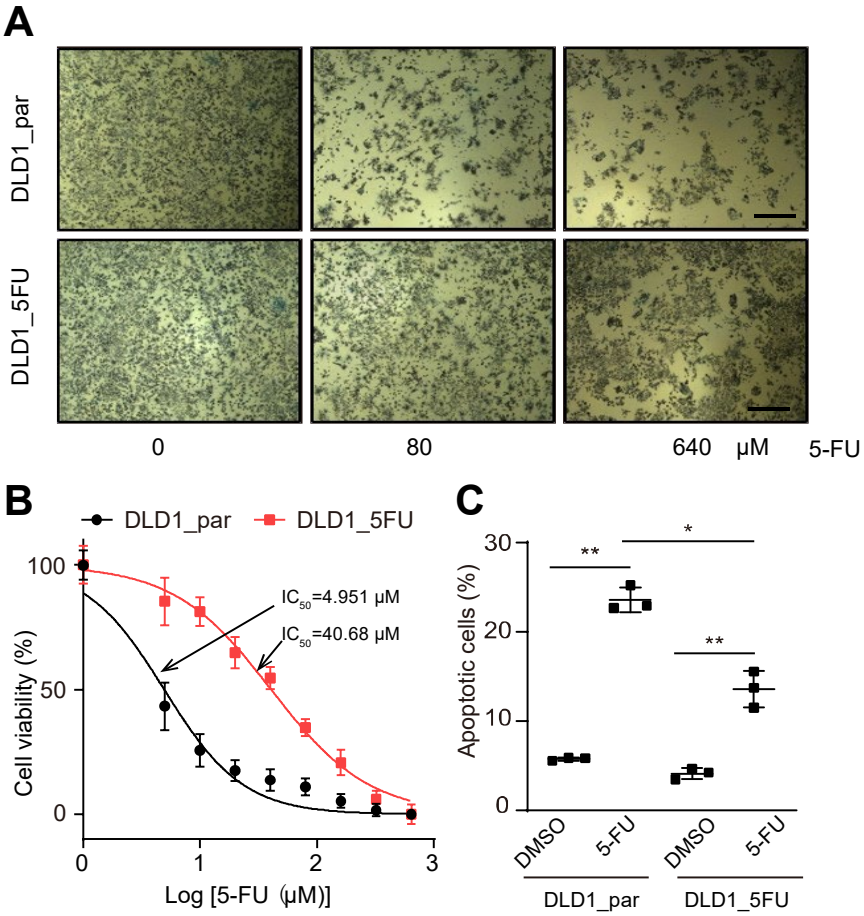

Figure 5.30

A, The indicated cell pools were treated with 5-FU for 48 hours and subsequently subjected to MTT assay. Micrographs show cell pools with formation of MTT formazan, which is directly proportional to the number of living cells Scale bars represent 200 µm.

B, IC_{50} determination of DLD1_par and DLD1_5FU cells in response to 5-FU. Cells were treated with the indicated concentrations of 5-FU for 48 hours and then subjected to an MTT assay.

C, Detection of apoptotic cells by Annexin V-FITC and PI staining after treatment with 5-FU for 36 hours.

In panels C mean values ± SD are provided. (*) $P < 0.05$ and (**) $P < 0.01$.

Interestingly, CSF1R expression was up-regulated concomitantly with down-regulation of miR-34a in DLD1_5FU cells when compared to DLD1_par cells (Figure 5.31 A and B). Similar results were obtained with HT29 cells, that were rendered resistant to 5-FU as described for above for DLD-1 cells (Figure 5.31 C).

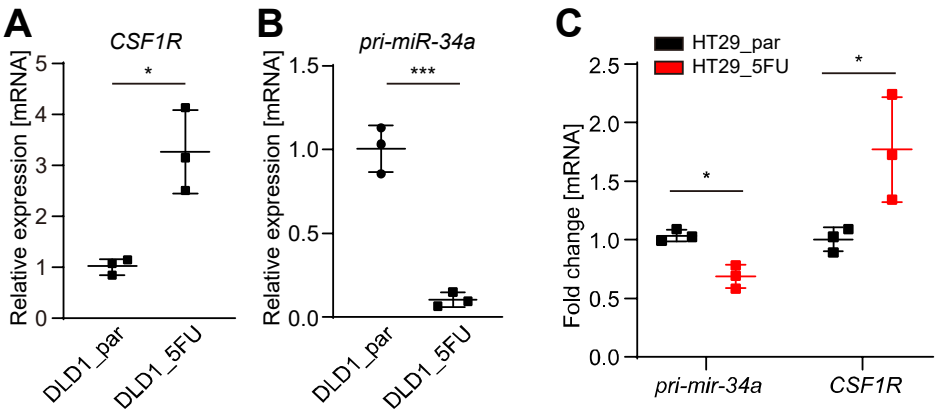

Figure 5.31

A, B, qPCR analysis of *CSF1R* (A) and *pri-miR34a* (B) expression in DLD1_par and DLD1_5FU cells.

C, Detection of pri-miR-34a and CSF1R expression in HT29_par and HT29_5FU cells. In panels A, B and C mean values ± SD are provided. (*) $P < 0.05$, (**) $P < 0.01$ and (***) $P < 0.001$

Furthermore, GSEA showed that increased *CSF1R* is negatively associated with apoptosis related gene expression (Figure 5.32 A). In addition, down-regulation of CSF1R in DLD_FU cells by specific siRNA pools resulted in decreased cell viability after 5-FU treatment (Figure 5.32 B) and was accompanied by an increase in apoptosis (Figure 5.32 C and D). Interestingly, ectopic expression of *pre-miR-34a* further enhanced apoptosis, indicating that miR-34a may target additional suppressors of apoptosis besides *CSF1R* in this context.

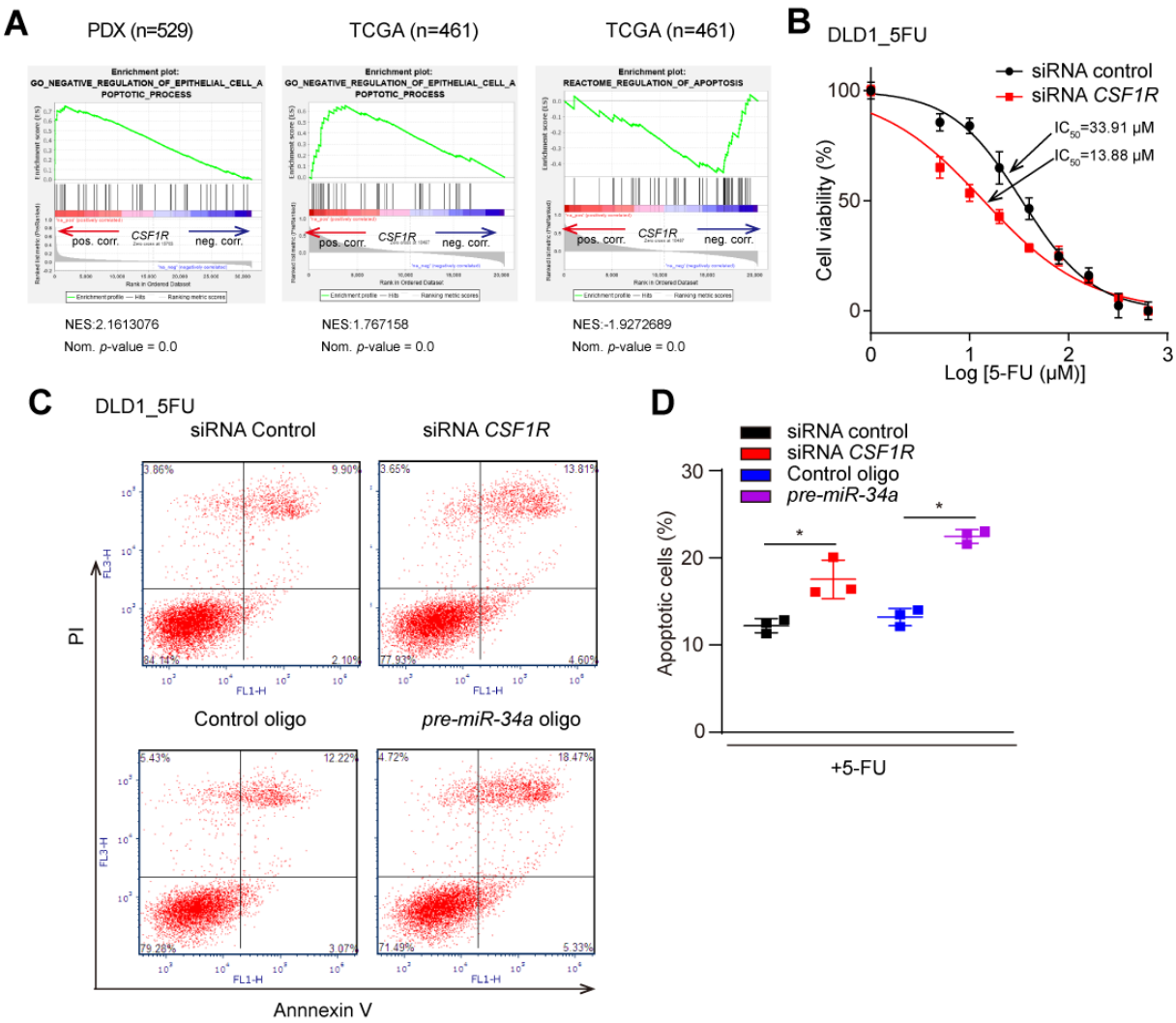

Figure 5.32

A, Genes were preranked by expression correlation coefficient (Pearson r) with CSF1R in descending order from left (positive correlation) to right (negative correlation) based on RNA expression data, and association of the indicated gene signatures with *CSF1R* expression was analyzed by GSEA. Pos. corr.: positive correlation, neg. corr.: negative correlation. NES: normalized enrichment score.

B, DLD1_5FU cells were transfected with control or *CSF1R*-specific siRNAs for 24 hours and subsequently treated with increasing concentrations of 5-FU for 48 hours. Then the IC50 was determined by an MTT assay.

C, D, DLD1_5FU cells were transfected with indicated oligonucleotides, subsequently treated with 5-FU for 36 hours and apoptotic cells were detected by Annexin V-FITC and PI staining.

In panels A, D, E, F, G and J mean values ± SD are provided. (*) $P < 0.05$, (**) $P < 0.01$ and (***) $P < 0.001$

Taken together, down-regulation of *miR-34a* and elevated expression of CSF1R is selected for during treatment with 5-FU and confers resistance of CRC cells to 5-FU.

5.8 CSF1R mediates EMT, migration, and invasion of 5-FU in CRC cells

Unlike parental DLD1 cells, DLD1_5FU cells displayed a mesenchymal-like morphology (Figure 5.33).

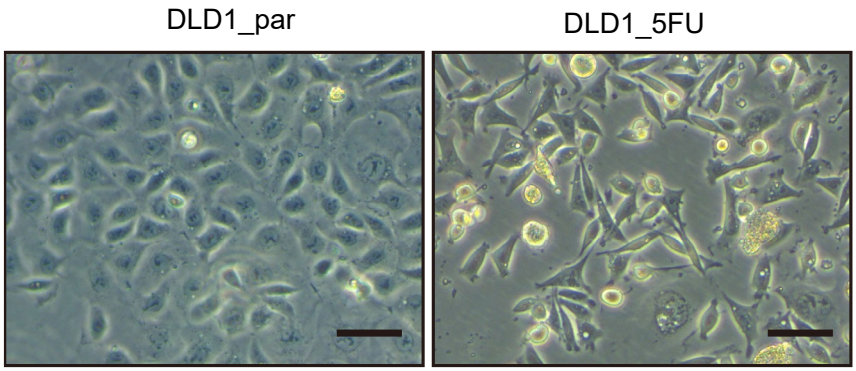

Figure 5.33
Representative phase-contrast pictures of DLD1_par and DLD1_5FU cells. Scale bars represent 25 µm.

Additionally, VIM, SNAIL and ZEB1 were upregulated at the mRNA and protein levels in DLD1_5FU cells when compared to the parental DLD-1 cells (Figure 5.34, A and B). On the contrary, E-cadherin protein expression was decreased in DLD1_5FU cells. In addition to *CSF1R* other target mRNAs of miR-34a, such as *AXL, PDGFR, c-Met, c-Kit, ZNF281 and CD44*, were up-regulated in DLD1_5FU cells. Consistent with the increased stemness known to be associated with EMT (Mani et al., 2008), the stemness markers *CD44*, *CD166, BMI1* and *CD24* were upregulated in DLD1_5FU cells.

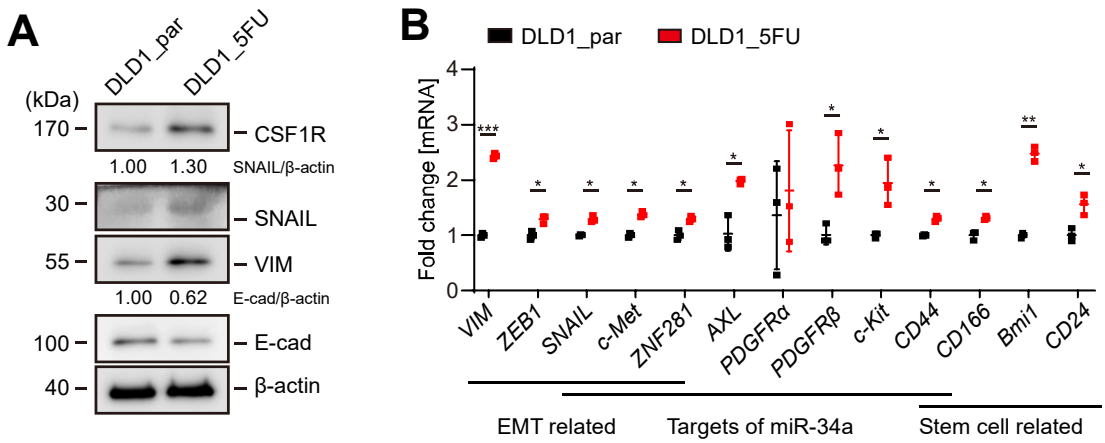

Figure 5.34
A, Western blot analysis of indicated proteins.
B, qPCR analysis of indicated mRNA.
In panels B mean values ± SD are provided. (*) $P < 0.05$, and (**) $P < 0.01$.

In line with a passage through an EMT, migration and invasion was significantly elevated in DLD1_5FU cells when compared to DLD1_par cells (Figure 5.35 A). Furthermore, ectopic expression of *pri-miR-34a* reduced VIM and SNAIL expression, and significantly inhibited migration and invasion in DLD1_5FU cells (Figure 5.35 B and C).

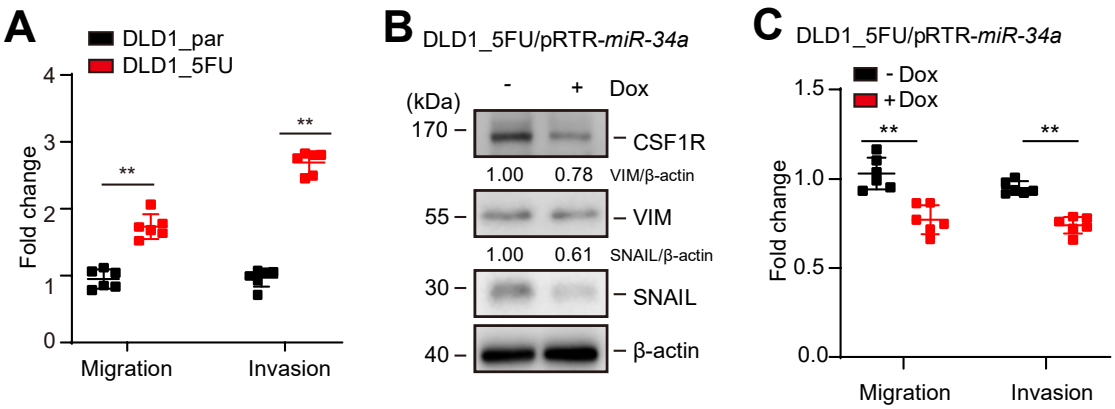

Figure 5.35
A, Analysis of relative invasion and migration using Boyden-chamber assays.
B, Western blot analysis of indicated proteins in DLD1_5FU/pRTR-*miR34a* cells after treatment with or without Dox for 72 hours.
C, Relative invasion and migration of DLD1_5FU/pRTR-*miR34a* cells after treatment with or without Dox for 72 hours.
In panels A and C mean values ± SD are provided. (**) $P < 0.01$.

Notably, down-regulation of CSF1R expression by specific siRNAs inhibited migration and invasion in DLD1_5FU cells to a similar extent as ectopic *pri-miR-34a* expression (Figure 5.36 A). Also, HT29_5FU cells displayed increased migration and invasion, which was repressed by *CSF1R*-specific siRNA or *pre-miR-34a* (Figure 5.36 B, C and D).

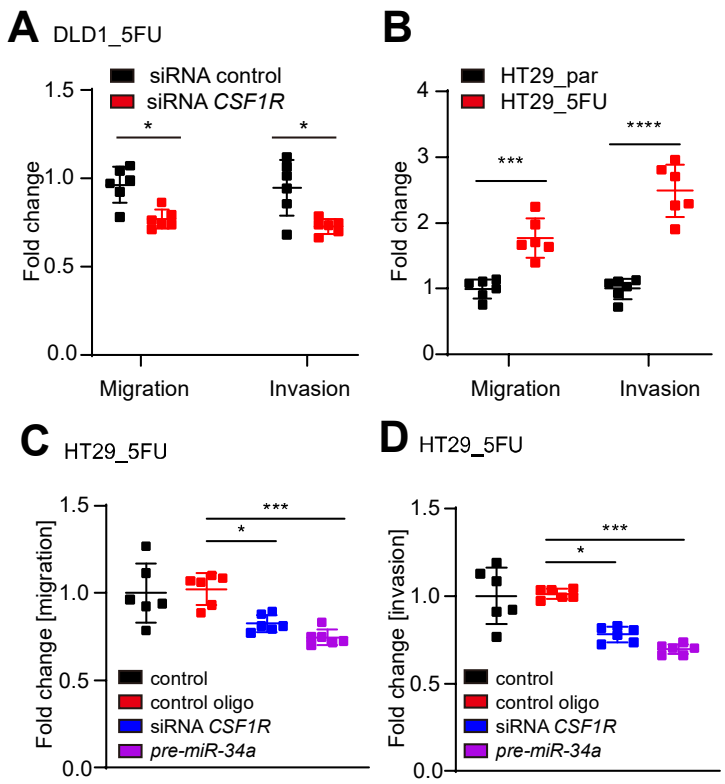

Figure 5.36

A, DLD1_5FU cells were transfected with control or *CSF1R*-specific siRNAs for 24 hours and then subjected to migration and invasion assays for another 36 hours. Subsequently, cells were fixed and stained with crystal violet.

B, Relative invasion and migration of HT29_par and HT29_5FU.

C, D, HT29_5FU cells were transfected with siRNA or *pre-miR-34a* oligo for 24 hours and then subjected to migration and invasion assays for another 36 hours.

In panels A, B, C, and D mean values ± SD are provided. (*) $P < 0.05$, (**) $P < 0.01$ and (***) $P < 0.001$.

Therefore, the enhancement of migration and invasion in 5-FU-resistant CRC cells is mediated, at least in part, by downregulation of *miR-34a* expression and the resulting up-regulation of CSF1R expression.

Treatment of DLD1_5FU cells with GW2580, a specific CSF1R inhibitor, suppressed invasion to a large extent as evidenced by a Boyden-chamber assay (Figure 5.37 A). Eight weeks after injection of DLD1_5FU cells into the tail vein of NOD/SCID mice their lungs displayed an increased number of metastases when compared to mice injected with DLD1_par cells (Figure 5.37 B and C). Pre-treatment of DLD1_5FU cells with the CSF1R-inhibitor GW2580 before injection suppressed metastasis formation in NOD/SCID mice.

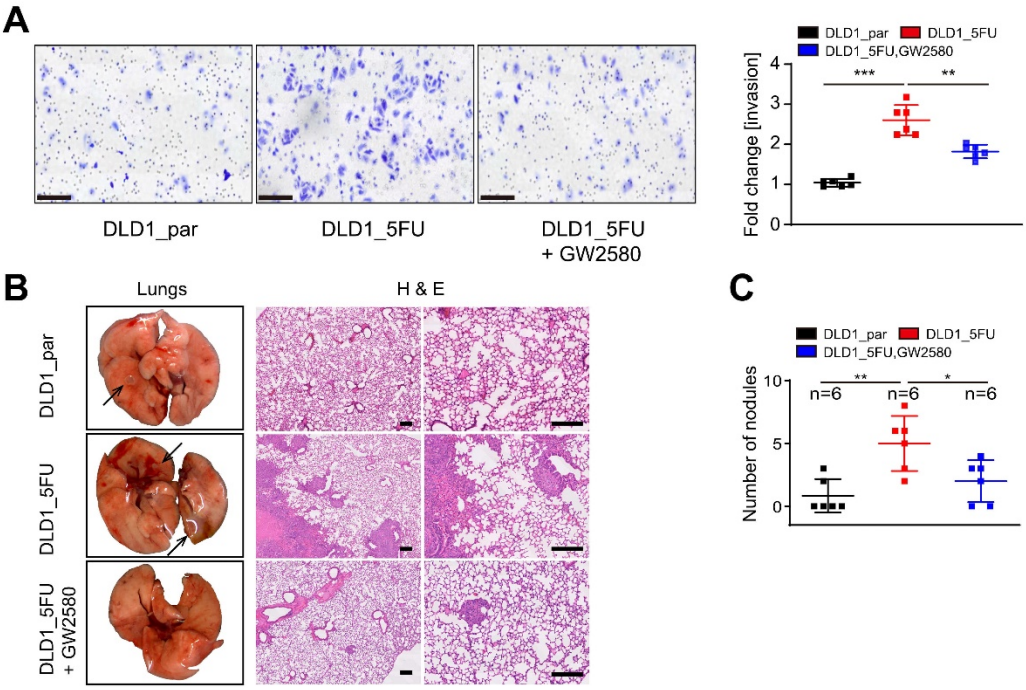

Figure 5.37

A, Cells were treated with or without inhibitor GW2580 for 48 hours and then subjected to an invasion assay in Boyden-chambers containing Matrigel for another 36 hours.

B, Left, lungs were resected 8 weeks after injection. Arrows, metastatic tumor nodules. Right, representative examples of the H&E staining of the resected lungs are shown. Scale bar, 200 µm.
C, Quantification of metastatic tumor nodules in the lung per mouse 8 weeks after tail-vein injection. Cells were treated as indicated for 48 hours and subsequently injected into the tail vein of NOD/SCID mice.
B: Xenograft experiments were performed by Dr. Matjaz Rokavec.
In panels A and C mean values ± SD are provided. (*) $P < 0.05$, (**) $P < 0.01$ and (***) $P < 0.001$.

Taken together, these results show that elevated CSF1R expression promotes metastases formation of chemo-resistant CRC cells.

5.9 Epigenetic silencing of *miR-34a* contributes to CSF1R up-regulation, 5-FU resistance and CRC progression

We have previously shown that methylation of the CpG island upstream of the *miR-34a* transcriptional start site (TSS) results in silencing of miR-34a expression (Lodygin et al., 2008). Therefore, we analyzed whether the down-regulation of miR-34a expression observed in DLD1_5FU cells is due to methylation of the *miR-34a* promoter. Whereas DLD1_par cells harboured both methylated and non-methylated *miR-34a* alleles as detected by MSP (methylation-specific PCR), DLD-1_5FU cells only displayed methylated *miR-34a* promoter alleles (Figure 5.38 A and B). In HT29_par cells only non-methylated *miR-34a* was detected, whereas HT29_5FU cells also showed methylated besides non-methylated *miR-34a* alleles. As reported previously, MiaPaCa2 pancreatic cancer cells displayed methylated and un-methylated *miR-34a* alleles (Lodygin et al., 2008). In addition, we performed a bisulfite sequencing analysis of the *miR-34a* promoter region as described before (Lodygin et al., 2008). Overall

methylation of the *miR-34a* promoter was significantly higher in DLD1_5FU than in DLD1_par cells (Figure 5.38 C).

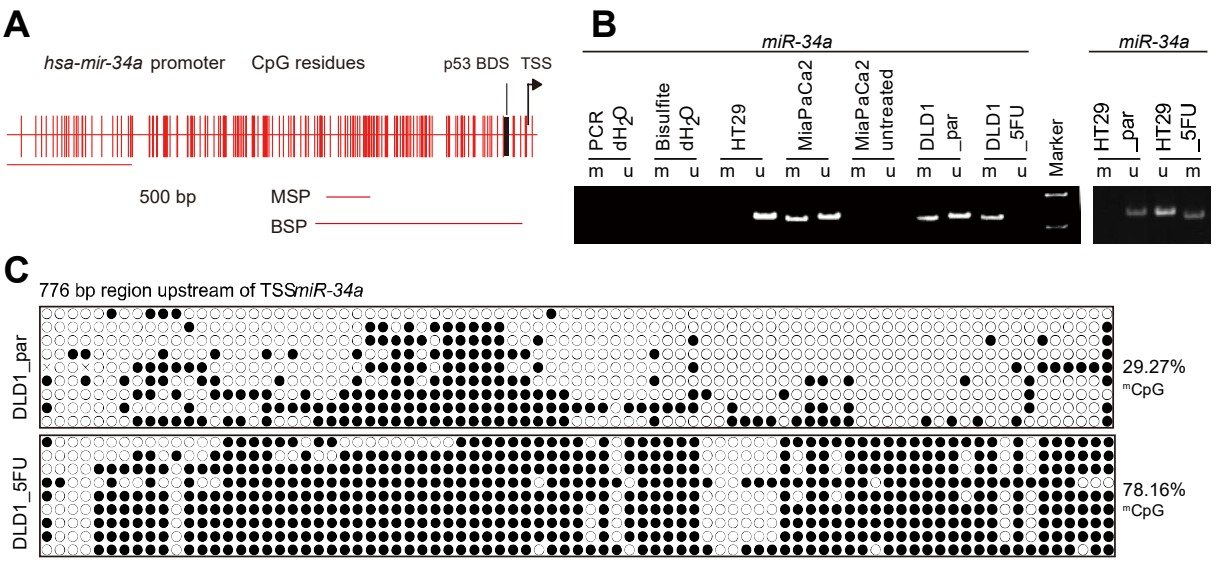

Figure 5.38

A, Genomic region 2.0 kbp upstream of the transcriptional start site (TSS, position indicated by arrow) within the human *miR-34a* gene. Vertical bars represent CpG-dinucleotides. The position of the p53 binding site (BDS) is indicated. The horizontal bars indicate PCR amplicons used for methylation-specific PCR (MSP) and bisulfite sequencing (BSP), respectively.

B, Representative results of methylation-specific PCR (MSP) analysis. M, methylation-specific PCR-product; U, un-methylated allele spec. PCR-product; Untreated: no bisulfite added; PCR dH2O, no DNA in PCR; bisulfite dH2O, no DNA input in bisulfite reaction; HT29, negative control; MiaPaCa2, positive control.

C, Bisulfite sequencing analysis of the *miR-34a* promoter in DLD1_par and DLD1_5FU cells. 9 subcloned amplification products were sequenced for each cell lines. Each horizontal line represents one individual clone, and each circle one single CpG dinucleotide. Open circles represent non-methylated and black circles methylated CpGs.

Furthermore, DLD1_5FU cells were treated with 5-aza-2'deoxycytidine (5-aza) and/or Trichostatin A (TSA), which are inhibitors of DNA methyl-transferases and histone deacetylases, respectively, in order to reactivate the expression of *miR-34a* silenced by CpG methylation. *Pri-miR-34a* was re-expressed after treatment of DLD1_5FU cells with 5-aza and further increased by the combined treatment with 5-aza and TSA (Figure 5.39 A). On the contrary, CSF1R expression was downregulated after treatment with 5-aza or the combination of 5-aza and TSA (Figure 5.39 B). Therefore, hyper-methylation of the *miR-34a* promoter decreased the expression of *miR-34a* and thereby presumably caused the up-regulation of CSF1R expression in 5-FU resistant cells.

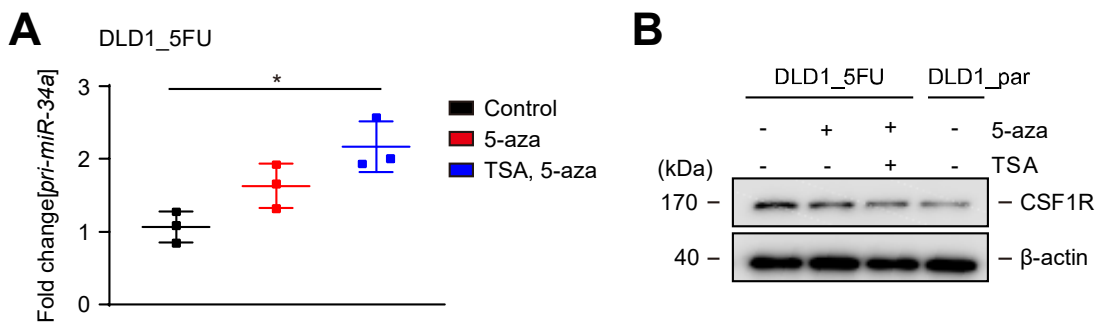

Figure 5.39

A, qPCR analysis of *pri-miR-34a* in DLD1_5FU cells after treatment with 5-aza for 72 hours or alternatively with 5-aza for 72 hours combined with TSA for the last 24 hours. **B**, Western blot analysis of cell lysates isolated from DLD1_5FU cells after treatment with 5-aza for 72 hours or alternatively with 5-aza for 72 hours combined with TSA for the last 24 hours.

In panels A mean values ± SD are provided. (*) $P < 0.05$.

Next, we determined whether the inverse correlation between *miR-34a* CpG-methylation and CSF1R expression is also present in primary CRCs. Therefore, the

expression of CSF1R protein was analyzed by immunohistochemistry in 90 CRC samples, for which the methylation status of *miR-34a* had been determined previously (Hahn et al., 2013). Notably, in CRCs with high *miR-34a* CPG methylation the expression of CSF1R protein was significantly higher than in CRCs with decreased *miR-34*a CpG methylation (Figure 5.40 A and B).

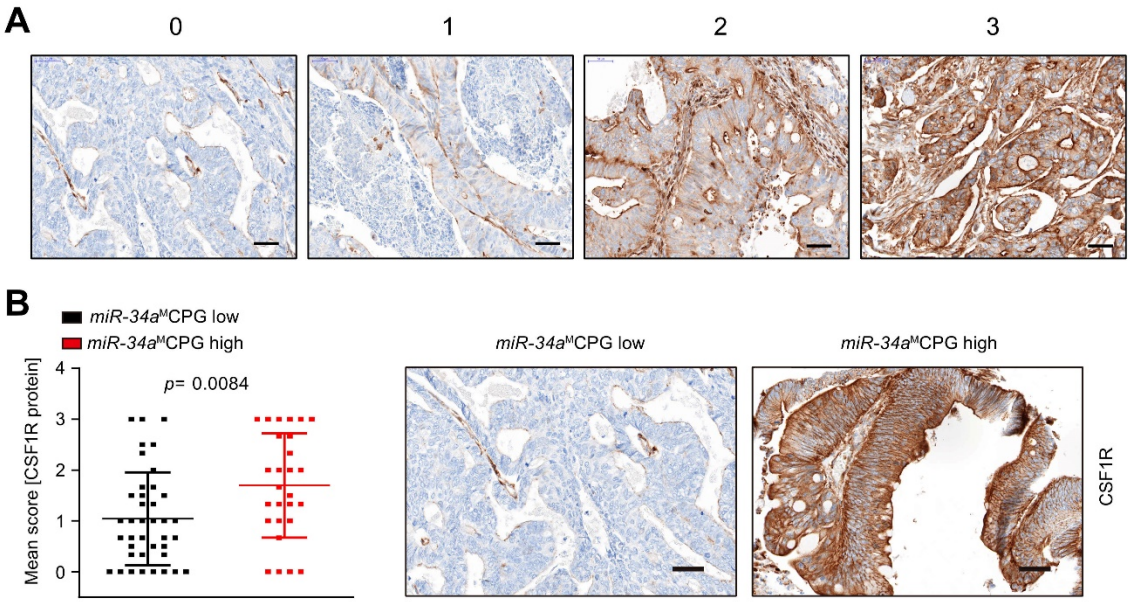

Figure 5.40

A, Immunohistochemistry score for CSF1R. The staining intensity score is 0 for absent, 1 for low, 2 for intermediate and 3 for strong signal. Representative examples are shown.

B, Left: Quantification of CSF1R protein expression in human CRC samples of 78 patients (left). The methylation status of *miR-34a* in these samples had been determined previously (Siemens, Neumann, et al., 2013). Right: Representative immunohistochemical detections of CSF1R protein in *miR-34a* $^{m}C_{P}G$ low and high tumors, respectively. Scale bar: 50 µm.

A, B: IHC was made by Professor Dr. David Horst.

Furthermore, CSF1R expression was elevated at the infiltrative tumor edge of primary CRCs that were accompanied by liver metastases (M1 tumors) when

compared to primary CRCs without liver metastases (M0; Figure 5.41). Therefore, the inverse correlation between *miR-34a* CpG-methylation and CSF1R expression was also found in primary CRCs. Furthermore, increased expression of CSF1R at the invasion front of primary CRCs was associated with distant metastasis.

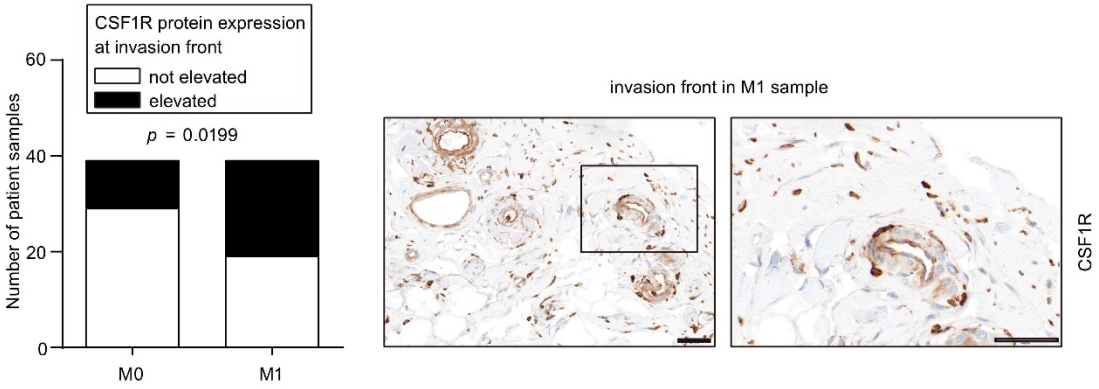

Figure 5.41

Evaluation of CSF1R protein expression at the invasion front in M0 and M1 CRCs (left chart) and examples of representative immunohistochemical detections (right panel). The presence of an invasion front was confirmed by DH, a certified pathologist. Results were analyzed using the chi-square test. Scale bar: 50 µm. IHC was made by Professor Dr. David Horst.

6. Discussion

Our results suggest that the reciprocal regulation between miR-34a and CSF1R controls EMT and chemo-sensitivity. The deregulation of this feedback loop during CRC progression may contribute to metastasis and chemo-resistance (see also the graphical abstract Figure 6.1). Since CSF1R is expressed at elevated levels in several types of tumors (Cioce et al., 2014; J. Menke et al., 2012; Patsialou et al., 2015), the regulations identified here may also be relevant to other entities. Not only CSF1R, but also its ligands CSF1 and IL34, are expressed at elevated levels in CRCs (Dang et al., 2016; Franze et al., 2018a; Mroczko et al., 2003). In the human colon expression of CSF1 is significantly higher than that of IL34, suggesting CSF1 is the main ligand for activation of CSF1R in CRC (Zwicker et al., 2015). Here, analysis of TCGA datasets and two additional cohorts of CRC patients showed that elevated mRNA levels of *CSF1R*, *CSF1* and *IL34* are associated with poor survival of CRC patients. The analysis of patient-derived xenografts (PDXs) and single cell sequencing data revealed tumor cell intrinsic expression of *CSF1R*. We determined that miR-34a directly targets CSF1R mRNA and thereby mediates the repression of CSF1R by p53. This is in line with a previous study that showed that a miR-34a mimic downregulates *csf1r* mRNA expression in rats (Chen et al., 2016). However, the authors did not provide evidence for a direct regulation nor did they study the miR-34a/CSF1R connection further. Since *CSF1R* represents a direct target of miR-34a, the elevated expression of CSF1R in CRCs may result from the epigenetic silencing of *miR-34a,* which frequently occurs in CRC (Lodygin et al., 2008; Vogt et al., 2011). Interestingly, ectopic expression of p53 not only repressed *CSF1R* via miR-34a, but also its ligand CSF1. The latter effect may be due to the induction of the microRNAs miR-148b and miR-1207 by p53, since both microRNAs are directly induced by p53 and target *CSF1* mRNA (Cimino et al., 2013;

Dang et al., 2016). Interestingly, a recent study showed that p53 deletion results in secretion of CSF1 in a pancreatic tumor model and was suggested to influence stromal cells, such as tumor-associated macrophages (Blagih et al., 2020). Our results suggest that the increased CSF1 secretion resulting from p53 inactivation/mutation may cooperate with increased CSF1R expression in a tumor cell autonomous manner.

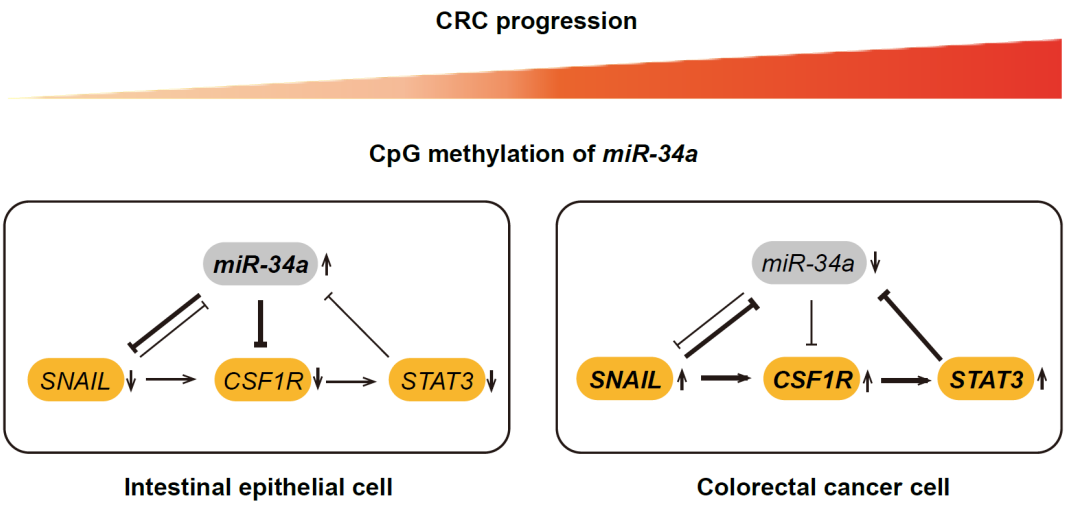

Figure 6.1
Summarizing model of the regulatory loops characterized here and their alterations during colorectal cancer progression. The thickness of the lines and arrows corresponds to the relative degrees of the indicated inhibitions and activations of expression.

Here we show that CSF1R is directly and indirectly induced by SNAIL in a coherent feed-forward loop, which involves the down-regulation of its repressor miR-34a by SNAIL (see also scheme in Figure 5.20). The regulatory circuit characterized here also involves STAT3, which is activated by CSF1R and itself represses *miR-34a*. We have previously reported, that *miR-34a* is repressed directly by STAT3, which contributes to IL6-induced EMT and invasion in CRCs and colitis-associated colon cancer (Rokavec, Oner, et al., 2014). Besides mediating SNAIL-induced invasion,

activation of CSF1R by CSF1 or IL34 induced EMT in CRC cell lines which was associated with increased migration, invasion and lung metastases formation in a xenograft mouse model. The induction of EMT by CSF1R presumably induces a mesenchymal state in primary CRCs which allows invasion, intravasation, and extravasation during metastatic spread. Interestingly, CSF2/GM-CSF has recently been shown to induce EMT in colon cancer cells and may thereby contribute to CRC progression as well (Chen et al., 2017).

5-FU-based chemotherapy represents the most common chemotherapeutic regime for CRC patients with metastatic tumors (Tong et al., 2016). However, long-term use of 5-FU usually results in drug resistance, which is a major cause of therapeutic failure (Housman et al., 2014). Here we describe the establishment of 5-FU-resistant CRC cell lines that display increased mesenchymal characteristics when compared to the parental cell lines. We found that downregulation of miR-34a and increased expression of CSF1R critically contribute to 5-FU resistance. Additional targets of miR-34a, such as *AXL, PDGFR, c-Met, c-Kit, ZNF281 and CD44*, were also upregulated in chemo-resistant DLD1 cells, suggesting that the acquisition of chemo-resistance may involve several additional factors and signaling pathways. Re-expression of miR-34a or silencing of CSF1R in DLD1_5FU and HT29_5FU cells restored the sensitivity to 5-FU, indicating the importance of the dysregulation of miR-34a and CSF1R in 5-FU resistance. Therefore, inhibiting CSF1R in combination with restoring miR-34a function may have therapeutic potential for the treatment of CRC. We have previously characterized the RTK c-kit as a miR-34a target and found that its down-regulation sensitizes CRC cells to 5-FU (Siemens, Jackstadt, Kaller, & Hermeking, 2013). In addition, other RTKs, such as AXL and PDGFR, have been characterized as miR-34a targets (Garofalo et al., 2013; Kaller et al., 2011; Silber et

al., 2012). Therefore, the repression of RTKs may represent an important mechanism of tumor suppression by miR-34a.

During the establishment of 5-FU-resistant CRC cells, *miR-34a* expression was downregulated as a consequence of CpG methylation of its promoter. This event and the resulting up-regulation of CSF1R expression critically contributed to resistance towards 5-FU. We have previously shown that the silencing of *miR-34a* in primary tumors is associated with metastasis in CRC patients and in combination with the elevated expression of c-Met and β-Catenin predicts a poor outcome (Hahn et al., 2013). Here, CSF1R was expressed at elevated levels at the invasion front of primary CRCs. Therefore, up-regulation of CSF1R expression due to *miR-34a* silencing may promote CRC progression and result in decreased survival of CRC patients. The results presented here suggest that targeting the miR-34a/CSF1R pathway might be a feasible approach to inhibit CRC metastasis and overcome resistance to 5-FU-based therapy. Taken together, targeting CSF1R may not only affect the tumor microenvironment and boost immune cells targeting the tumor (15), but may also directly inhibit tumor initiation and progression via the mechanisms described here.

7. Summary

The *miR-34a* gene is a direct target of p53 and is commonly silenced in colorectal cancer (CRC). In primary CRCs increased expression of the receptor tyrosine kinase *colony stimulating factor 1 receptor*/*CSF1R* was associated with a mesenchymal-like subtype and poor patient survival, and showed an inverse correlation with miR-34a expression, suggesting that it may represent a miR-34a target. Indeed, the 3'-UTR of *CSF1R* contains a miR-34a seed-matching site and *CSF1R* expression was directly inhibited by miR-34a. Furthermore, p53 repressed *CSF1R* via inducing *miR-34a*, whereas SNAIL and SLUG induced *CSF1R* both directly and indirectly, via repressing *miR-34a*. Activation of CSF1R inhibited *miR-34a* via STAT3. CSF1R activation was sufficient and required for EMT, migration, invasion and metastases formation of CRC cells. Acquired resistance of CRC cells to 5-FU was mediated by CpG-methylation of *miR-34a* and the resulting induction of *CSF1R*. Both alterations were required for EMT, invasion and metastases of 5-FU-resistant CRC cells. In primary CRCs elevated expression of CSF1R was detected at the invasion front and was associated with CpG methylation of the *miR-34a* promoter as well as formation of distant metastases. In conclusion, the reciprocal regulation of miR-34a and CSF1R identified here controls EMT, metastasis and chemo-sensitivity of CRC cells.

8. Zusammenfassung

Das miR-34a-Gen ist ein direktes Ziel von p53 und wird beim Kolorektal-Karzinom (KRK) in den meisten Fällen epigenetisch inaktiviert. In primären KRKs war eine erhöhte Expression des Rezeptor-Tyrosinkinase-Kolonie-stimulierenden Faktor-1-Rezeptors / CSF1R mit einem mesenchymalen Subtyp und einem schlechten Patientenüberleben assoziiert und zeigte eine inverse Korrelation mit der miR-34a-Expression, was darauf hindeutet, dass es sich bei der CSF1R mRNA möglicherweise um ein miR-34a Ziel handelt. Tatsächlich enthält der 3'-UTR von CSF1R eine miR-34a-Bindungs-Stelle und die CSF1R-Expression wurde direkt durch miR-34a inhibiert. Darüber hinaus unterdrückte p53 CSF1R durch Induktion von miR-34a, während SNAIL und SLUG CSF1R sowohl direkt als auch indirekt durch Unterdrückung von miR-34a induzierten. Die Aktivierung von CSF1R inhibierte miR-34a über STAT3. Die CSF1R-Aktivierung war ausreichend und notwendig für EMT, Migration, Invasion und Metastasenbildung von KRK-Zellen. Die erworbene 5-FU-Resistenz von KRK-Zellen wurde durch CpG-Methylierung von miR-34a und die daraus resultierende Induktion von CSF1R vermittelt. Beide Veränderungen waren für EMT, Invasion und Metastasierung von 5-FU-resistenten KRK-Zellen erforderlich. In primären KRKs wurde eine erhöhte Expression von CSF1R an der Invasionsfront nachgewiesen und war mit der CpG-Methylierung des miR-34a-Promotors sowie der Bildung von Fernmetastasen verbunden. Zusammenfassend lässt sich sagen, dass die hier identifizierte wechselseitige Regulation von miR-34a und CSF1R die EMT, Metastasierung und Chemosensitivität von KRK-Zellen steuert.

9. Acknowledgements

First of all, my deepest gratitude goes first and foremost to my supervisor, Prof. Heiko Hermeking, for offering me the opportunity to work in such a great laboratory, for his continuous support, scientific input, and help during my doctoral study. I have learned much from him about what the characteristics of a respected scientist are. His passion for science will influence me in my future research. This thesis could not be finished without his consistent and patient guidance.

Moreover, I would like to thank all the former and present members of AG Hermeking for their kind help and support in the past years. Especially I would like to thank Dr. Markus Kaller for the initial experiments, helpful discussion, and priceless knowledge. He is so smart that knows everything and can solve all the problems that I met. I would like to thank Ursula Götz for her great technical support and help with every problem in the lab.

Furthermore, I would like to express my gratitude to Dr. Longchang Jiang, Dr. Huihui Li, Dr. Yina Zhang, Jinjiang Chou, Fangteng Liu, Wenjing Shi, Chunfeng Liu and Zekai Huang for their great scientific help and support.

And last but not least I would like to express my gratitude to my wife who has always been supporting me without a word of complaint. Words are powerless to express my love to her.

10. References

Amati, B., Frank, S. R., Donjerkovic, D., & Taubert, S. (2001). Function of the c-Myc oncoprotein in chromatin remodeling and transcription. *Biochimica et Biophysica Acta, 1471*(3), M135-145.

Bencheikh, L., Diop, M. K., Riviere, J., Imanci, A., Pierron, G., Souquere, S., . . . Droin, N. (2019). Dynamic gene regulation by nuclear colony-stimulating factor 1 receptor in human monocytes and macrophages. *Nat Commun, 10*(1), 1935. doi: 10.1038/s41467-019-09970-9

Blagih, J., Zani, F., Chakravarty, P., Hennequart, M., Pilley, S., Hobor, S., . . . Vousden, K. H. (2020). Cancer-Specific Loss of p53 Leads to a Modulation of Myeloid and T Cell Responses. *Cell Rep, 30*(2), 481-496 e486. doi:10.1016/j.celrep.2019.12.028

Boire, A., Brastianos, P. K., Garzia, L., & Valiente, M. (2020). Brain metastasis. *Nature Reviews: Cancer, 20*(1), 4-11. doi:10.1038/s41568-019-0220-y

Bolos, V., Peinado, H., Perez-Moreno, M. A., Fraga, M. F., Esteller, M., & Cano, A. (2003). The transcription factor Slug represses E-cadherin expression and induces epithelial to mesenchymal transitions: a comparison with Snail and E47 repressors. *Journal of Cell Science, 116*(Pt 3), 499-511. doi:10.1242/jcs.00224

Bray, F., Ferlay, J., Soerjomataram, I., Siegel, R. L., Torre, L. A., & Jemal, A. (2018). Global cancer statistics 2018: GLOBOCAN estimates of incidence and mortality worldwide for 36 cancers in 185 countries. *CA Cancer J Clin, 68*(6), 394-424. doi:10.3322/caac.21492

Brenner, H., Kloor, M., & Pox, C. P. (2014). Colorectal cancer. *Lancet, 383*(9927), 1490-1502. doi:10.1016/S0140-6736(13)61649-9

Byrne, P. V., Guilbert, L. J., & Stanley, E. R. (1981). Distribution of cells bearing rece ptors for a colony-stimulating factor (CSF-1) in murine tissues. *Journal of Cell Biology, 91*(3 Pt 1), 848-853.

Calon, A., Lonardo, E., Berenguer-Llergo, A., Espinet, E., Hernando-Momblona, X., Ig lesias, M., . . . Batlle, E. (2015). Stromal gene expression defines poor-progno sis subtypes in colorectal cancer. *Nat Genet, 47*(4), 320-329. doi:10.1038/ng.3 225

Cancer Genome Atlas, N. (2012). Comprehensive molecular characterization of hum an colon and rectal cancer. *Nature, 487*(7407), 330-337. doi:10.1038/nature11 252

Cannarile, M. A., Weisser, M., Jacob, W., Jegg, A. M., Ries, C. H., & Ruttinger, D. (20 17). Colony-stimulating factor 1 receptor (CSF1R) inhibitors in cancer therapy. *J Immunother Cancer, 5*(1), 53. doi:10.1186/s40425-017-0257-y

Chen, Y., Cao, S., Xu, P., Han, W., Shan, T., Pan, J., . . . Wang, X. (2016). Changes i n the Expression of miR-34a and its Target Genes Following Spinal Cord Injur y In Rats. *Med Sci Monit, 22*, 3981-3993. doi:10.12659/msm.900893

Chen, Y., Zhao, Z., Chen, Y., Lv, Z., Ding, X., Wang, R., . . . Chen, G. (2017). An epit helial-to-mesenchymal transition-inducing potential of granulocyte macrophage colony-stimulating factor in colon cancer. *Sci Rep, 7*(1), 8265. doi:10.1038/s41 598-017-08047-1

Chockalingam, S., & Ghosh, S. S. (2014). Macrophage colony-stimulating factor and cancer: a review. *Tumour Biol, 35*(11), 10635-10644. doi:10.1007/s13277-014-2627-0

Christoffersen, N. R., Shalgi, R., Frankel, L. B., Leucci, E., Lees, M., Klausen, M., . . . Lund, A. H. (2010). p53-independent upregulation of miR-34a during oncogene

-induced senescence represses MYC. *Cell Death Differ, 17*(2), 236-245. doi:10.1038/cdd.2009.109

Cimino, D., De Pitta, C., Orso, F., Zampini, M., Casara, S., Penna, E., . . . Taverna, D. (2013). miR148b is a major coordinator of breast cancer progression in a relapse-associated microRNA signature by targeting ITGA5, ROCK1, PIK3CA, NRAS, and CSF1. *FASEB Journal, 27*(3), 1223-1235. doi:10.1096/fj.12-214692

Cioce, M., Canino, C., Goparaju, C., Yang, H., Carbone, M., & Pass, H. I. (2014). Autocrine CSF-1R signaling drives mesothelioma chemoresistance via AKT activation. *Cell Death Dis, 5*, e1167. doi:10.1038/cddis.2014.136

Coussens, L., Van Beveren, C., Smith, D., Chen, E., Mitchell, R. L., Isacke, C. M., . . . Ullrich, A. (1986). Structural alteration of viral homologue of receptor proto-oncogene fms at carboxyl terminus. *Nature, 320*(6059), 277-280. doi:10.1038/320277a0

Dang, W., Qin, Z., Fan, S., Wen, Q., Lu, Y., Wang, J., . . . Ma, J. (2016). miR-1207-5p suppresses lung cancer growth and metastasis by targeting CSF1. *Oncotarget, 7*(22), 32421-32432. doi:10.18632/oncotarget.8718

De Craene, B., & Berx, G. (2013). Regulatory networks defining EMT during cancer initiation and progression. *Nature Reviews: Cancer, 13*(2), 97-110. doi:10.1038/nrc3447

Dekker, E., Tanis, P. J., Vleugels, J. L. A., Kasi, P. M., & Wallace, M. B. (2019). Colorectal cancer. *Lancet, 394*(10207), 1467-1480. doi:10.1016/S0140-6736(19)32319-0

Favoriti, P., Carbone, G., Greco, M., Pirozzi, F., Pirozzi, R. E., & Corcione, F. (2016). Worldwide burden of colorectal cancer: a review. *Updates Surg, 68*(1), 7-11. doi:10.1007/s13304-016-0359-y

Fearon, E. R., & Vogelstein, B. (1990). A genetic model for colorectal tumorigenesis. *Cell, 61*(5), 759-767. doi:10.1016/0092-8674(90)90186-i

Franze, E., Dinallo, V., Rizzo, A., Di Giovangiulio, M., Bevivino, G., Stolfi, C., . . . Monteleone, G. (2018a). Interleukin-34 sustains pro-tumorigenic signals in colon cancer tissue. *Oncotarget, 9*(3), 3432-3445. doi:10.18632/oncotarget.23289

Franze, E., Dinallo, V., Rizzo, A., Di Giovangiulio, M., Bevivino, G., Stolfi, C., . . . Monteleone, G. (2018b). Interleukin-34 sustains pro-tumorigenic signals in colon cancer tissue. *Oncotarget, 9*(1949-2553 (Electronic)), 3432-3445. doi:10.18632/oncotarget.23289

Garofalo, M., Jeon, Y. J., Nuovo, G. J., Middleton, J., Secchiero, P., Joshi, P., . . . Croce, C. M. (2013). MiR-34a/c-Dependent PDGFR-alpha/beta Downregulation Inhibits Tumorigenesis and Enhances TRAIL-Induced Apoptosis in Lung Cancer. *PLoS One, 8*(6), e67581. doi:10.1371/journal.pone.0067581

Gill, J. G., Langer, E. M., Lindsley, R. C., Cai, M., Murphy, T. L., Kyba, M., & Murphy, K. M. (2011). Snail and the microRNA-200 family act in opposition to regulate epithelial-to-mesenchymal transition and germ layer fate restriction in differentiating ESCs. *Stem Cells, 29*(5), 764-776. doi:10.1002/stem.628

Guilbert, L. J., & Stanley, E. R. (1980). Specific interaction of murine colony-stimulating factor with mononuclear phagocytic cells. *Journal of Cell Biology, 85*(1), 153-159.

Guinney, J., Dienstmann, R., Wang, X., de Reynies, A., Schlicker, A., Soneson, C., . . . Tejpar, S. (2015). The consensus molecular subtypes of colorectal cancer. *Nat Med, 21*(11), 1350-1356. doi:10.1038/nm.3967

Hahn, S., & Hermeking, H. (2014). ZNF281/ZBP-99: a new player in epithelial-mesen chymal transition, stemness, and cancer. *J Mol Med (Berl), 92*(6), 571-581. do i:10.1007/s00109-014-1160-3

Hahn, S., Jackstadt, R., Siemens, H., Hunten, S., & Hermeking, H. (2013). SNAIL an d miR-34a feed-forward regulation of ZNF281/ZBP99 promotes epithelial-mes enchymal transition. *EMBO J, 32*(23), 3079-3095. doi:10.1038/emboj.2013.23 6

Heisterkamp N Fau - Groffen, J., Groffen J Fau - Stephenson, J. R., & Stephenson, J. R. (1983). Isolation of v-fms and its human cellular homolog. *Virology, 126*(1), 248-258.

Hermeking, H. (2007). p53 enters the microRNA world. *Cancer Cell, 12*(5), 414-418. doi:10.1016/j.ccr.2007.10.028

Hermeking, H. (2012). MicroRNAs in the p53 network: micromanagement of tumour s uppression. *Nature Reviews: Cancer, 12*(9), 613-626. doi:10.1038/nrc3318

Housman, G., Byler, S., Heerboth, S., Lapinska, K., Longacre, M., Snyder, N., & Sark ar, S. (2014). Drug resistance in cancer: an overview. *Cancers (Basel), 6*(3), 1 769-1792. doi:10.3390/cancers6031769

Hunten, S., Kaller, M., Drepper, F., Oeljeklaus, S., Bonfert, T., Erhard, F., . . . Hermek ing, H. (2015). p53-Regulated Networks of Protein, mRNA, miRNA, and lncRN A Expression Revealed by Integrated Pulsed Stable Isotope Labeling With Ami no Acids in Cell Culture (pSILAC) and Next Generation Sequencing (NGS) An alyses. *Mol Cell Proteomics, 14*(10), 2609-2629. doi:10.1074/mcp.M115.05023 7

Isella, C., Brundu, F., Bellomo, S. E., Galimi, F., Zanella, E., Porporato, R., . . . Bertott i, A. (2017). Selective analysis of cancer-cell intrinsic transcriptional traits defin

es novel clinically relevant subtypes of colorectal cancer. *Nat Commun, 8*, 151 07. doi:10.1038/ncomms15107

Isella, C., Terrasi, A., Bellomo, S. E., Petti, C., Galatola, G., Muratore, A., . . . Medico, E. (2015). Stromal contribution to the colorectal cancer transcriptome. *Nature Genetics, 47*(4), 312-319. doi:10.1038/ng.3224

Jackstadt, R., Roh, S., Neumann, J., Jung, P., Hoffmann, R., Horst, D., . . . Hermekin g, H. (2013). AP4 is a mediator of epithelial-mesenchymal transition and metas tasis in colorectal cancer. *J Exp Med, 210*(7), 1331-1350. doi:10.1084/jem.201 20812

Jass, J. R. (2007). Classification of colorectal cancer based on correlation of clinical, morphological and molecular features. *Histopathology, 50*(1), 113-130. doi:10. 1111/j.1365-2559.2006.02549.x

Jiang, L., & Hermeking, H. (2017). miR-34a and miR-34b/c Suppress Intestinal Tumo rigenesis. *Cancer Res, 77*(10), 2746-2758. doi:10.1158/0008-5472.CAN-16-21 83

Kaller, M., Liffers, S. T., Oeljeklaus, S., Kuhlmann, K., Roh, S., Hoffmann, R., . . . Her meking, H. (2011). Genome-wide characterization of miR-34a induced change s in protein and mRNA expression by a combined pulsed SILAC and microarra y analysis. *Mol Cell Proteomics, 10*(8), M111 010462. doi:10.1074/mcp.M111. 010462

Kang, Y., & Massague, J. (2004). Epithelial-mesenchymal transitions: twist in develop ment and metastasis. *Cell, 118*(3), 277-279. doi:10.1016/j.cell.2004.07.011

Khazaei, S., Rezaeian, S., Khazaei, S., Mansori, K., Sanjari Moghaddam, A., & Ayub i, E. (2016). Effects of Human Development Index and Its Components on Col

orectal Cancer Incidence and Mortality: a Global Ecological Study. *Asian Pac J Cancer Prev, 17*(S3), 253-256. doi:10.7314/apjcp.2016.17.s3.253

Krebs, A. M., Mitschke, J., Lasierra Losada, M., Schmalhofer, O., Boerries, M., Busch, H., . . . Brabletz, T. (2017). The EMT-activator Zeb1 is a key factor for cell plasticity and promotes metastasis in pancreatic cancer. *Nature Cell Biology, 19*(5), 518-529. doi:10.1038/ncb3513

Laibe, S., Lagarde, A., Ferrari, A., Monges, G., Birnbaum, D., Olschwang, S., & Project, C. O. L. (2012). A seven-gene signature aggregates a subgroup of stage II colon cancers with stage III. *OMICS, 16*(10), 560-565. doi:10.1089/omi.2012.0039

Lemmon, M. A., & Schlessinger, J. (2010). Cell signaling by receptor tyrosine kinases. *Cell, 141*(7), 1117-1134. doi:10.1016/j.cell.2010.06.011

Li, H., Courtois, E. T., Sengupta, D., Tan, Y., Chen, K. H., Goh, J. J. L., . . . Prabhakar, S. (2017). Reference component analysis of single-cell transcriptomes elucidates cellular heterogeneity in human colorectal tumors. *Nature Genetics, 49*(5), 708-718. doi:10.1038/ng.3818

Li, H., Rokavec, M., Jiang, L., Horst, D., & Hermeking, H. (2017). Antagonistic Effects of p53 and HIF1A on microRNA-34a Regulation of PPP1R11 and STAT3 and Hypoxia-induced Epithelial to Mesenchymal Transition in Colorectal Cancer Cells. *Gastroenterology, 153*(2), 505-520. doi:10.1053/j.gastro.2017.04.017

Liberzon, A., Birger, C., Thorvaldsdottir, H., Ghandi, M., Mesirov, J. P., & Tamayo, P. (2015). The Molecular Signatures Database (MSigDB) hallmark gene set collection. *Cell Syst, 1*(6), 417-425. doi:10.1016/j.cels.2015.12.004

Livak, K. J., & Schmittgen, T. D. (2001). Analysis of relative gene expression data using real-time quantitative PCR and the 2− ΔΔCT method. *Methods, 25*(4), 402-408.

Lodygin, D., Tarasov, V., Epanchintsev, A., Berking, C., Knyazeva, T., Korner, H., . . . Hermeking, H. (2008). Inactivation of miR-34a by aberrant CpG methylation in multiple types of cancer. *Cell Cycle, 7*(16), 2591-2600. doi:10.4161/cc.7.16.6533

Manfredi, S., Lepage, C., Hatem, C., Coatmeur, O., Faivre, J., & Bouvier, A. M. (2006). Epidemiology and management of liver metastases from colorectal cancer. *Ann Surg, 244*(2), 254-259. doi:10.1097/01.sla.0000217629.94941.cf

Mani, S. A., Guo, W., Liao, M. J., Eaton, E. N., Ayyanan, A., Zhou, A. Y., . . . Weinberg, R. A. (2008). The epithelial-mesenchymal transition generates cells with properties of stem cells. *Cell, 133*(4), 704-715. doi:10.1016/j.cell.2008.03.027

Marisa, L., de Reynies, A., Duval, A., Selves, J., Gaub, M. P., Vescovo, L., . . . Boige, V. (2013). Gene expression classification of colon cancer into molecular subtypes: characterization, validation, and prognostic value. *PLoS Med, 10*(5), e1001453. doi:10.1371/journal.pmed.1001453

Menke, J., Kriegsmann, J., Schimanski, C. C., Schwartz, M. M., Schwarting, A., & Kelley, V. R. (2012). Autocrine CSF-1 and CSF-1 Receptor Co-expression Promotes Renal Cell Carcinoma Growth. *Cancer Research, 72*(1), 187-200. doi:10.1158/0008-5472.CAN-11-1232

Menke, J., Kriegsmann, J., Schimanski, C. C., Schwartz, M. M., Schwarting, A., & Kelley, V. R. (2012). Autocrine CSF-1 and CSF-1 receptor coexpression promotes renal cell carcinoma growth. *Cancer Res, 72*(1), 187-200. doi:10.1158/0008-5472.can-11-1232

Menssen, A., Epanchintsev, A., Lodygin, D., Rezaei, N., Jung, P., Verdoodt, B., . . . H ermeking, H. (2007). c-MYC delays prometaphase by direct transactivation of MAD2 and BubR1: identification of mechanisms underlying c-MYC-induced D NA damage and chromosomal instability. *Cell Cycle, 6*(3), 339-352.

Mroczko, B., Szmitkowski, M., & Okulczyk, B. (2003). Hematopoietic growth factors in colorectal cancer patients. *Clin Chem Lab Med, 41*(5), 646-651. doi:10.1515/C CLM.2003.098

Nandi, S., Cioce, M., Yeung, Y. G., Nieves, E., Tesfa, L., Lin, H., . . . Stanley, E. R. (2 013). Receptor-type protein-tyrosine phosphatase zeta is a functional receptor for interleukin-34. *J Biol Chem, 288*(30), 21972-21986. doi:10.1074/jbc.M112.4 42731

Natarajan, S. K., Stringham, B. A., Mohr, A. M., Wehrkamp, C. J., Lu, S., Phillippi, M. A., . . . Mott, J. L. (2017). FoxO3 increases miR-34a to cause palmitate-induce d cholangiocyte lipoapoptosis. *Journal of Lipid Research, 58*(5), 866-875. doi:1 0.1194/jlr.M071357

Network, C. G. A. (2012). Comprehensive molecular characterization of human colon and rectal cancer. *Nature, 487*(7407), 330.

Nieto, M. A., Huang, R. Y., Jackson, R. A., & Thiery, J. P. (2016). Emt: 2016. *Cell, 16 6*(1), 21-45. doi:10.1016/j.cell.2016.06.028

Novak, U., Harpur, A. G., Paradiso, L., Kanagasundaram, V., Jaworowski, A., Wilks, A. F., & Hamilton, J. A. (1995). Colony-stimulating factor 1-induced STAT1 and STAT3 activation is accompanied by phosphorylation of Tyk2 in macrophages and Tyk2 and JAK1 in fibroblasts. *Blood, 86*(8), 2948-2956.

Okita, A., Takahashi, S., Ouchi, K., Inoue, M., Watanabe, M., Endo, M., . . . Ishioka, C. (2018). Consensus molecular subtypes classification of colorectal cancer as

a predictive factor for chemotherapeutic efficacy against metastatic colorectal cancer. *Oncotarget, 9*(27), 18698-18711. doi:10.18632/oncotarget.24617

Oner, M. G., Rokavec, M., Kaller, M., Bouznad, N., Horst, D., Kirchner, T., & Hermeking, H. (2018). Combined Inactivation of TP53 and MIR34A Promotes Colorectal Cancer Development and Progression in Mice Via Increasing Levels of IL6R and PAI1. *Gastroenterology, 155*(6), 1868-1882. doi:10.1053/j.gastro.2018.08.011

Patsialou, A., Wang, Y., Pignatelli, J., Chen, X., Entenberg, D., Oktay, M., & Condeelis, J. S. Autocrine CSF1R signaling mediates switching between invasion and proliferation downstream of TGFbeta in claudin-low breast tumor cells. (1476-5594 (Electronic)).

Patsialou, A., Wang, Y., Pignatelli, J., Chen, X., Entenberg, D., Oktay, M., & Condeelis, J. S. (2015). Autocrine CSF1R signaling mediates switching between invasion and proliferation downstream of TGFbeta in claudin-low breast tumor cells. *Oncogene, 34*(21), 2721-2731. doi:10.1038/onc.2014.226

Peinado, H., Ballestar, E., Esteller, M., & Cano, A. (2004). Snail mediates E-cadherin repression by the recruitment of the Sin3A/histone deacetylase 1 (HDAC1)/HDAC2 complex. *Molecular and Cellular Biology, 24*(1), 306-319. doi:10.1128/mcb.24.1.306-319.2004

Pillai, R. S., Bhattacharyya, S. N., Artus, C. G., Zoller, T., Cougot, N., Basyuk, E., . . . Filipowicz, W. (2005). Inhibition of translational initiation by Let-7 MicroRNA in human cells. *Science, 309*(5740), 1573-1576. doi:10.1126/science.1115079

Pixley, F. J., & Stanley, E. R. (2004). CSF-1 regulation of the wandering macrophage: complexity in action. *Trends in Cell Biology, 14*(11), 628-638. doi:10.1016/j.tcb.2004.09.016

Pyonteck, S. M., Akkari, L., Schuhmacher, A. J., Bowman, R. L., Sevenich, L., Quail, D. F., . . . Joyce, J. A. (2013). CSF-1R inhibition alters macrophage polarizatio n and blocks glioma progression. *Nat Med, 19*(10), 1264-1272. doi:10.1038/n m.3337

Richardsen, E., Uglehus, R. D., Johnsen, S. H., & Busund, L. T. (2015). Macrophage-colony stimulating factor (CSF1) predicts breast cancer progression and mortal ity. *Anticancer Research, 35*(2), 865-874.

Rokavec, M., Kaller, M., Horst, D., & Hermeking, H. (2017). Pan-cancer EMT-signatur e identifies RBM47 down-regulation during colorectal cancer progression. *Sci Rep, 7*(1), 4687. doi:10.1038/s41598-017-04234-2

Rokavec, M., Li, H., Jiang, L., & Hermeking, H. (2014). The p53/miR-34 axis in develo pment and disease. *J Mol Cell Biol, 6*(3), 214-230. doi:10.1093/jmcb/mju003

Rokavec, M., Oner, M. G., Li, H., Jackstadt, R., Jiang, L., Lodygin, D., . . . Hermeking, H. (2014). IL-6R/STAT3/miR-34a feedback loop promotes EMT-mediated colo rectal cancer invasion and metastasis. *J Clin Invest, 124*(4), 1853-1867. doi:10. 1172/JCI73531

Roussel, M. F., Downing, J. R., Rettenmier, C. W., & Sherr, C. J. (1988). A point muta tion in the extracellular domain of the human CSF-1 receptor (c-fms proto-onco gene product) activates its transforming potential. *Cell, 55*(6), 979-988. doi:10. 1016/0092-8674(88)90243-7

Roussel, M. F., Dull, T. J., Rettenmier, C. W., Ralph, P., Ullrich, A., & Sherr, C. J. (19 87). Transforming potential of the c-fms proto-oncogene (CSF-1 receptor). *Nat ure, 325*(6104), 549-552. doi:10.1038/325549a0

Roussel, M. F., Sherr, C. J., Barker, P. E., & Ruddle, F. H. (1983). Molecular cloning of the c-fms locus and its assignment to human chromosome 5. *J Virol, 48*(3), 770-773.

Sale, M. J., Balmanno, K., Saxena, J., Ozono, E., Wojdyla, K., McIntyre, R. E., . . . Cook, S. J. (2019). MEK1/2 inhibitor withdrawal reverses acquired resistance driven by BRAF(V600E) amplification whereas KRAS(G13D) amplification promotes EMT-chemoresistance. *Nat Commun, 10*(1), 2030. doi:10.1038/s41467-019-09438-w

Septisetyani, E. P., Ningrum, R. A., Romadhani, Y., Wisnuwardhani, P. H., & Santoso, A. (2014). Optimization of Sodium Dodecyl Sulphate as a Formazan Solvent and Comparison of 3-(4,-5-Dimethylthiazo-2-Yl)-2,5-Diphenyltetrazolium Bromide (Mtt) Assay with Wst-1 Assay in Mcf-7 Cells. *Indonesian Journal of Pharmacy, 25*(4), 245. doi:10.14499/indonesianjpharm25iss4pp245

Shi, L., Jackstadt, R., Siemens, H., Li, H., Kirchner, T., & Hermeking, H. (2014). p53-induced miR-15a/16-1 and AP4 form a double-negative feedback loop to regulate epithelial-mesenchymal transition and metastasis in colorectal cancer. *Cancer Res, 74*(2), 532-542. doi:10.1158/0008-5472.CAN-13-2203

Siemens, H., Jackstadt, R., Hunten, S., Kaller, M., Menssen, A., Gotz, U., & Hermeking, H. (2011). miR-34 and SNAIL form a double-negative feedback loop to regulate epithelial-mesenchymal transitions. *Cell Cycle, 10*(24), 4256-4271. doi:10.4161/cc.10.24.18552

Siemens, H., Jackstadt, R., Kaller, M., & Hermeking, H. (2013). Repression of c-Kit by p53 is mediated by miR-34 and is associated with reduced chemoresistance, migration and stemness. *Oncotarget, 4*(9), 1399-1415. doi:10.18632/oncotarget.1202

Siemens, H., Neumann, J., Jackstadt, R., Mansmann, U., Horst, D., Kirchner, T., & H ermeking, H. (2013). Detection of miR-34a promoter methylation in combinatio n with elevated expression of c-Met and beta-catenin predicts distant metastas is of colon cancer. *Clin Cancer Res, 19*(3), 710-720. doi:10.1158/1078-0432.C CR-12-1703

Silber, J., Jacobsen, A., Ozawa, T., Harinath, G., Pedraza, A., Sander, C., . . . Huse, J. T. (2012). miR-34a repression in proneural malignant gliomas upregulates e xpression of its target PDGFRA and promotes tumorigenesis. *PLoS One, 7*(3), e33844. doi:10.1371/journal.pone.0033844

Smith, R. A., Andrews, K. S., Brooks, D., Fedewa, S. A., Manassaram-Baptiste, D., S aslow, D., . . . Wender, R. C. (2018). Cancer screening in the United States, 20 18: A review of current American Cancer Society guidelines and current issues in cancer screening. *CA Cancer J Clin, 68*(4), 297-316. doi:10.3322/caac.214 46

Subramanian, A., Tamayo, P., Mootha, V. K., Mukherjee, S., Ebert, B. L., Gillette, M. A., . . . Mesirov, J. P. (2005). Gene set enrichment analysis: a knowledge-base d approach for interpreting genome-wide expression profiles. *Proc Natl Acad S ci U S A, 102*(43), 15545-15550. doi:10.1073/pnas.0506580102

Sveen, A., Bruun, J., Eide, P. W., Eilertsen, I. A., Ramirez, L., Murumagi, A., . . . Loth e, R. A. (2018). Colorectal Cancer Consensus Molecular Subtypes Translated to Preclinical Models Uncover Potentially Targetable Cancer Cell Dependencie s. *Clin Cancer Res, 24*(4), 794-806. doi:10.1158/1078-0432.CCR-17-1234

Tarasov, V., Jung, P., Verdoodt, B., Lodygin, D., Epanchintsev, A., Menssen, A., . . . Hermeking, H. (2007). Differential regulation of microRNAs by p53 revealed by

massively parallel sequencing: miR-34a is a p53 target that induces apoptosis and G1-arrest. *Cell Cycle, 6*(13), 1586-1593. doi:10.4161/cc.6.13.4436

Thiery, J. P., Acloque, H., Huang, R. Y., & Nieto, M. A. (2009). Epithelial-mesenchymal transitions in development and disease. *Cell, 139*(5), 871-890. doi:10.1016/j.cell.2009.11.007

Tong, M., Zheng, W., Li, H., Li, X., Ao, L., Shen, Y., . . . Guo, Z. (2016). Multi-omics landscapes of colorectal cancer subtypes discriminated by an individualized prognostic signature for 5-fluorouracil-based chemotherapy. *Oncogenesis, 5*(7), e242. doi:10.1038/oncsis.2016.51

Ullrich, A., & Schlessinger, J. (1990). Signal transduction by receptors with tyrosine kinase activity. *Cell, 61*(2), 203-212. doi:10.1016/0092-8674(90)90801-k

Vogt, M., Munding, J., Gruner, M., Liffers, S. T., Verdoodt, B., Hauk, J., . . . Hermeking, H. (2011). Frequent concomitant inactivation of miR-34a and miR-34b/c by CpG methylation in colorectal, pancreatic, mammary, ovarian, urothelial, and renal cell carcinomas and soft tissue sarcomas. *Virchows Arch, 458*(3), 313-322. doi:10.1007/s00428-010-1030-5

Wang, H., Shao, Q., Sun, J., Ma, C., Gao, W., Wang, Q., . . . Qu, X. (2016). Interactions between colon cancer cells and tumor-infiltrated macrophages depending on cancer cell-derived colony stimulating factor 1. *Oncoimmunology, 5*(4), e1122157. doi:10.1080/2162402X.2015.1122157

Wang, Y., Szretter, K. J., Vermi, W., Gilfillan, S., Rossini, C., Cella, M., . . . Colonna, M. (2012). IL-34 is a tissue-restricted ligand of CSF1R required for the development of Langerhans cells and microglia. *Nature Immunology, 13*(8), 753-760. doi:10.1038/ni.2360

Welch, C., Chen, Y., & Stallings, R. L. (2007). MicroRNA-34a functions as a potential tumor suppressor by inducing apoptosis in neuroblastoma cells. *Oncogene, 26* (34), 5017-5022. doi:10.1038/sj.onc.1210293

Wyckoff, J., Wang W Fau - Lin, E. Y., Lin Ey Fau - Wang, Y., Wang Y Fau - Pixley, F., Pixley F Fau - Stanley, E. R., Stanley Er Fau - Graf, T., . . . Condeelis, J. A pa racrine loop between tumor cells and macrophages is required for tumor cell m igration in mammary tumors. (0008-5472 (Print)).

Yarden, Y., & Ullrich, A. (1988). Growth factor receptor tyrosine kinases. *Annual Revi ew of Biochemistry, 57*, 443-478. doi:10.1146/annurev.bi.57.070188.002303

Zhao, P., Gao, D., Wang, Q., Song, B., Shao, Q., Sun, J., . . . Qu, X. (2015). Respons e gene to complement 32 (RGC-32) expression on M2-polarized and tumor-as sociated macrophages is M-CSF-dependent and enhanced by tumor-derived I L-4. *Cell Mol Immunol, 12*(6), 692-699. doi:10.1038/cmi.2014.108

Zwicker, S., Martinez, G. L., Bosma, M., Gerling, M., Clark, R., Majster, M., . . . Bostro m, E. A. (2015). Interleukin 34: a new modulator of human and experimental in flammatory bowel disease. *Clin Sci (Lond), 129*(3), 281-290. doi:10.1042/CS20 150176

11. Curriculum Vitae

Xiaolong Shi

Date of birth: 24.03.1984

Place of birth: Shaanxi, China

Education:

2005-2009 Shaanxi Normal University, Xi'an, China

Major subject: Bioscience

07.2009 Bachelor Degree of Science

2011-2014 Shaanxi Normal University, Xi'an, China

Major subject: Science of Chinese Pharmacology

07.2014 Master Degree of Medical

Research experience:

Since 05.2015 Dr. rer. nat. student,

Supervisor: Prof. Dr. rer. nat. Heiko Hermeking

(Head of Experimental and Molecular Pathology,

Institute of Pathology, LMU, Munich)